The University of Vermont

Load Monitoring for Safe Construction

Final Performance Report

Submitted to: National Institute of Occupational Safety and Health
Center for Disease Control and Prevention
Grant Number: NIOSH 5 R01 OH03157-03

Principal Investigator: Dryver R. Huston
Institution: Department of Mechanical Engineering
University of Vermont
Burlington, VT 05405

Co-Investigator: Peter L. Fuhr
Institution: Department of Electrical and Computer Engineering
University of Vermont
Burlington, VT 05405

Co-Investigator: Wai-Fah Chen
Institution: School of Civil Engineering
Purdue University
West Lafayette, IN 47907

Co-Investigator: David V. Rosowsky
Institution: Department of Civil Engineering
Clemson University
Clemson, SC 29634

March 22, 1998

2. TABLE OF CONTENTS

3. List of Abbreviations

α'_s = slab shore stiffness ratio.

Δ_{slab}= the total deflection at the center of a slab.

Δ_{cr} = deflection at the center of a slab due to creep.

Δ_{shr} = deflection at the center of a slab due to shrinkage.

Δ_{ea} = deflection at the center of a slab due to elastic accumulation.

ΔL = the change in length of the shore.

ΔP = the calculated change in shore load due to the temperature gradient.

A = the cross-sectional area of the shore.

C_t = accumulated load effects.

E = the elastic modulus of the steel.

EULD = equivalent uniform load distribution.

F_i = the new value of the force in the shore leg after changing length.

F_i = the new value of the shore force after changing the shore length.

F_m = the maximum force of the system before changing length.

L_i = the length of the shore after length change.

L_o = the original length of the shore before length change.

L_r = the length change ratio.

R_g = the global force amplification ratio at a shore leg.

R_L = the local force amplification ratio at a shore leg.

S_g = global sensitivity at a particular shore.

S_L = local sensitivity at a particular shore.

4. List of Figures

5. List of Tables

6. Significant Findings

This study generated a large amount of results in terms of experimental data and mechanical analyses. The significant results from the field studies, laboratory studies, and mechanical analyses are listed below.

Field measurements of shore loads were taken at four sites: 1. Beckley WV, 2. East Ave., 3. Pomeroy Hall, and 4. Boston Museum Towers. An extensive analysis of the data has been completed for only the Beckley site. An analysis of the data from East Ave., Pomeroy Hall, and the Boston Museum Towers is currently underway. One of the significant features of the field data is that it may be the first set of lateral load measurements on this type of shoring.

For the data that have been analyzed to date, the following results have been identified:

1. The observed lateral shore loads were typically on the order of ±10% of the corresponding (i.e., simultaneous) vertical load.

2. A magnification factor on the order of 2.0 may be appropriate to account for the (spatial) variability among a group of shores in a common pour area. The degree of variability shore-to-shore appears to be a function of the amount of precompression imparted during installation.

3. The suggested ACI design load, including equipment, appears to be adequate for the slab areas considered in this study. The simpler "tributary analysis" design load well approximates the average shore load, while the more conservative ACI load (including equipment) well approximates the maximum shore load. However, an error in the installation of a shore can result in that shore being seriously overloaded.

4. An area-effect may exist which serves to reduce the maximum shore load for a given pour area (i.e., the ACI design load becomes more conservative as the effective slab area increases). A reduction in design load for construction may be a function of pour area, slab thickness, formwork arrangement, and concrete placement procedures.

5. Significant load variations in steel shores may result from large daily (or other) temperature variations. These variations were particularly evident during curing periods, even when there were no additional externally applied loads.

6. A small decrease in shore load was observed during the curing period. This decrease in shore load is likely a function either of creep effects in the concrete or gain in strength and stiffness of the slab. The decrease in load appears to become greater with increasing effective slab area.

7. Shore removal can induce significant loads on the slab and shores, often of an impact nature. The magnitude of these loads is a function of the amount of compression in the shore at the time of its removal and the removal procedure used. Shore removal loads take two forms: (1) additional compression due to the removal procedure, and (2) load redistribution following the removal of a nearby shore. The amount of load redistribution is largely a function of the supporting formwork arrangement. Very large effective impact loads may be imparted to the (early-age) slab during formwork removal.

8. The use of drophead shoring can eliminate highly dangerous reshoring operations, while possibly improving the efficiency of construction operations.

The laboratory measurements of shoring mechanics focused on the effects of various situations on the loads and stability of shoring systems. Some of the significant findings are:

1. The shore loads experienced by individual shores can be highly sensitive to small length changes in the individual shores.

2. Uplift can be measured by measuring the axial force in the individual shores.

3. The sequence of loading on the shore system can affect the final state of the loads in the shore. The test data indicated that the maximum force of the shoring system when loaded asymmetrically is about 20% greater than that when it is loaded symmetrically.

4. Soft footings can result in an uneven distribution of forces in the slab-shoring system, with the neighboring shores carrying the extra load of the shore with the soft footing.

5. For the particular case of the steel shoring system, the critical tilt angle of collapse was about 5.5 degrees. The collapse was presaged by tilts leading up to 5 degrees. A level of 2 degrees might be a reasonable alarm level.

The significant results of the mechanical analyses of shoring can be summarized as follows:

1. The analysis of nonuniform construction loads on structures can be quite complicated. A simplified procedure based on the equivalent uniform load distribution (EULD) method is adopted in this study due to its simplicity for practical use.

2. An analysis of the mechanics of load distribution in shoring systems indicates that an asymmetric loading of shoring systems increased the maximum loads experienced by individual loads by up to 20% over a symmetric loading.

3. An analysis of loads that are transferred to the shores by shore removal indicated that the safest pattern is that shores should be removed first from the center of a panel and then toward the outside columns.

4. Design tables for the simplified analysis of multi-level shoring systems is given in Tables 10.1 and 10.2.

7. Usefulness of Findings

Most of the findings reported in Section 6 have useful application in increasing the safety of shoring systems. These are:

1. The observed lateral shore loads were typically on the order of ±10% of the corresponding (i.e., simultaneous) vertical load.

2. A magnification factor on the order of 2.0 may be appropriate to account for the (spatial) variability among a group of shores in a common pour area. The degree of variability shore-to-shore appears to be a function of the amount of precompression imparted during installation.

3. The suggested ACI design load, including equipment, appears to be adequate for the slab areas considered in this study. The simpler "tributary analysis" design load well approximates the average shore load, while the more conservative ACI load (including equipment) well approximates the maximum shore load. However, an error in the installation of a shore can result in that shore being seriously overloaded.

4. An area-effect may exist which serves to reduce the maximum shore load for a given pour area (i.e., the ACI design load becomes more conservative as the effective slab area increases). A reduction in design load for construction may be a function of pour area, slab thickness, formwork arrangement, and concrete placement procedures.

5. Shore removal can induce significant loads on the slab and shores, often of an impact nature. The magnitude of these loads is a function of the amount of compression in the shore at the time of its removal and the removal procedure used. Shore removal loads take two forms: (1) additional compression due to the removal procedure, and (2) load redistribution following the removal of a nearby shore. The amount of load redistribution is largely a function of the supporting formwork arrangement. Very large effective impact loads may be imparted to the (early-age) slab during formwork removal.

6. The use of drophead shoring can eliminate highly dangerous reshoring operations, while possibly improving the efficiency of construction operations.

7. The shore loads experienced by individual shores can be highly sensitive to small length changes in the individual shores.

8. Uplift can be measured by measuring the axial force in the individual shores.

9. The sequence of loading on the shore system can affect the final state of the loads in the shore. The test data indicated that the maximum force of the shoring system when loaded asymmetrically is about 20% greater than that when it is loaded symmetrically.

10. Soft footings can result in an uneven distribution of forces in the slab-shoring system, with the neighboring shores carrying the extra load of the shore with the soft footing.

11. For the particular case of the steel shoring system, the critical tilt angle of collapse was about 5.5 degrees. The collapse was presaged by tilts leading up to 5 degrees. A level of 2 degrees might be a reasonable alarm level.

12. The analysis of nonuniform construction loads on structures can be quite complicated. A simplified procedure based on the equivalent uniform load distribution (EULD) method is adopted in this study due to its simplicity for practical use.

13. An analysis of loads that are transferred to the shores by shore removal indicated that the safest pattern is that shores should be removed first from the center of a panel and then toward the outside columns.

14. Design tables for the simplified analysis of multi-level shoring systems is given in Tables 10.1 and 10.2.

8. Abstract

This project was concerned with measuring the loads and behavior of temporary support structures that are used in the construction of reinforced concrete buildings. The main features of this work included: 1. Measuring and horizontal shoring loads at four sites – a federal prison in Beckley WV, a library storage facility on East Ave. on the University of Vermont campus, a reconstructed old building (Pomeroy Hall) on the University of Vermont campus, and a 25-story building referred to as the Boston Museum Towers; 2. Measurement of shore load effects including load sequence effects, soft footing effects and lateral instabilities in the laboratory; 3. A detailed mechanical and reliability analysis of shoring systems using both the simplified and modified simplified techniques that account for elasticity and creep; and 4. A comparison of the measured loads with those specified by the design codes. The field studies and the code comparisons resulted in a set of tentative recommendations for construction practice and a refinement of the codes. The laboratory studies concluded that shore loads are highly sensitive to member length variations, soft footings, and load application sequences. Symmetric load applications result in smaller member loads by about 20%. The laboratory experiments also indicated that shore member tilt can be used as a precursor warning measurement for lateral instabilities.

9. Introduction and Project Objectives

9. 1 Specific Aims

The overall goal of this project was to measure the vertical and lateral loads experienced by the shoring system of a reinforced concrete building under construction and to use the measurements to evaluate and improve shoring system design codes so that future construction site collapses can be prevented. The development and use of this shoring instrumentation was proposed to have four main phases:

1. **Design, develop and verify the load-monitoring instrumentation** - This involves assembling, and testing of load cells and data processing equipment that measure the vertical and lateral loads experienced by shoring systems during construction.

2. **Conduct field measurements** - The instrumentation assembled in Phase 1 will be used on 3 construction sites to measure both static and dynamic vertical shoring loads.

3. **Analyze data** - The data collected in Phase 2 will be analyzed to identify critical loading situations and load effects.

4. **Produce applications, guidelines and recommendations** - This will include at a minimum: suggested modifications to current code-specified design loads, methods of accounting for impact loads and procedures for instrumenting other large-scale construction projects.

The fundamental hypotheses of this project are that the loading history of shoring systems are a primary cause of catastrophic collapses, the measurement of these loads can be useful in preventing collapses, and that the shoring loads can be measured efficiently using relatively simple techniques.

At present, the most shoring system design procedures are based on computer or hand calculations with engineering judgement serving as a guide for the safety factors. The actual load environment experienced by a shoring system during construction, in particular those caused by impacts, side loads and poorly-sequenced pouring operations, may be significantly different than those predicted by standard analysis techniques. It is hypothesized that if these loads are measured rather than just calculated, then the design calculations and codes could be improved and would presumably be safer.

The project was a joint effort by researchers from the University of Vermont (UVM), Purdue University and Clemson University. The UVM group was involved primarily in the instrumentation development, field tests, and overall project management. The Purdue and Clemson groups were involved primarily in the data analysis, and the development of new design procedures.

9.2. Background and Significance

Structural engineers generally have paid a great deal of attention to ensuring the safety of the structure during its service life by satisfying code safety requirements. Unfortunately a similar degree of attention has often been missed in the consideration of safety during construction. The failure of structural systems during construction can often have tragic consequences. In April 1987 the L'Ambiance Plaza in Bridgeport Connecticut collapsed, killing 28 construction workers. The plaza was 60% complete at the time of collapse. Since there were minimal onsite measurements of the performance of the structure and its shoring system, the cause of the collapse is not certain and is still be debated. Unfortunately, this was not an isolated incident. Over the past 25 years there have been more than 85 collapses that have been directly attributed to formwork or shoring failures (Hadipriono and Wang, 1986).

In general, the primary causes of formwork failures are: 1) excessive loads, 2) premature removal of forms or shores, and 3) inadequate lateral support for the shoring members (Chen and Mossallam, 1991). Hadipriono and Wang (1986) determined that 48% of the recorded failures were due to inadequate vertical shores. Ayyub and Eldukair (1989) report that errors in design and construction procedures are responsible for about 51% and 57% of construction failures in the United States, respectively. A detailed discussion of various shoring failures appears in ACI SCM-19(89) (Anon. 1989).

If a shoring system does not have sufficient strength and stability to carry the imposed loads, the results can be disastrous. Consequently, it is essential to determine the load distribution during construction to assure safety. A number of attempts have been made at developing analytical and computer models to evaluate the load distribution and safety of a formwork structure. Nielsen (1952) was one of the first to study the distribution of loads on shores and slabs in multistory building structure by modeling the slabs and formwork as a highly-indeterminate elastic system. The analysis procedure was quite tedious for practical use, especially considering the lack of computers at the time. Grundy and Kabaila (1963) produced a simplified analysis procedure that treats the shoring as being infinitely rigid. Taylor (1967) showed that by judiciously releasing the shores between poured floors, the magnitude of the load carried by the most stressed floors can be reduced. Sbarounis (1984) extended Grundy and Kabaila's work to include cracking in the supporting slab. Liu, et al. (1985) developed a 2-D computer model to check the assumptions of Grundy and Kabaila's simplified method. They concluded that the simplified method is fairly accurate, but that the slab moments and shore loads should be corrected by a modification coefficient. Liu et al. (1988) extended this work to 3-D to examine the effects of boundary conditions, foundation rigidity, and nonlinear creep of the concrete and shores. Most of these effects were found to be negligible. El-Sheikh and Chen (1990) studied the behavior of telescopic steel shores under uniaxial loads. El-Sheikh and Chen (1988) examined such factors as rate of construction, out-of-straightness of shores. Liu, Lee and Chen (1988) developed a simplified method for the mathematical formulation of several construction operations. This enabled a computer-based evaluation of slab safety at any construction stage by comparing the applied loads with the available slab strength. Liu and Chen (1987) conducted a probabilistic analysis of the maximum shore load distribution in multistory concrete buildings using a 3-D model. They concluded that the variation of the construction live load influences the maximum shore load significantly. Lee, Liu and Chen (1990) examined the failure probability of time-dependent reinforced concrete structures. They showed that a structure during construction is much more critical and dangerous than one during its normal usage.

It should be noted that none of the foregoing methods have been chosen by the present codes and standards for the analysis of reinforced concrete buildings during construction. ACI Committee 347 references them as acceptable analysis techniques. The principal nationally-applicable codes and standards for concrete construction are:

1. The ACI Committee 347(1988), "Guide to Formwork for Concrete," which replaces a previous standard, ACI 347-78, "Recommended Practice for Concrete Formwork".

2. ANSI A10.9 (1983), the American National Standards Institute "American National Standard for Construction and Demolition Operations-Concrete and Masonry Work-Safety Requirements".

3. Chapter 6 of ACI 318 (1989) "Building Code Requirements for Reinforced Concrete," which deals with construction practices.

4. OSHA Subpart Q (Hurd, 1988) of the Federal Construction Safety and Health Regulations.

These codes give extensive explicit procedures for the design of the shoring systems to sustain static vertical loads. The dynamic loads due to impact and other effects are not covered in much detail. Neither are the design guidelines for lateral loads and stability. A primary cause for the brevity of treatment is the design codes is the lack of available load data. Typical is ACI 347-88 Sect. 2.6 which states:

> The formwork system should be designed to transfer all horizontal loads to the ground or to completed construction in a manner as to insure safety at all times. Diagonal bracing should be provided in vertical and horizontal planes where required to resist lateral loads and to prevent instability of individual members...

An inherent limitation of computer or hand calculations is that they can not anticipate unusual or extreme circumstances that may occur at the site. For example, fires have been known to cause formwork failures, as has the failure of the components themselves. Furthermore, it is known that construction crews do not always follow the shoring system design. Hence a computer model may not correctly represent the loads present at the actual site (Hadapriono and Wang, 1986). The documentation of live load variations in various types of concrete construction using different placement procedures would be invaluable in establishing realistic design requirements for live loads (Chen and Mosallam, 1991).

The literature reporting the actual measurement of loads on shoring systems during construction is somewhat more limited. Agarwal and Gardner (1974) compared the field measurements of the construction loads from two high-rise flat slab buildings with the loads predicted by the Grundy-Kabaila method. The field measurements of the construction loads agreed with acceptable accuracy with those predicted by the simplified method of Grundy and Kabaila. However, the field measurements were static in nature and could not measure short-term dynamic overloads such as those due to impacts and pouring and conveying operations. A rather comprehensive set of static-only shoring load measurements was reported by Fattal (1983). This study indicated that the vertical loads experienced by the shoring were appropriately accounted for by the design codes. However, no dynamic or lateral shoring loads were measured. Other reported estimates of live loads on shoring include those of Karshenas (1989) and Karshenas (1990) in which inventories of load situations on constructions site were taken and the live loads estimated. Huston et al. (1992) report results from a study in which a reinforced concrete building was instrumented with embedded optical fiber and conventional sensors. While these studies were aimed at embedding sensors in the building structure for long-term performance monitoring, they demonstrated the viability of instrumenting a building system during construction without impeding the construction crew. Kubo et al. (1989) report measurements taken of the wind loads and responses of the prestressed concrete Yukubo Bay cable-stayed bridge while it was under construction. Masahiro et al. (1990) and Tanaka et al. (1987) report the use of real-time load and deflection measurements to control the cable tensioning process during the construction of cable-stayed bridges. To date there appears to be no comprehensive studies reported in the literature in which load impacts, such as those caused by a cement bucket, or lateral loads, have been measured on a real construction site.

The literature reporting on the measurement of in-service loads and responses of civil structures is actually somewhat more extensive. The use of these techniques has traditionally been cumbersome due to the cost of the transducers, cabling, installation, and data processing. As a result most of the instrumented structures are selected major structures or smaller structures undergoing scrutiny as part of a research project. However, the ever-increasing reduction in costs and advancement in the power of electronic and electro-optical equipment has made it much more practical to conduct structural measurements. Considerable activity has occurred in the aerospace industry in the 1980's for high-performance vehicles through the development of embedding sensing and fabrication processing techniques. This technology has been termed "Smart Skins" or "Smart Structures." Smart structures techniques have been employed on a modest scale for civil structures, Huston (1991). The primary impediments to using smart structures techniques in civil structures are the overall cost versus the relative benefit and relatively conservative nature of the civil engineering community. The majority of civil structures are designed to last 50 years or more with a minimum of maintenance or observation. The use of on board instrumentation to monitor the health of constructed facilities on a routine basis can only be justified if it makes engineering and economic sense.

9.3 Research Design and Methods

The research project had four main phases:

1. Field Testing

Data were taken at four buildings under construction: 1. A federal prison in Beckley WV, 2. A library storage facility on the UVM campus on East Ave., 3. An old building undergoing reconstruction on the UVM campus (Pomeroy Hall), and 4. A 25-story building referred to as the Boston Museum Towers.

The field testing procedure was essentially quite similar to that originally proposed for the project. Eight 3-axis load cells were custom-built by Hitec Corp. of Westford MA. The load cells were tested in the UVM laboratory. Initially the load cells were found to have an off-axis sensitivity in the vertical direction. This was corrected by changing the strain gage circuits from 4-gage to 8-gage Wheatstone bridges. A Megadac 3108 data acquisition system was used to acquire the data and store it in digital format on optical media. A laptop computer controlled the testing operations. A ruggedized steel box provided weatherproofing and protection for the electronic equipment. Ruggedized cables and connectors were used to make the connections from the load cells to the data acquisition system.

The first site to be tested was a federal prison in Beckley WV. This site consisted of a series of five story low-rise buildings. Measurements were taken at one of the buildings during August and September 1994. The second site to be tested was a library storage facility on East Ave. on the UVM campus. The building on East Ave. is a low-rise structure. Measurements were taken at East Ave. from September to October 1994. Torrential rains hampered the East Ave. field measurements.

Following the Beckley and East Ave. site measurements, it proved extremely difficult to find another suitable building for measurements. The reason was threefold. First, there was an overall downturn in building construction in the Northeastern and Midwestern United States during this period. Second, the price of steel became quite low and most of the buildings that were built were built of steel, not concrete. Third, liability concerns of the owners restricted access to the sites. This happened, in particular, for a very promising site in suburban Chicago during the summer of 1996.

Finally in 1997 sites began to become available. One was Pomeroy Hall. This was an old building that was being reconstructed on the University of Vermont campus. Vertical shoring was used to hold the roof up during reconstruction. Measurements were taken of the roof shore loads in January and February 1997. The second site was a 25-story residential building under construction in Cambridge MA, known as the Boston Museum Towers. Data were taken at the Boston Museum Towers from the 8^{th} to the 22^{nd} floor in a period that ranged from June to August 1998.

2. Laboratory Testing

During the lull between field measurements, a series of laboratory tests on model shoring systems were completed. The purpose of these tests was to examine the mechanics of shoring systems. The effects that were examined were uplift, sensitivity of load to shore member length variation, sensitivity of loads to soft footing conditions, sensitivity to load sequences and lateral stability.

The tests were conducted on two sets of model shores. The first was a wood multistory structure that was used in the uplift, and load sensitivity studies. The second was a steel structure the was used in the lateral stability studies.

Overall, the experimental studies were successful. The wood shore tests demonstrated sensitivity of the load distribution to member length variations, soft footings and load sequence. The steel shore study demonstrated lateral instability in heavily loaded shoring systems. It also demonstrated that measurement of shore leg tilt angle can be used as a early-warning of impending lateral collapse.

3. Mechanical Analysis

A detailed analysis of shoring systems was also undertaken. M. Duan and W.-F. Chen of Purdue performed most of the mechanical analysis. The analysis examined the effect of loads and varying concrete properties in multistory construction. The overall result was a set of simplified design guideline for safe concrete building construction. An interesting result of the analysis was also that asymmetric load sequences cause an increase in the local member loads. This effect was observed in the model shoring tests.

4. Comparison with Codes and Recommendations.

At this point only the load data measured at the Beckley site has undergone an extensive analysis. This data has been compared with the ACI codes. In general, the codes and the data show a fair amount of agreement. Tentative recommendations for modifications and refinements to the codes appear in Section 16 of this report. D. Rosowsky et al. has carried out the bulk of the code comparison analysis at Clemson University.

The data from the other sites is currently being analyzed and results should be forthcoming in the early summer of 1998.

10. Mechanical Analyses of Shoring

One of the key features in establishing proper concrete shoring construction procedures is to have an understanding of the mechanical behavior of shoring systems. To this end, M. Duan, under the direction of Professor W. Chen at Purdue University conducted an extensive theoretical and computational analysis of shoring system mechanics, with a comparison to some of the Beckley WV field data. This line of research formed the basis of a PhD dissertation with the title "Design Guidelines for Safe Construction of Concrete Buildings" (Duan, 1996). This dissertation was written, in part, as part of this research project. The following is a synopsis of the key features of Duan's dissertation.

10.1 Introduction and Literature Review

There are more accidents occurring during construction than during the service life for concrete buildings (Chen and Mosallam, 1991). In the existing design code (ACI Committee 318, 1995), the main part only specifies the technical requirements to ensure predictable level of safety for a structure during its service period, however, there are very few considerations of safety requirements for temporary supporting systems during construction. Failure accidents can occur in various stages during construction. About half of these accidents occur during concrete placement, and about 12 percent occur during formwork removal. In summary, the causes of failure can be classified into three categories: (1) *Triggering causes of failure:* failure due to concrete placement, impact load, strong wind, heavy rain, improper formwork removal and other unclear sources. Most of these causes are essentially actions of excessive loads exerted during construction operations. (2) *Enabling causes of failure:* failure due to the deficiency of the supporting structural system such as inadequate formwork design and cross-bracing, inadequate formwork component and connection, inadequate formwork foundation, inadequate shoring and reshoring, etc.; (3) *Procedural causes of failure:* failure due to inadequate review of formwork design and construction, lack of inspection of formwork during concrete placement and inadequate procedures of construction. Design guidelines need to account for all these factors.

There are four available references presently in the USA for construction practice of concrete buildings: (1) ACI Committee 347 (1988), "Guide to Formwork for Concrete"; (2) ANSI A10.9 (1983), "American National Standards for Construction and Demolition Operation"; (3) Chapter 6 of ACI 318 (1995), "Building Code Requirements for Reinforced Concrete; and (4) OSHA (1988): Construction Safety and Health Regulations. In addition, the ASCE Structural Division also worked out a draft (1995), Proposed Guide/Standard for Design Loads on Structures during Construction. ACI Committee 347 recommends a um construction live load of 50 psf (2.5 kPa) for workmen, equipment, runways and impact, or 75 psf (3.71 kPa) when using buggy transport. The minimum design load for combined dead and live loads should be 100 psf (5.0 kPa), or 125 psf (6.25 kPa) when using buggy transport. The OSHA safety standard requires that a minimum 20 psf (1.0 kPa) be used for live load and weight of formwork.

ANSI AIO.9 does not provide a numerical value but leaves the determination of live load to the formwork designers or contractors. It is evident that there are no adequate specifications for safe construction within these codes, and the suggested minimum 100-lb/linear ft (1.5 kN/m) of floor edge or 2 percent of the total dead load of the floor, whichever is greater. Both ACI 347-88 and ANSI Standard A10.9 require a minimum design wind load of 15 psf (720 Pa). A more rational method was given by Rosowsky (1995) using a conversion factor to transform the design wind load in service life to the design wind load during construction.

For multilevel slab-shore systems, Grundy and Kabaila (1963) developed a simplified method to calculate construction loads distribution in slabs and shores. There are four basic assumptions in the simplified method:

(1) Shores are infinitely rigid in comparison with the slabs in vertical deflection.
(2) The effects of creep and shrinkage are neglected.
(3) Loads applied to slabs are distributed between slabs in proportion to their relative flexural stiffness.
(4) The slab stiffness can be treated as either a constant or a variable.

The above four assumptions define a simple calculation method for shore load distributions. It is called the simplified method. The simplified method was later suggested as an analysis method in formwork design by ACI Committee (Hurd, 1989). Agarwal and Gardner (1974) compared the simplified method with the field measurements for shore loads and found the simplified method agreed well with field measurements in some cases.

Liu, et al. (1985) developed a refined 2-D finite element analysis model to check the major assumptions of the simplified method by taking elastic shortening into account. The result of the study was that the simplified method is adequate for predicting the location of maximum slab moments and shore loads, but may underestimate the maximum moments and loads by 10%. The finite element refinement of considering shore elastic shortening was developed further by Liu, et al. (1988) and Chen and Mossalum (1991) with the program SHORING2 to check the safety of slabs during construction. This program considers slab strength development, the manner of shoring and reshoring, type of construction and construction rates. Further refinements to the mechanical modeling of shoring are to consider creep (Liu and Chen, 1987; and Lee et al., 1991), effects of fast rate construction (El-Sheikh and Chen, 1988), and construction loads on early-age slabs (Sbarounis, 1984a-c).

One method of estimating the safety of shoring systems is to use probabilistic, i.e. reliability-based, methods. Liu and Chen (1987) conducted probabilistic analyses of maximum shore load distributions using a 3-D model. El-Shahhat, et al. (1993a,b) performed a structural reliability for slabs during construction.

10.2 Design Considerations For Safe Construction Of Concrete Buildings

In the construction of multistory RC buildings, the early-age concrete slabs with partial strength and the formwork support all of the loads that occur during construction. This supporting system must be designed to work safely. However, as with most engineering systems, there is a need to balance safety and economy in developing design specifications (Corotis, 1985).

There are many factors that affect the behaviors of slab-formwork (or slab-shore) supporting systems. These factors can be classified into the following three categories:

(1) *Design decisions:* including concrete types, column and slab sizes and reinforcement arrangement, etc.
(2) *Construction schedules:* including shoring and reshoring, construction cycle, method of concrete placement such as concrete bucket dropping, pumping, and concrete placing paths, etc.
(3) *Environmental conditions:* ambient temperatures, wind conditions, and other possible natural excitations.

To develop proper design guidelines for safe construction, all of these factors should be accounted for. Thus, the general design formula for slabs at any critical time can be written as:

$$\text{Resistance} \geq \text{Effect of factored loads}$$

The design of the supporting system for a given construction schedule includes two parts as

(1) *For slabs*: to assure the safety of the partial strength slabs during construction;
(2) *For formwork:* to determine the specified load effect on formwork designed by the allowable stress design method.

The loads on the formwork are primarily vertical gravity loads and lateral loads. The gravity loads consist of dead and live loads. ACI 347 recommends a minimum design load for combined dead and live loads of 100 psf (5.0 kPa), or 125 psf (6.25 kPa) when using buggies to transport the concrete. Dead loads tend to have less variation than live loads. Field measurements at 20 construction sites in Taiwan were reported by Huang (1995) for dead and live loads during concrete pumping. The average dead load was about 110 psf (5.5 kPa), which included slab and beam weights, as well as some part of the column weight. The coefficient of variation (COV) of dead load is 0.22. higher than that of the service dead load. The average live load is about 15 psf (0.72 kPa).

Horizontal loads can be treated in a simple way as suggested by ACI 347 (1988) as either 100 lb/ linear ft (1.5 kN/m) or 2 percent of the total superposed dead load, whichever is larger. Both ACI 347-88 and ANSI Standard A10.9 require a minimum design wind load of 15 psf (720 Pa). A more rational method was given by Rosowsky (1995) using a conversion factor to transform the design wind load in service time to the design wind load during construction.

Some special loads also arise including temperature variations and earthquakes. Field measurements (Philbrick and Rosowsky, 1995) show that the temperature changes can cause variations of self-balanced internal forces in slab-shoring system during curing. This effect can be neglected due to its small magnitude. Earthquake loads are not considered for ordinary building construction because the construction period is usually short.

For formwork design, the specified load effect of dead and live loads is reached during concrete placement. For concrete slabs, the accumulated factored dead and live loads occur during the processes of concrete placement and shore removal.

Construction loads during concrete placement influence formwork and slabs differently, and thus should be studied separately. The *Equivalent Uniform Load Distribution* (EULD) method is adopted in this study due to its simplicity for practical use. Thus, all nonuniform loading effects are transformed into uniform loading effects at first in the present load effect analysis.

The EULD for the factored slab load is determined during concrete placing and shore removal for slab load evaluation. The paths of concrete placement and nonuniform configuration of shoring locations have little influence on slab load and hence, can be neglected. Then, the load effect on slabs can be calculated using the simplified method (Grundy and Kabaila, 1963) or the refined simplified methods (Liu, et, al., 1985, Duan and Chen, 1995a). In slab-shore load analysis, it is necessary to

(1) Establish the EULD model for dead and live loads.
(2) Account for slab-shore stiffness ratio.
(3) Account for creep and shrinkage.

The possible maximum EULD (specified load) effect on shore load is determined during concrete placement by amplifying the dead load. The effects of nonuniform loading, impact loading and material storage during concrete placement should be considered for formwork design.

In general, a construction schedule includes the selected procedure of shoring and reshoring, the construction cycle and the method of concrete placement. The goal of design here is to check construction schedules so that construction load effects will not be greater than the capacity of early-age slabs at any critical time. For a given construction schedule, the slab safety check can be performed in the following steps:

(1) Determine factored construction load in the form of EULD;
(2) Calculate accumulated factored load effects;
(3) Calculate the capacity of partial strength slabs;
(4) Check the safety of slabs.

10.3 Improved Simplified Method for Slab and Shore Load Analysis During Construction

Two possible methods of further refining and improving the simplified method are to account for variation in slab stiffness and the flexibility of the shores. An important factor in this regard is the slab shoring stiffness ratio. The stiffness ratio between the slab and the shores varies between 0.05 and 1.0. Usually panels with large spacing have a small slab-shore stiffness ratio and are suitable for the simplified method.

Based on the present study, the following recommendations are made for the analysis of distributions of construction loads in multilevel shoring systems:

(1) *For calculation of dead load distribution in construction* - When the slab shore stiffness ratio $\alpha'_s < 0.4$, use the simplified method. Otherwise, use the improved simplified method.
(2) *For calculation of live load distribution in construction* - When $\alpha'_s < 0.2$, use the simplified method. Otherwise, use the improved simplified method.
(3) *Tables 10.1 and 10.2 can be used to simplify the improved simplified method.* Linear interpolation can be used if the slab-shore stiffness ratio is between the values given in the tables. To use these tables, the difference in stiffness between each slab should be small and the shoring conditions are the same in each level. Otherwise, use the original formulas in Duan (1996).

shoring case		slab-shore stiffness ratio K_{shore} / K_{slab}				shoring layout (on rigid ground)
	slab load	$\alpha_s' = 0.0$ (strong-shoring)	$\alpha_s' = 0.5$	$\alpha_s' = 1.0$	$\alpha_s' = 2.0$ (weak-shoring)	
two-level shoring	P_2	0.00	0.33	0.50	0.67	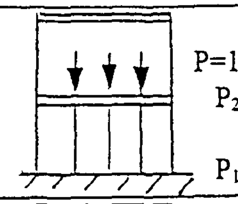
	P_1	1.00	0.67	0.50	0.33	
three-level shoring	P_3	0.00	0.45	0.60	0.73	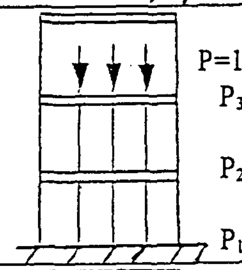
	P_2	0.00	0.18	0.20	0.18	
	P_1	1.00	0.36	0.20	0.09	
four-level shoring	P_4	0.00	0.49	0.61	0.73	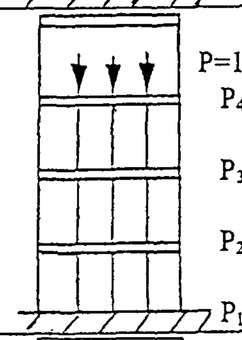
	P_3	0.00	0.23	0.23	0.19	
	P_2	0.00	0.01	0.08	0.05	
	P_1	1.00	0.19	0.08	0.03	
five-level shoring	P_5	0.00	0.49	0.62	0.73	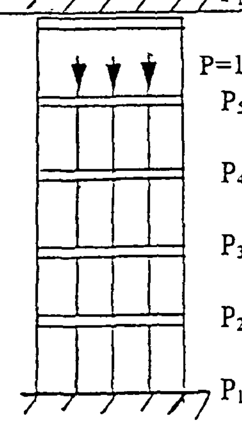
	P_4	0.00	0.25	0.24	0.20	
	P_3	0.00	0.12	0.09	0.05	
	P_2	0.00	0.05	0.03	0.01	
	P_1	1.00	0.09	0.03	0.01	

Table 10.1 Slab load distribution under unit force for typical shoring cases with the same slab rigidity and shoring condition in each level and the bottom shoring is on rigid ground (Duan, 1996).

shoring case	slab load	slab-shore stiffness ratio K_{shore}/K_{slab}				shoring layout
		$\alpha'_s = 0.0$ (strong-shoring)	$\alpha'_s = 0.5$	$\alpha'_s = 1.0$	$\alpha'_s = 2.0$ (weak-shoring)	
two-level shoring	P_2	0.50	0.60	0.67	0.75	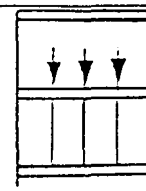 P=1 P_2
	P_1	0.50	0.40	0.33	0.25	P_1
three-level shoring	P_3	0.33	0.52	0.62	0.73	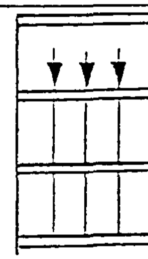 P=1 P_3
	P_2	0.33	0.29	0.25	0.20	P_2
	P_1	0.33	0.19	0.13	0.07	P_1
four-level shoring	P_4	0.25	0.51	0.62	0.73	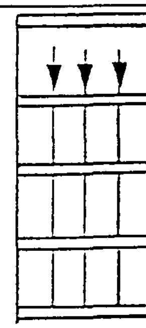 P=1 P_4
	P_3	0.25	0.26	0.24	0.20	P_3
	P_2	0.25	0.14	0.10	0.05	P_2
	P_1	0.25	0.09	0.05	0.02	P_1
five-level shoring	P_5	0.20	0.50	0.62	0.73	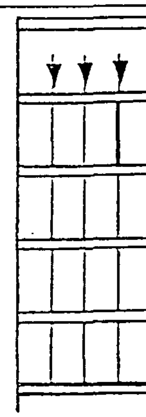 P=1 P_5
	P_4	0.20	0.25	0.24	0.20	P_4
	P_3	0.20	0.13	0.09	0.05	P_3
	P_2	0.20	0.07	0.04	0.01	P_2
	P_1	0.20	0.05	0.02	0.00	P_1

Table 10.2 Slab load distribution under unit force for typical shoring cases with the same slab rigidity and shoring condition in each level and the bottom shoring is on a slab (Duan, 1996).

10.4 Effects Of Creep and Shrinkage on Slab-Shore Loads and Deflections during Construction

The total deflection at the center of a slab, Δ_{slab}, during curing consists of three parts: creep, Δ_{cr}; shrinkage, Δ_{shr}; and elastic accumulation Δ_{ea}:

$$\Delta_{slab} = \Delta_{cr} + \Delta_{shr} + \Delta_{ea}$$

The elastic accumulation is caused by the dramatic change of elastic modulus in early-age slabs while under a changing slab load during curing.

A test of the creep model for stress relaxation in a slab is made by comparing the loads measured at Beckley WV (Huston 1995) with a creep model. The results are quite reasonable, Figures 10.1 and 10.2.

Based on the present study, the following suggestions are made to modify the simplified or the refined simplified methods considering the creep and shrinkage effects on supporting systems for a construction cycle of about 7 days:

(1) *In the case of steel shores*, the creep and shrinkage effect can be neglected when the slab-shore stiffness ratio α'_s is larger than 0.40. Otherwise, consider increasing the slab load on the topmost slab by 10% and reducing the other slab loads equally.

(2) *In the case of wooden shores*, creep and shrinkage effects should be considered by increasing the slab load on the topmost slab by 15% and by reducing other slab loads equally.

(3) *The long-term deflection of a slab* can be predicted using Eqs. (4.27) to (4.29) in Duan (1996)if the history of construction load on slabs can be evaluated.

(4) *The numerical analysis* is performed by custom software written in FORTRAN 77, which is shown in Appendix B (Duan, 1996).

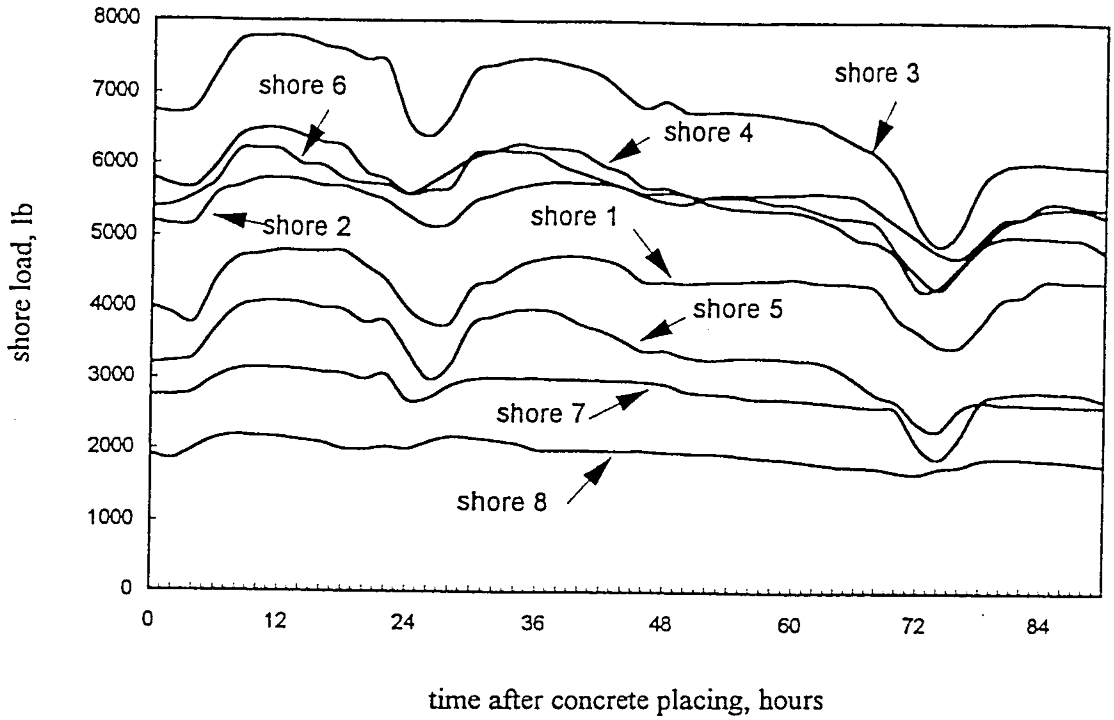

Figure 10.1 Shore load measured during curing for large spacing at Beckley, WV.

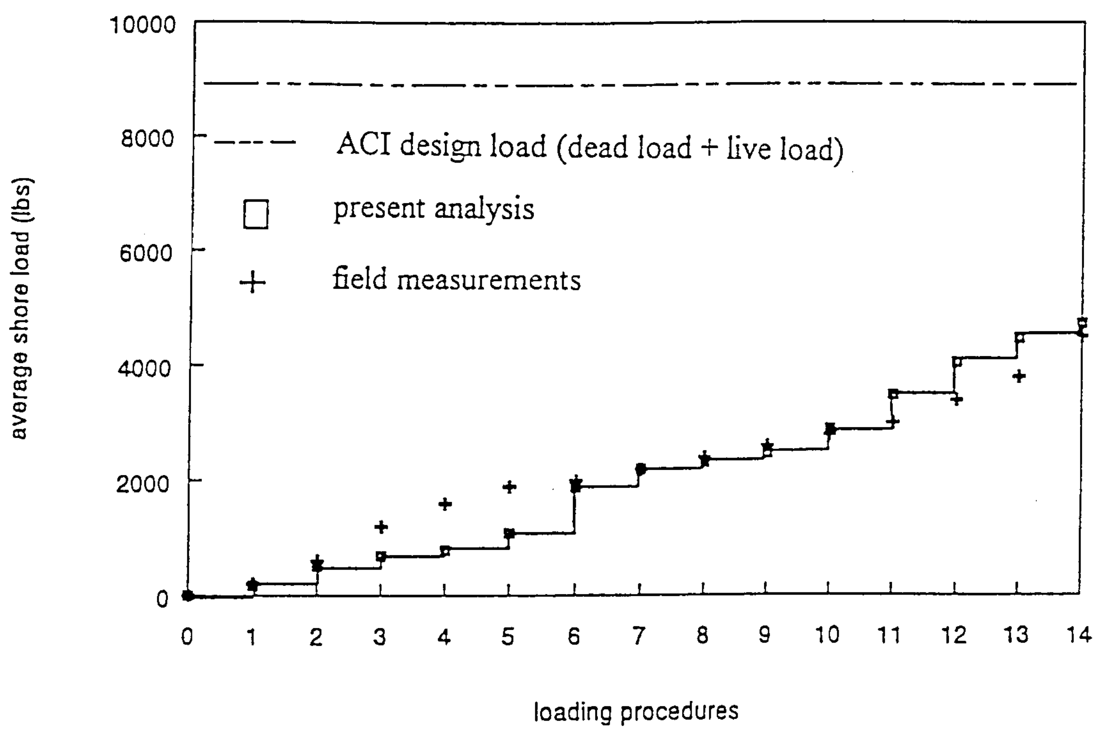

Figure 10.2 Average shore load measured and predicted during curing for large spacing at Beckley, WV.

10.5 Nonuniform and Impact Loading On Slab-Shores in Concrete Placement and Shore Removal During Construction

Concrete placement and shore removal are two critical stages during construction. As pointed out by Hadipriono and Wang (1986), more than sixty percent of accidents in construction occur in these two stages. A slab-shoring system may be overloaded and nonuniform concrete placement and impact load may cause the uplift and shift of shores from formwork. The supporting system may be loosened as a result. In addition, removing shores too early or in an improper way is another cause of slab-shoring system failures. Thus, the reasons for a structural failure can be explained and design guidelines are developed to prevent its occurrence.

Construction loads during concrete placement transmit to shores and supporting slabs occur in different manners, and should be considered differently. Maximum shore loads in the topmost level of shoring system are influenced by concrete placing sequences. Nonuniform load effects have little influence on slabs and shores in lower parts of a multilevel supporting system. Uplift effects on shores may occur during concrete placement. Hence the shores in a supporting system should be braced properly. The effect of impact loads from concrete dropping while using crane buckets on shore loads and slab load occurs simultaneously and can be very significant.

A detailed analysis of loads that are transferred to the shores by shore removal indicates that the pattern of shore removal is important. The safest pattern is for the shores at the center of the slab to be removed first. Then the shores from the outside part of the panel should be removed.

As a test of the mechanical models to predict the shore loads during pouring a comparison of shore load data taken at Beckley WV and with the model was conducted. Figure 10.3 shows the bucket pouring sequence on the slab. Figure 10.4 shows the pour loads used in the model. A comparison between the model and the measured data appears in Figure 10.5. The comparison is quite good.

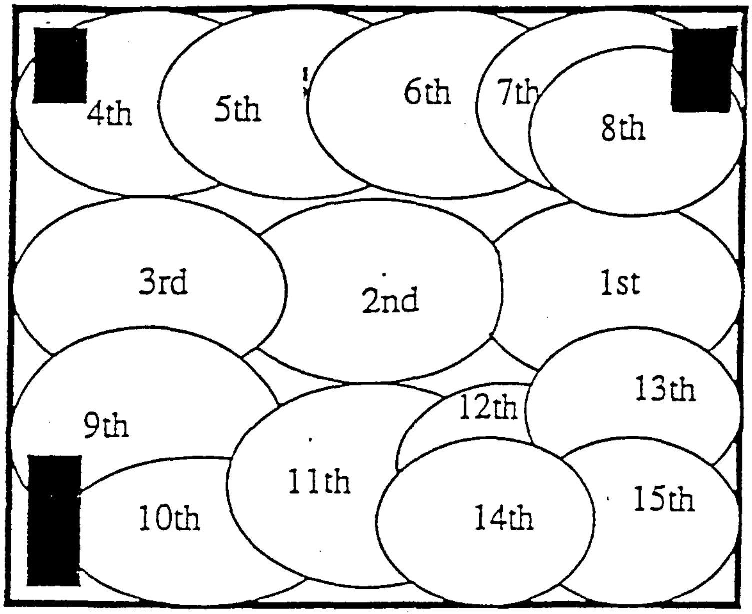

Figure 10.3 Sequence of concrete placing at Beckley site.

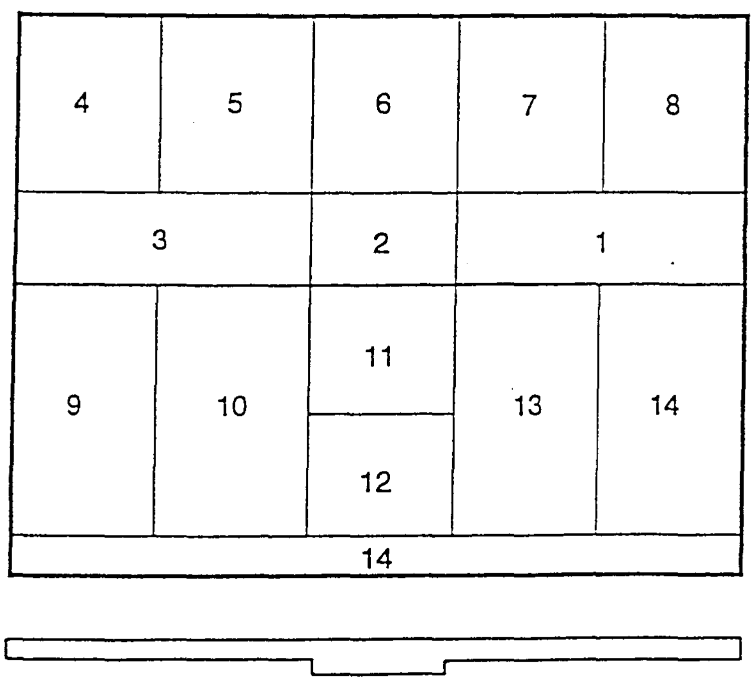

Figure 10.4 Simplified sequence of concrete placing at Beckley site.

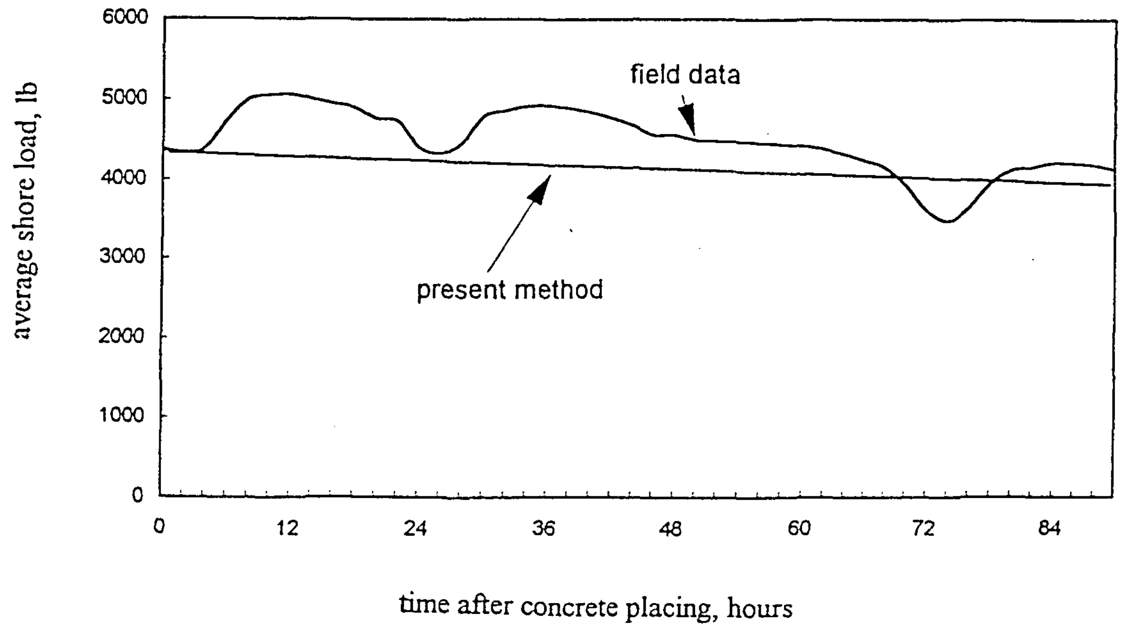

Figure 10.5 Histories of average shore loads from present analysis and field measurements at Beckley site.

10.6 General Design Guidelines for Safe Construction of Concrete Buildings

The slab-shore supporting system must carry all possible loads during a complete construction process. Slabs must attain sufficient strength and rigidity before concrete placement or shore removal so as to not generate excessive stress and deflections. Formwork must be designed to have sufficient strength to safely transmit gravity load to slabs during concrete placement and horizontal load to permanent structures before and during concrete placement.

In planning a construction schedule using multilevel shoring system, the following factors should be considered:

(1) The *design loads* for slabs during service.
(2) The *design weight* of the concrete including the weight of the slab, beam, and formwork.
(3) The *construction live load* involved, such as crews, equipment, material storage, path of concrete placement, impact due to concrete dropping and equipment moving.

(4) The *construction cycle.*
(5) The *developed strength of concrete* at the time it is required to support new load.
(6) The *type of formwork system*, i.e., steel or wooden shores, individual shore load.
(7) The *span and thickness of slabs* and the *elasticity of shores.*
(8) The *wind* during concrete placement and *temperature* during curing.

In general, a construction schedule includes the selected procedure of shoring and reshoring, construction cycle and the method of concrete placement. The goal of design here is to find feasible construction schedules such that the construction load effect will not be greater than the capacity of early-age slabs and formwork at any critical times. For a given construction schedule, the procedures for safe construction can be performed as:

(1) *Slab Safety Check* – This involves determining the dead load; determining the factored construction load in terms of EULD, which accounts for workers, equipment, material storage, and impact loads; calculating the accumulated load effects C_t with either the simplified or improved simplified methods; calculating the capacity of partial strength slabs; and then checking the safety of the slab.
(2) *Serviceability of the Slab* – Long-term deflections, while not a serious safety issue, do affect the performance and utility of the completed structure, and have a bearing on formwork design and usage.
(3) *Formwork Design* – Designing the formwork requires determining the construction load in terms of an EULD, designing the formwork under vertical load effects using the allowable stress design method; and providing sufficient bracing for shores to resist the horizontal loads and to assure the stability of the shores.

The following checklist has been developed to enable the safe use of shoring reinforced concrete building construction.

Concrete Placement:

(1) The selection of the path of concrete placement. This should be symmetric in order to minimize nonuniform loading effects on shore loads.
(2) Low height and slow speed of concrete dropping are helpful to reduce impact effects on slabs and shores.

Shore Removal:

(1) Before shore removal, make sure that the slabs have attained sufficient strength.
(2) Shore removal operations should be performed smoothly to avoid dynamic effects.
(3) If shores are removed one by one, the safe pattern of shore removal should be from the center of a panel toward outside columns.

Lateral Bracing

(1) Single post shores should be laced and braced to reach sufficient stability to prevent buckling and being unstable when uplift occurs.
(2) The bracing system must be tied to a solid ground or permanent structure unless it is multi-directional with sufficient X-bracing to give its internal rigidity.

10.7 Decision Making Models for Reliability of Slab and Formwork Systems during Construction

The design and use of shoring systems for the safe construction of reinforced concrete buildings requires a tradeoff between the cost of safety and the cost of accidents. Figure 10.6 gives and indication of the relation between the cost of safety and the cost of accidents. Estimating the costs of safety and the cost of accidents is a difficult problem. One of the hindrances in performing such an analysis is reliable reliability data. Nonetheless, if such data were available, Duan (1996, Chapter 7) lays the groundwork for such an analysis.

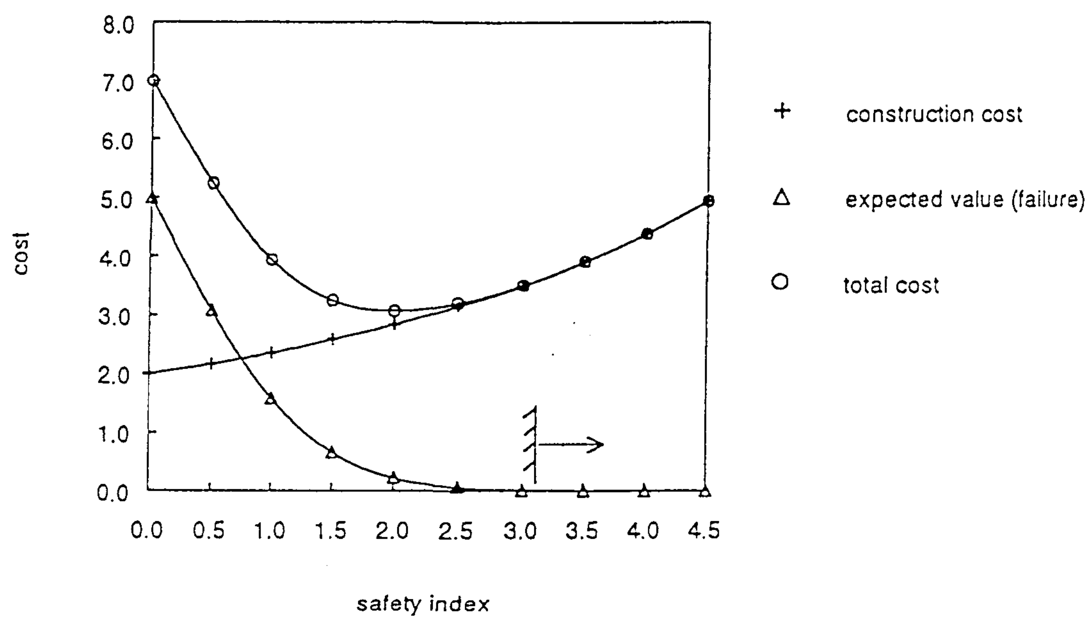

Figure 10.6 Relationship between total cost and target safety index of construction.

10.8 Inspection of Safety and Quality of Concrete Buildings during Construction

To ensure a safe and qualitative construction, adequate inspection should be provided. Contractors and on-site inspectors should work together to supervise a construction project. The main checklist items are summarized in the following.

Construction:

(1) Material approval and shop drawing approval.
(2) Check shoring and reshoring planning and scheduling.
(3) Check field and laboratory material testing procedures.
(4) Check actual construction loads, mechanical equipment loads, etc., against design loads.
(5) Check temporary bracing.

Reinforced Concrete:

(1) Study the specifications and drawings.
(2) Check the reinforcing-steel grade.
(3) Check the concrete mix: water/cement ratio (slump test, Kellyball test), temperature in casting and admixtures.
(4) Check the dimensions of all concrete members, and concrete cover.
(5) Check rebar details: length, size, location of rebars; spacers, bar chairs, hoops effective depth of top bars.
(6) Check the integrity reinforcing construction joints.
(7) Check the actual rate of casting and temperature against design.
(8) Check concrete vibration requirements.
(9) Check dimensional tolerances.
(10) Check curing requirements.

Formwork Construction

(1) Study the specifications and drawings.
(2) Review formwork erection plan.
(3) Perform formwork analysis.
(4) Lateral cross bracing against lateral loads.

10.9 Conclusions and Recommendations for Further Study

In the present study (Duan 1996) developed design guidelines for the safe construction of concrete buildings. The main contributions covered are:

(1) Improved method for load effect analysis.
(2) Analysis of the creep and shrinkage effects.
(3) Effects of nonuniform loading and impact.
(4) Design procedures.
(5) Slab safety checks.
(6) Formwork safety checks.
(7) Reliability analysis.

In addition a series of recommendations for further study were proposed, which included:

(1) Refining the design guidelines.
(2) Study on lateral load and resistance.
(3) Load factor analysis.
(4) Concrete bridge construction.

11. Laboratory Studies of Shoring

11.1 Overview

A series of laboratory tests were undertaken in an attempt to understand some of the mechanical principles of shoring systems. Four sets of experiments were conducted: 1. A study of the *sensitivity of shoring loads to length changes*; 2. A study of the *sensitivity of shoring loads to uplift*; 3. A study of the *sensitivity of shoring loads to soft footings*; and 4. An examination of the *stability of shoring systems under combined lateral and vertical loads*.

The primary results of these studies are: 1. The load on an individual shore can be highly sensitive to changes in the length of the shore; 2. Uplift and soft footings are measurable effects; 3. Load application sequence can affect the load in the shores; and 4. Small measurable changes in tilt angle are precursors to lateral collapse. Details of the experiments and results follow.

11.2 Member Shoring Load Sensitivity Due To Length Variation

11.2.1 Introduction

Field measurements by Fattal (1983) indicated that non-uniform residual forces on the shores may exist, when they are first installed. A full-scale simulation test of a single-story shoring structure under different loading routines was carried out in Taiwan (Huang, 1995). Huang studied shoring system buckling with a full-scale simulation test, data was obtained about the force distribution in the shores and the effect of load sequences. Field measurements in Beckley, WV indicated that shore loads can be highly variable (Huston et al., 1995).

One hypothesis for explaining the variable shore loads is that since a shoring system is highly indeterminate, the loads in the individual members are sensitive to changes in the length of the members. In order to quantify and gain a better understanding of the sensitivity of shoring loads due to variations in the member lengths, laboratory scale model tests of a three story and three bay slab-shoring system were conducted. A three story, three bay slab-shoring system was modeled with wood shore bays and plywood boards, Figure 11.1. Nine large buckets were filled and placed on the plywood boards to simulate the loads due to concrete pouring. Filling the buckets in symmetric and asymmetric sequences simulated different concrete pour sequences. Shims were placed under the shores to very the shore lengths. Twelve load cells measured the resulting loads. Local and global load force amplification ratios were used to quantitatively assess the effect of length variations. It was found that the shoring load was very sensitive to shoring length changes, even though the length change ratio was very small. The amount of variation depends on the structural characteristics and parameters of the system.

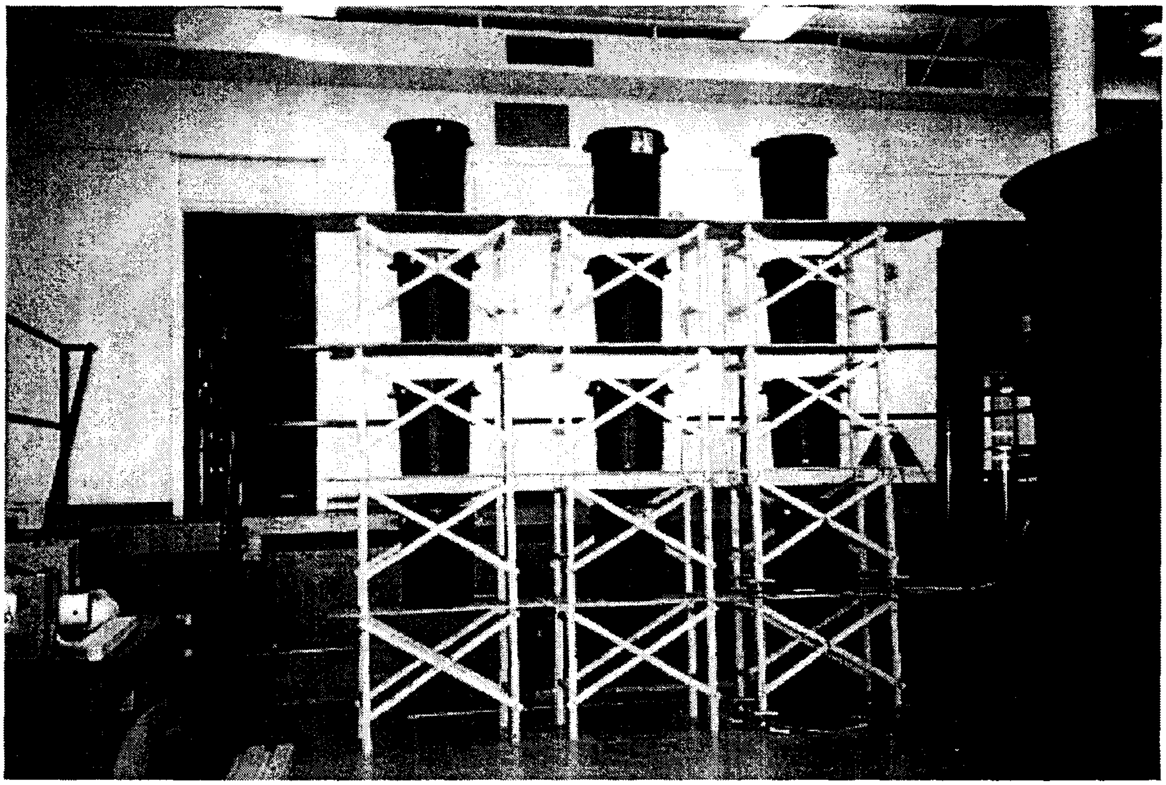

Figure 11.1 Three story, three bay wood model shoring system.

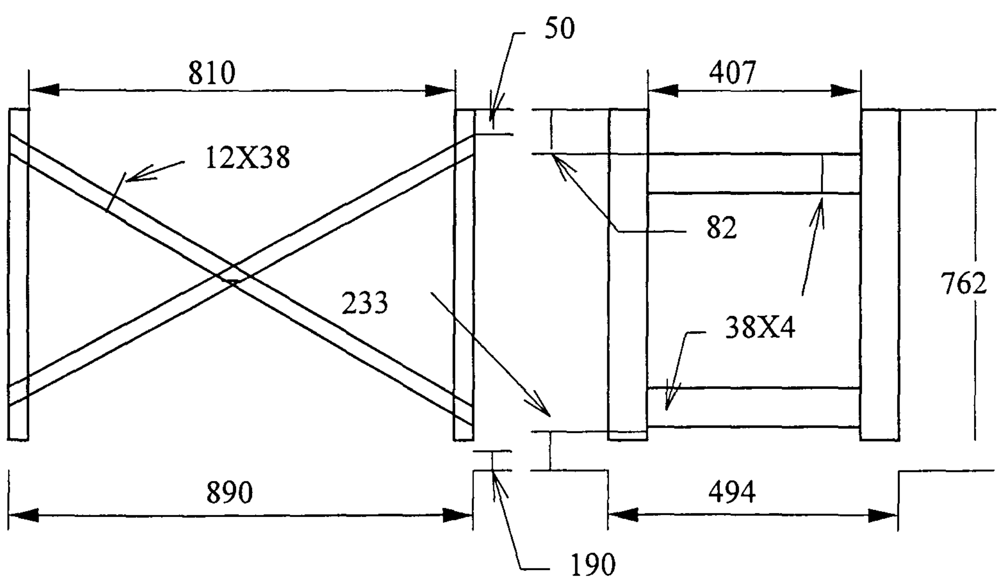

Figure 11.2 Dimensions of wood shoring model in mm.

11.2.2 Description

A simplified model of an approximately 1/3 scale shoring system was fabricated as shown in figures 11.1 and 11.2. Pine wood space trusses with four legs were built, the size of the shore legs were 40x44x762 mm.

The shore loads were measured with eight 3-axis Hitec load cells with a range of +/- 10,000 lb., and four single-axis Geokon load cells with a range of 0 to 300,000 lb. In compression. Vishay 2310 Strain Gage amplifiers were used to boost the level of the signal from each Geokon load cell. Load cell signals were recorded with a Megadac 3108AC, digital data acquisition system.

The buckets were filled with water to simulated concrete pouring. The 20-gallon buckets buckets weighed about 150 lb. when full. Filling each bucket took about four minutes, with a loading rate of about 38 lb. per minute. This was a quasi-static loading, not dynamic.

The test configuration of the instrumentation is shown in Figure 11.3.

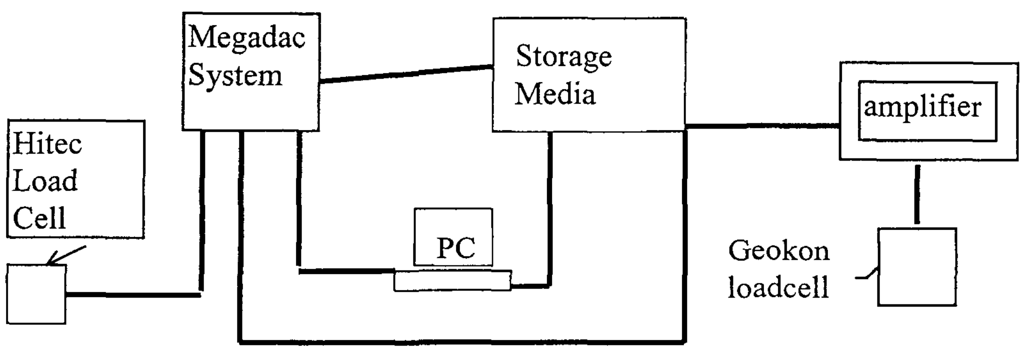

Figure 11.3 Configuration of Instrumentation for Wood Shoring Model

The three story, three bay slab-shoring model without beams is shown in Figure 11.4. The slab was modeled with a 3/4-inch thick plywood board, 4 feet wide by 8 feet long. The three shore bays were evenly distributed on each level. Three buckets were placed just above the center of the shore bay. Eight Hitec load cells were placed at the outer two shore bays while four Geokon load cells were placed at the center shore bay.

In certain tests, the structural properties of the three story, three bay slab-shoring model were varied by stiffening the floors with wood 2x4 beams.

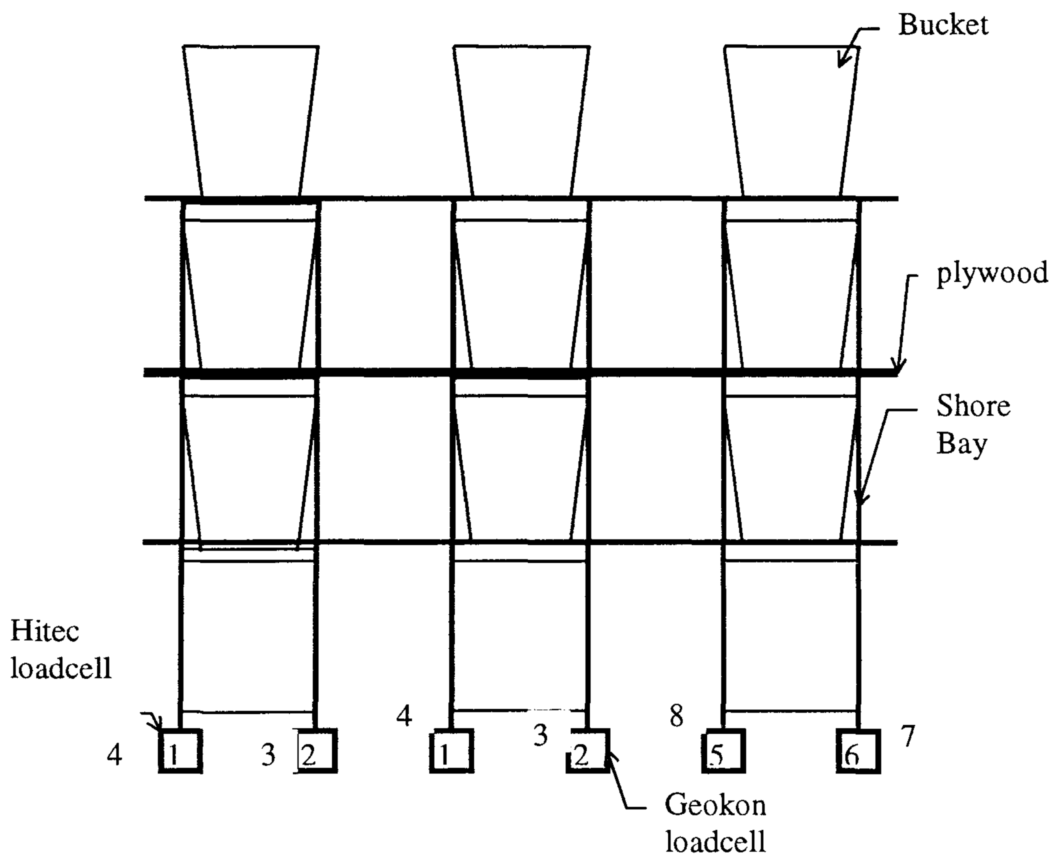

Figure 11.4 Three story, three bay slab-shoring system model without beams.

11.2.3 Test Procedure

Variations in the lengths of the shores were simulated by adding shims to the shore legs on the first level. Three shims were used and specified as Shim #1, Shim #2, and Shim #3 with a thickness of 1.83 mm, 3.23 mm, and 5.68 mm, respectively.

Two different types of tests were conducted. In the first test, the shim was added to the top of the first story shore leg of the shore bay. Then the load was applied by filling the buckets with water. In the second test, the shim was added after the buckets had been filled with water. In this case, a jack was used to raise the plywood so the shim could be added. These two test procedures were used to examine the effects of load sequencing.

In each case, load data was recorded during the entire pour and shim cycle.

11.2.4 Data Processing and Results

The statistics and measures used in the analysis are defined as follows.

1. *Local force amplification ratio* - the ratio of the force increase to the original force.

$$R_L = (F_i - F_o) / F_o \tag{11.1}$$

Where R_L = The local force amplification ratio at a shore leg.
F_i = The new value of the force in the shore leg after changing length.
F_o = The original force value of the shore leg before changing length.

2. *Global force amplification ratio* - the ratio of the force increase to the system maximum force.

$$R_g = (F_i - F_m) / F_m \tag{11.2}$$

Where R_g = The global force amplification ratio at a shore leg.
F_i = The new value of the force in the shore leg after changing length.
F_m = The maximum force of the system before changing length.

3. *Length change ratio* - the ratio of the change in length to the original length.

$$L_r = (L_i - L_o) / L_o \tag{11.3}$$

Where L_r = length change ratio

L_i = the length of the shore after length change.

L_o = the original length of the shore before length change.

4. *Local sensitivity* - the ratio of the local force amplification ratio to the length change ratio.

$$S_L = [(F_i - F_o) / F_o] / [(L_i - L_o) / L_o \\ = R_L / L_r \tag{11.4}$$

Where S_L = local sensitivity at a particular shore.

R_L = the local force amplification ratio.

L_r = the length change ratio.

5. *Global sensitivity* - the ratio of the global force amplification ratio to the length change ratio.

$$S_g = [(F_i - F_m) / F_m]/ [(L_i - L_o) / L_o] \\ = R_g / L_r \tag{11.5}$$

Where S_g = global sensitivity at a particular shore.

R_g = the global force amplification ratio.

L_r = the length change ratio.

Figure 11.5 shows the data recorded while three shims were placed sequentially onto the shore leg over Hitec load cell #2, after filling the nine buckets with water, and without stiffening beams between the plywood and shore bays. In the figure 11.5, there are five time segments for each load cell force curve. The first and last sections are the state of with no shims. The second, third, and fourth sections from the left correspond to shim #1, #2, and #3, respectively. It is apparent that that the force in Hitec loadcell #2 increased by about 60%. However, the maximum force of the slab-shoring model occurs at Geokon loadcell #1 when no shims are used. When shim #1 is placed onto the shore leg above Hitec loadcell #2, the maximum force occurs at the Hitec loadcell #2. The value is about 310 lb. for the model system. Therefore, the total force is changed very little for the whole model system. When shim #3 is put onto the leg, i.e. the shore length at Hitec loadcell #2 on the first level is increased 0.74%, the maximum force increases by about 50% to the normal maximum force for the model system.

In Figure 11.6 the shims are placed onto Geokon loadcell #1, this is where the maximum force of the system takes place. Here, the maximum force increases by about 45% while the leg length increased by 0.24% and about 100% while the leg length is increased 0.74%.

Figure 11.7 shows the data gathered while adding shims sequentially onto Hitec loadcell #3 when the system was holding nine buckets of water. The local force amplification ratio and local sensitivity are shown in Figure 11.8 and Figure 11.9. The global force amplification ratio and sensitivity are shown in Figure 11.10, and Figure 11.11.

Table 11.1 contains the data in Figure 11.6 for the sensitivity and force amplification ratio due to shore length change while adding shims above Geokon loadcell #1. Table 11.2 is the computation of global force amplification ratio and global sensitivity while adding shims above Hitec loadcell #3.

Leng. Rat.	loadz 1 lb.	loadz 2 lb.	loadg 1 lb.	loadg 2 lb.	loadz 5 lb.	Loadz 6 lb.	Loadz 4 lb.	loadz 3 lb.	loadg 4 lb.	loadg 3 lb.	loadz 8 lb.	loadz 7 lb.
0	128.	32.91	296	241.3	129.4	106.9	125.1	157.6	232.1	216.1	144.6	137.5
0.24%	123	-13.4	428.5	156.4	136.1	113.1	126.8	138.3	241.6	228.9	143.5	140.1
0.42%	98.3	-23.7	495.6	109.9	137.7	112.9	139.8	121.6	244.8	226.9	145.6	140.2
0.74%	53.9	-24.2	589.8	98.71	100.6	103	164.4	107.8	233.5	221.2	139.6	171.6
0	180.	56.38	213.4	237.4	169.6	127.5	78.92	137.9	314.4	243.7	112.1	106.8
Global force amplification ratio												
Leng. Rat.	loadz 1 lb.	loadz 2 lb.	loadg 1 lb.	loadg 2 lb.	loadz 5 lb.	Loadz 6 lb.	Loadz 4 lb.	loadz 3 lb.	loadg 4 lb.	loadg 3 lb.	loadz 8 lb.	loadz 7 lb.
0.24%	-0.58	-1.04	0.448	-0.35	-0.41	-0.51	-0.45	-0.40	0.041	0.059	-0.01	0.019
0.42%	-0.67	-1.08	0.675	-0.54	-0.41	-0.51	-0.40	-0.48	0.055	0.05	0.007	0.019
0.74%	-0.83	-1.08	0.993	-0.59	-0.57	-0.56	-0.29	-0.54	0.006	0.023	-0.04	0.248
Global sensitivity												
Leng. Rat.	loadz 1 lb.	loadz 2 lb.	loadg 1 lb.	loadg 2 lb.	loadz 5 lb.	Loadz 6 lb.	Loadz 4 lb.	loadz 3 lb.	loadg 4 lb.	loadg 3 lb.	loadz 8 lb.	loadz 7 lb.
0.24%	-244	-436	186.6	-147	-172	-214	-189	-169	17.1	24.6	-3.25	7.971
0.42%	-159	-257.	160.6	-129.	-96.8	-122	-94.7	-113	13.07	11.87	1.6	4.632
0.74%	-111	-146.	134.1	-79.8	-76.5	-75.1	-39.4	-72.4	0.858	3.154	-4.70	33.5

Table 11.1 Computation of the global force amplification ratio and sensitivity.

Lr	loadz1 lb.	Loadz2 lb.	loadg1 lb.	loadg2 lb.	loadz5 lb.	Loadz6 lb.	Loadz4 lb.	loadz3 lb.	loadg4 lb.	loadg3 lb.	loadz8 lb.	loadz7 lb.
0	210.2	101.4	238.6	153.1	129.1	205.8	23.76	112.6	381.6	333.2	135.6	38.4
0.24%	162.5	114.2	249.3	178.7	136.3	175.4	-3.802	269.5	270.4	321.6	137.1	65.64
0.42%	162.8	83.56	265.1	199.4	138.9	160.1	-43.34	396.2	218.9	297.5	146.8	81.13
0.74%	141.2	57.92	280.1	224.2	150.4	137.4	-43.34	479	180.7	245.6	152.1	98.46
0	131.7	162.1	264.9	185.5	113.6	163.8	137.8	24.52	338.9	320.9	158.4	80.08
Calculation for the global force amplification ratio												
Lr	loadz1 lb.	Loadz2 lb.	loadg1 lb.	loadg2 lb.	loadz5 lb.	Loadz6 lb.	loadz4 lb.	loadz3 lb.	loadg4 lb.	loadg3 lb.	loadz8 lb.	loadz7 lb.
0.24%	-0.574	-0.701	-0.347	-0.532	-0.643	-0.54	-1.01	-0.294	-0.292	-0.035	0.011	0.709
0.42%	-0.573	-0.781	-0.305	-0.477	-0.636	-0.581	-1.114	0.038	-0.426	-0.107	0.082	1.113
0.74%	-0.63	-0.848	-0.266	-0.412	-0.606	-0.64	-1.114	0.255	-0.526	-0.263	0.122	1.564
Calculation for the global sensitivity												
Lr	loadz1 lb.	Loadz2 lb.	loadg1 lb.	loadg2 lb.	loadz5 lb.	Loadz6 lb.	loadz4 lb.	loadz3 lb.	loadg4 lb.	loadg3 lb.	loadz8 lb.	loadz7 lb.
0.24%	-239.2	-291.9	-144.4	-221.5	-267.8	-225.1	-420.8	-122.4	-121.5	-14.53	4.579	295.6
0.42%	-136.5	-186	-72.72	-113.7	-151.4	-138.2	-265.1	9.085	-101.5	-25.5	19.61	265
0.74%	-85.12	-114.6	-35.94	-55.72	-81.87	-86.48	-150.5	34.47	-71.15	-35.54	16.48	211.4

Table 11.2 The computation of Global force Amplification Ratio and Sensitivity

11.2.5 Discussion

From the force amplification ratio it is apparent that the slab-shoring system model is very sensitive to shore length variation. The global force amplification ratio is as large as 100% when the length change ratio is only 0.74%.

The slab-shoring system is usually set up and adjusted by hand in the construction field sites. It is an unavoidable consequence that there exist initial uneven lengths in the slab-shoring system, i.e. a shore length variation. According to these tests, the shore force amplification ratio depends on the location of the shore and the length change ratio, as well as the structural parameters of the slab-shoring system. In the worst case scenario, the uneven initial loads may results in a local structural failure and cause a progressive global structural collapse.

On the other hand, the uneven initial length also affects the load routine. From this model test, the maximum force amplification ratio can reach 25% of the normal maximum force.

In summary, the uneven initial length of shores in the slab-shoring system belongs to the geometry error. The distributions of shore force are very sensitive to length variations. This matter warrants deeper analysis and more field-testing.

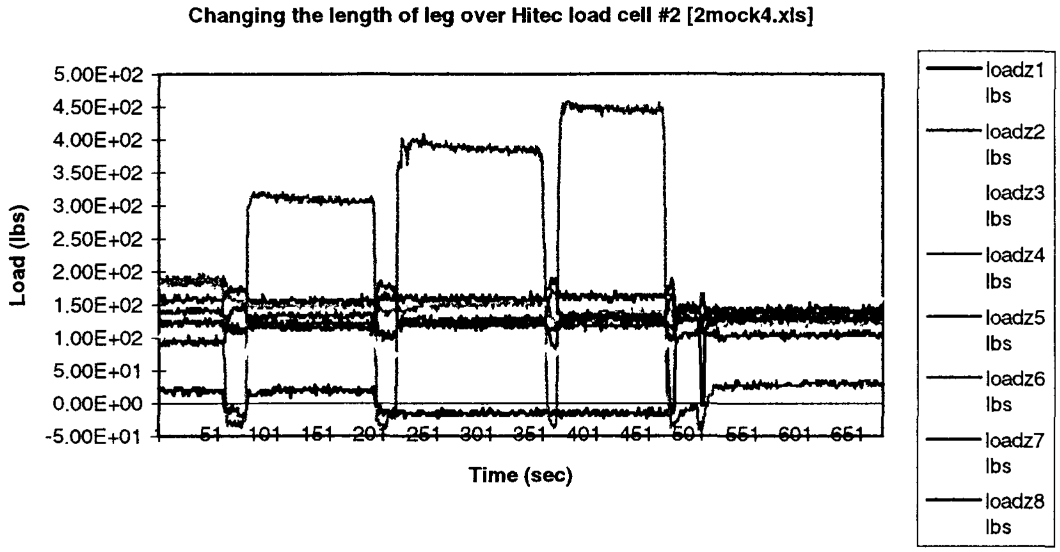

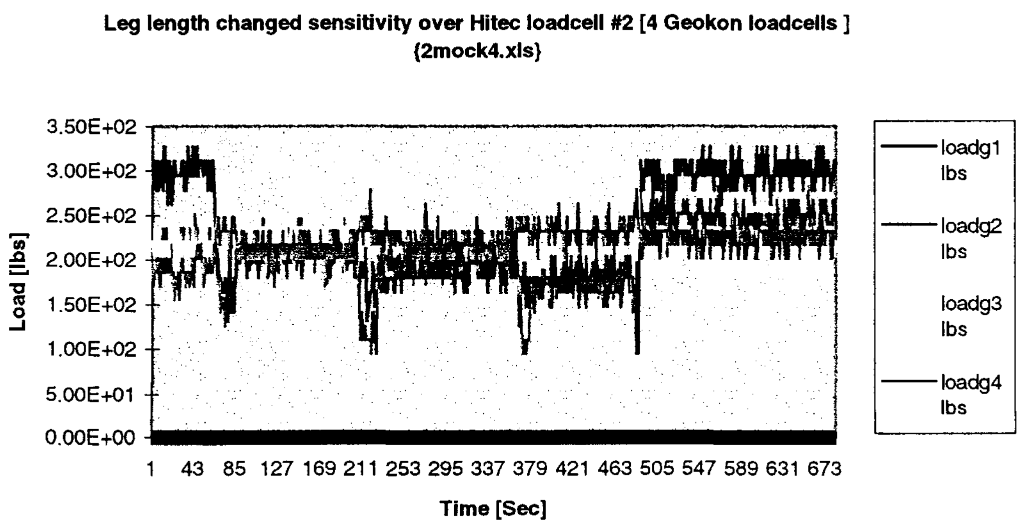

Figure 11.5 Test data of shore forces while adding shims above Hitec loadcell #2

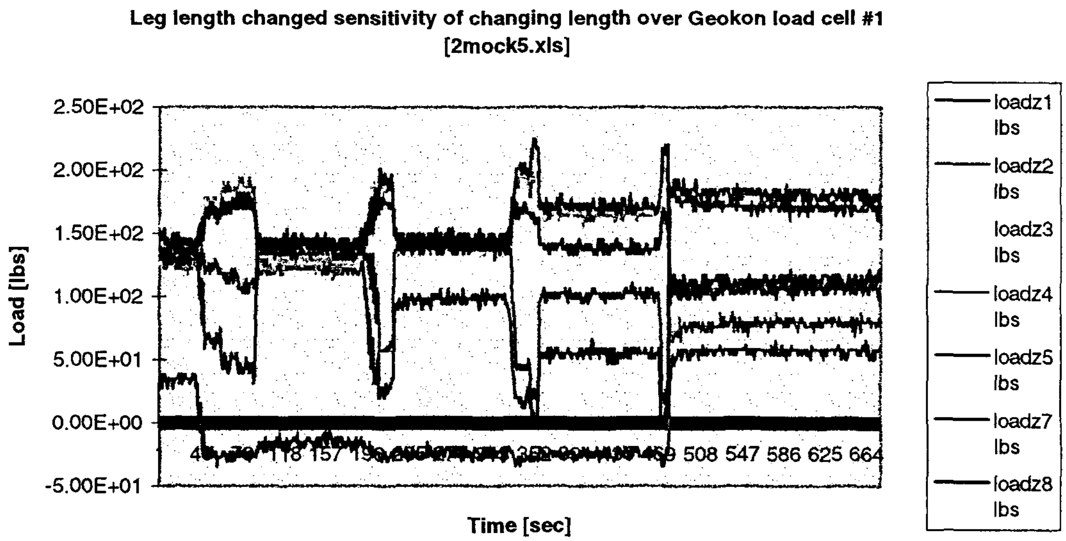

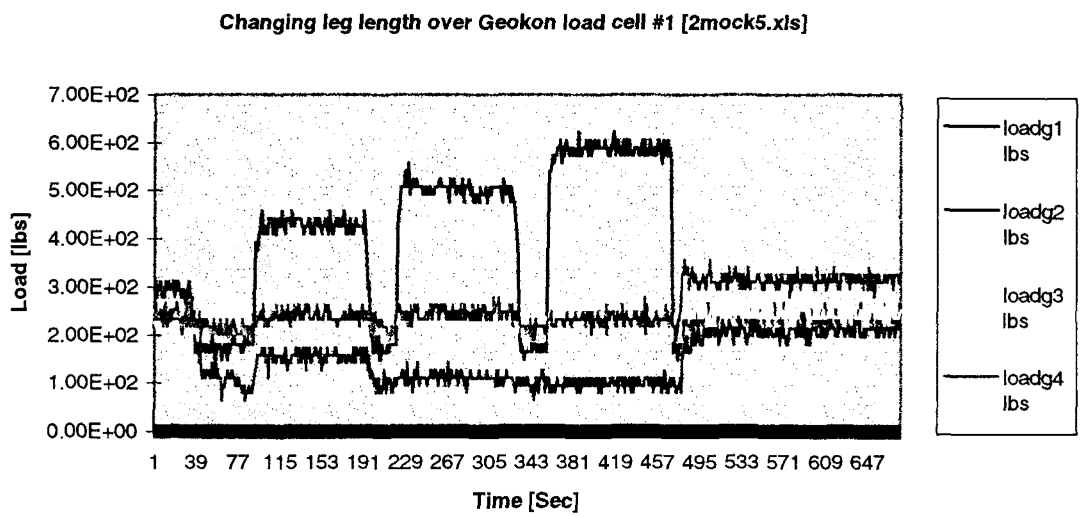

Figure 11.6 Test data while adding shims above Geokon loadcell #1.

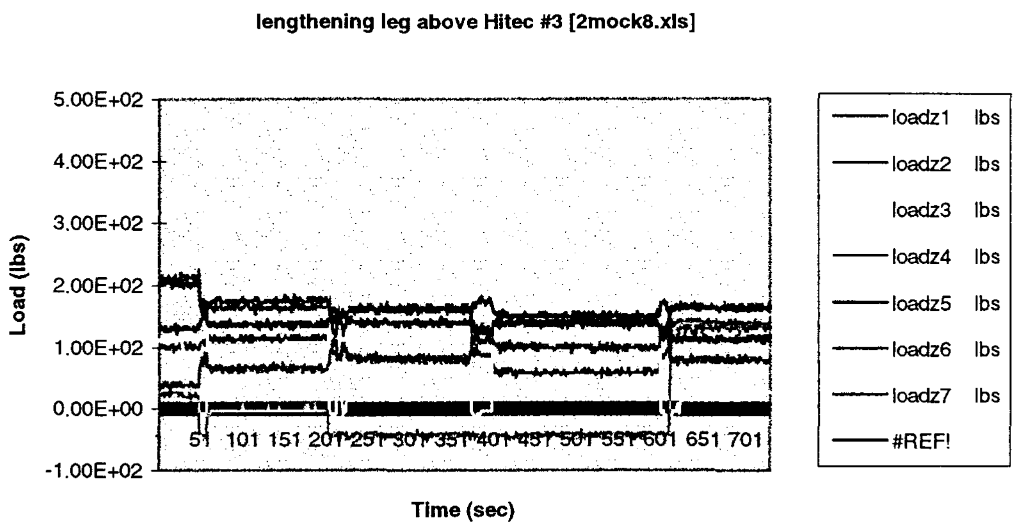

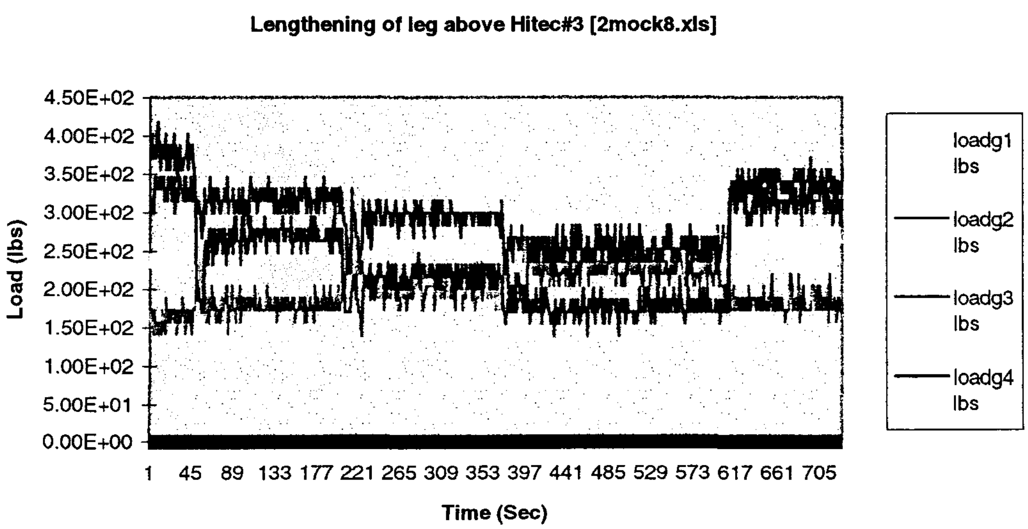

Figure 11.7 Test data while adding shims above Hitec Loadcell #3.

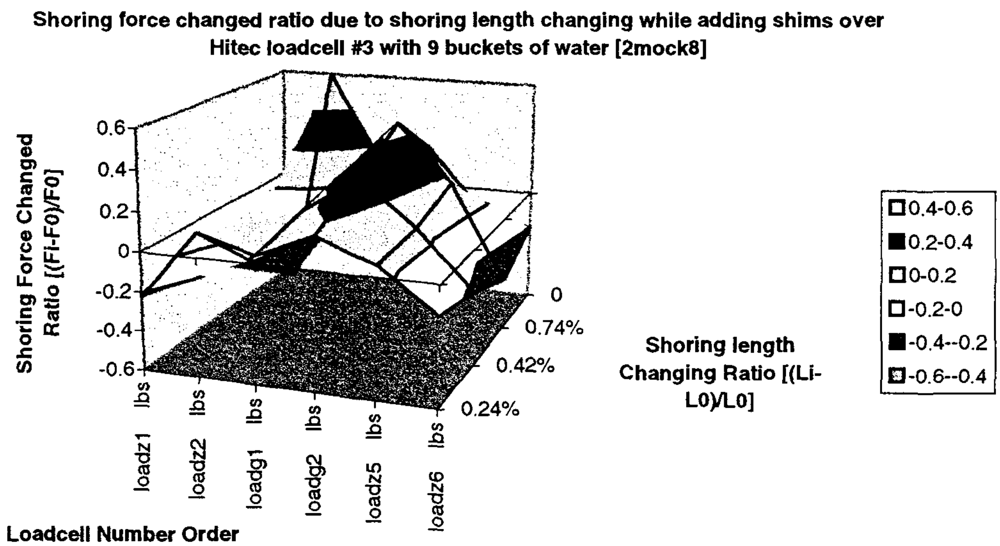

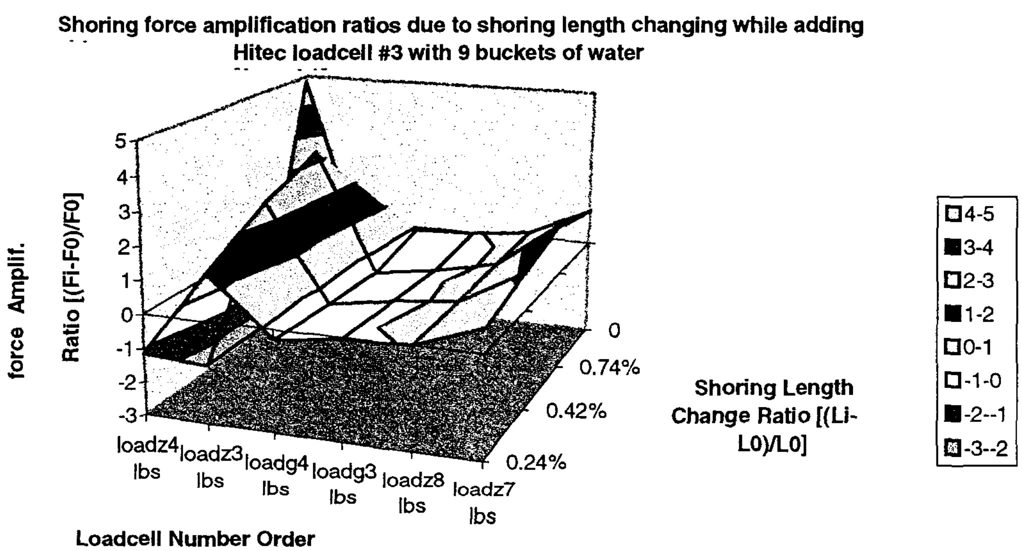

Figure 11.8 Local force amplification ratio while adding shims above Hitec loadcell #3.

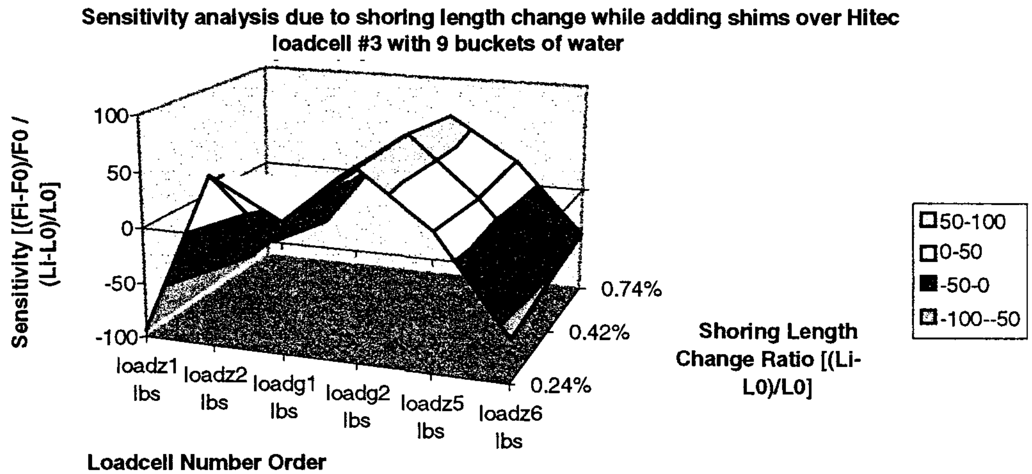

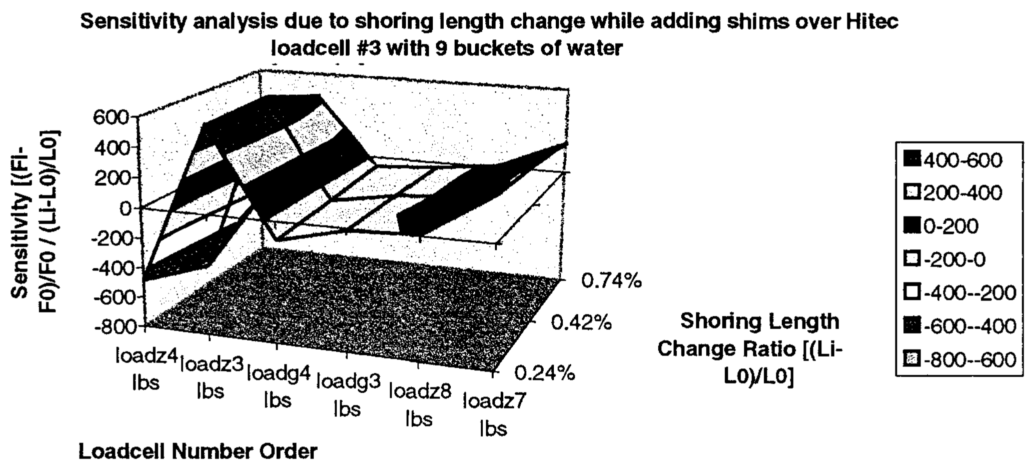

Figure 11.9 Local sensitivity while adding shims above Hitec loadcell #3

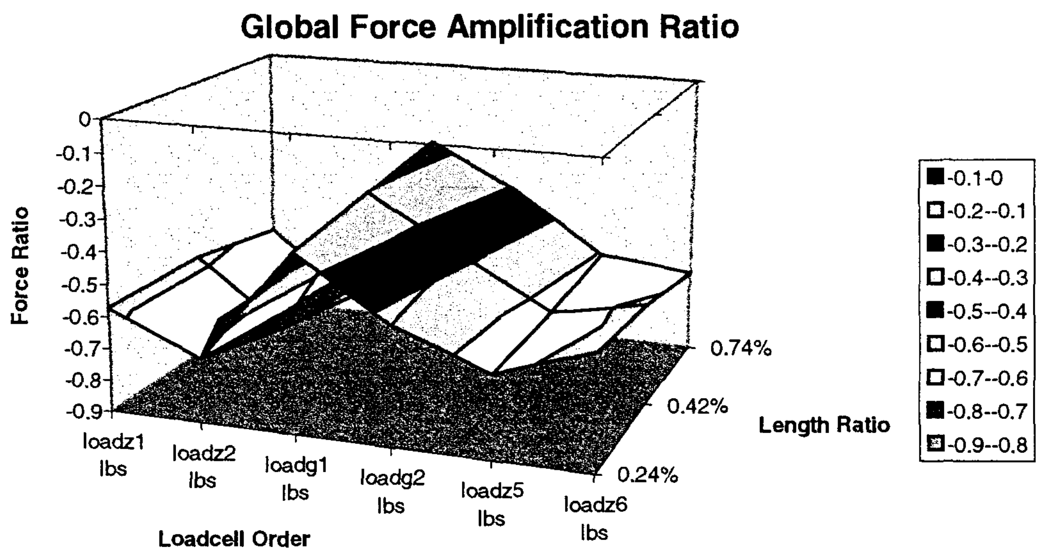

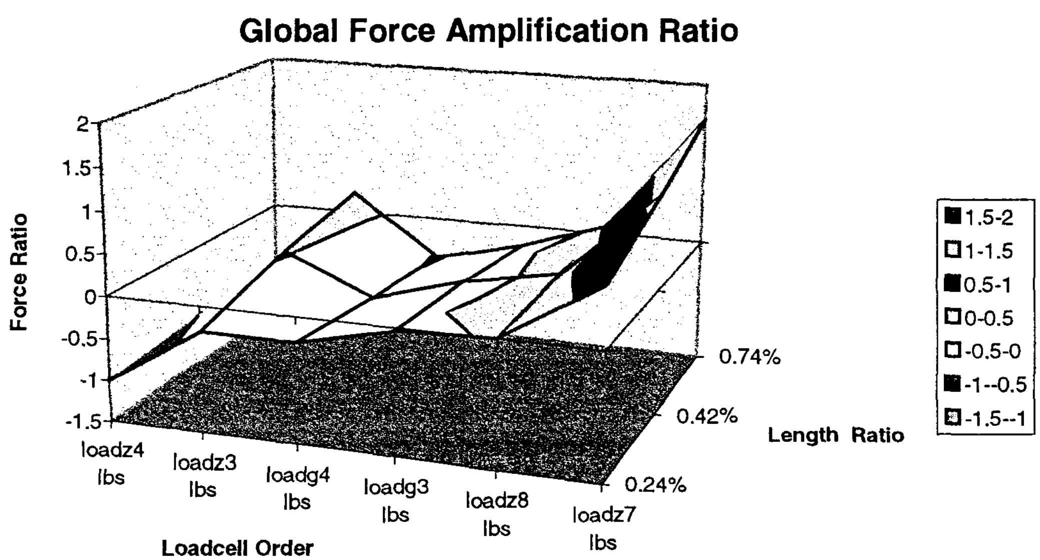

Figure 11.10 Global Force Amplification Ratio while adding shims above Hitec Loadcell #3 with 9 buckets of water without beams

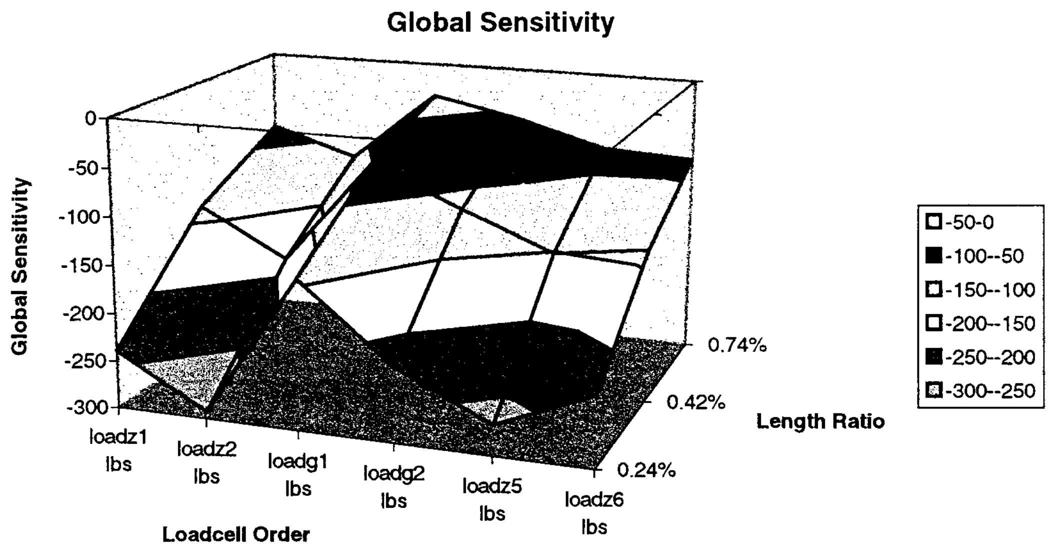

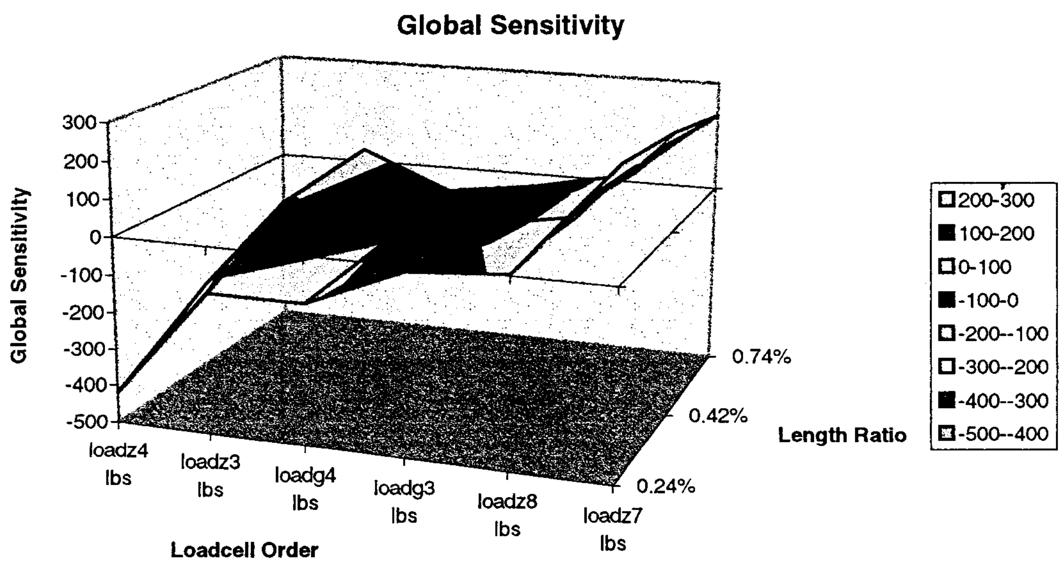

Figure 11.11 Global Force Sensitivity while adding shims above Hitec loadcell #3 with 9 buckets of water without stiffening beams

11.3 Uplift and Soft Footing Model Test of Slab Shoring Structural System

11.3.1 Introduction

Two causes of structural collapse during concrete construction are the actions of uplift and soft footings under shores. Uplift is where a large load on one point of the shoring system causess a negative bending moment in the formwork, which results in a vertical uplift of a different section of the formwork. The uplifting can cause an udetected shifting and weakening of the shoring system, which can lead to instabilities in subsequent construction operations. Soft footings occur when the foundation (usually earthen) under a particular location in the shoring system is unable to support the structure above it. The soft footing can cause a variety of problems that range from load distribution to other shores, excessive deformation of the formwork to progressive collapse of the structure.

In this study, the effects of uplift due to structure deformation and soft footings have been studied. Experimental wood slab-shoring system model tests have been completed to simulate these phenomena, which cannot be measured and made in field construction sites. Filling buckets with water in different sequences simulated different load application sequences in the concrete pouring. The effects of soft footings on the slab-shoring system has been studied and compared to firm footings using the experimental model test to simulate the field conditions.

11.3.2 Experimental Description

(a). Uplift Test

In this test a one level, two bay slab and shoring system was simulated with the model shoring system shown in Figure 11.1. Eight Hitec loadcells were used to support the eight legs of the two wood shoring models and measure the forces of the model legs. Three dial indicators were mounted at the centerline of the plywood and used to measure the displacement of the plywood board. The test used two, four, and five 20-gallon buckets full of water to simulate applied loads.

Several sets of tests with 2, 4 and 5 buckets of water were performed in order to obtain the details of the relation between the load and uplift. It took about 4 minutes to fill each bucket with about 75 kilogram of water. In order to measure the force data in Hitec loadcells during the entire test, pre-loads were placed on the plywood over loadcells #5, #6, #7, and #8. The uplifts were reduced at the cost of force reading on all the loadcells.

(b). Soft Footing Test

In the soft footing test, the test configurations consisted of four bay one story and three story models. On each story, four 20-gallon buckets were placed on the top of the plywood and centered over each bay. Eight Hitec loadcells were placed below the shore legs of the outer two bays. For this configuration, referred to as Hitec loadcell configuration #1, two different material pieces of foam (#1 and #2 was respectively) were placed under Hitec loadcell #2 to simulate the soft footing. The material of foam #2 was softer than that of foam #1. Symmetric and asymmetric sequences of water loading were used for both the one-story and three-story level system. In the tests, two 2 x 4 inches wood beams were placed on the first level in order to simulate a shoring system with lateral formwork beams and stringers.

(c). Firm Footing Test

For a firm footing test, the setup was the same as in the soft footing test except that firm (concrete slab and plywood shim) footings were used. Test data during symmetric and asymmetric loadings were measured to provide a control experiment and to determine the effect of the loading sequence.

11.3.3 Measurement Instrumentation

All of these model tests used eight Hitec three-axis load cells for shore load measurement. The load data was acquired with a Megadac multi-channel data acquisition system and stored on rewritable optical disk media. A PC served as the system controller and as a post processor of the data.

11.3.4 Experimental Results and Discussion

(a). Uplift Test

The objective of the uplift test was to verify that uplift exists due to structural deformation under somewhat realistic conditions. The dial indicator readings with 4 and 5 buckets of water appear in Table 11.3. In this table, the displacements of the points were measured with dial indicators that were placed between the model structure and the laboratory reference frame. Negative dial indicator readings mean the direction of displacement was down toward the ground. The positive values of displacement indicate uplift at this measured point. The uplift displacement values were rather small. This is largely due to the use of pre-load weights on the plywood over Hitec loadcells #5-8 so as to ensure a continuous measurement of changes in axial load due to uplift.

Figures 11.12 and 11.13 are the time histories of loading while filling the buckets with water.

Load Case	Four Buckets			Five Buckets		
Indicator No.	Unloaded	Loaded	Displace	Unloaded	Loaded	Displace
Dial # 1	-0.0368	-0.2528	-0.216	-0.0412	-0.2974	-0.2562
Dial # 2	-0.4241	-0.3693	0.0548	-0.4161	-0.3263	0.0898
Dial # 3	-0.2918	-0.3064	-0.0146	-0.339	-0.3591	-0.0201

Table 11.3 Uplift Displacement of One Level Story Model System (units = inches).

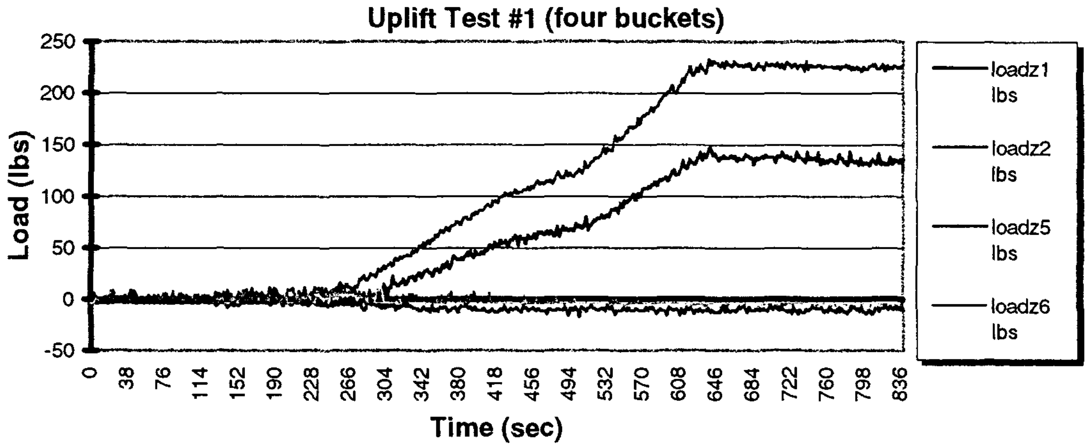

Figure 11.12 One level model uplift test with 4 buckets of water

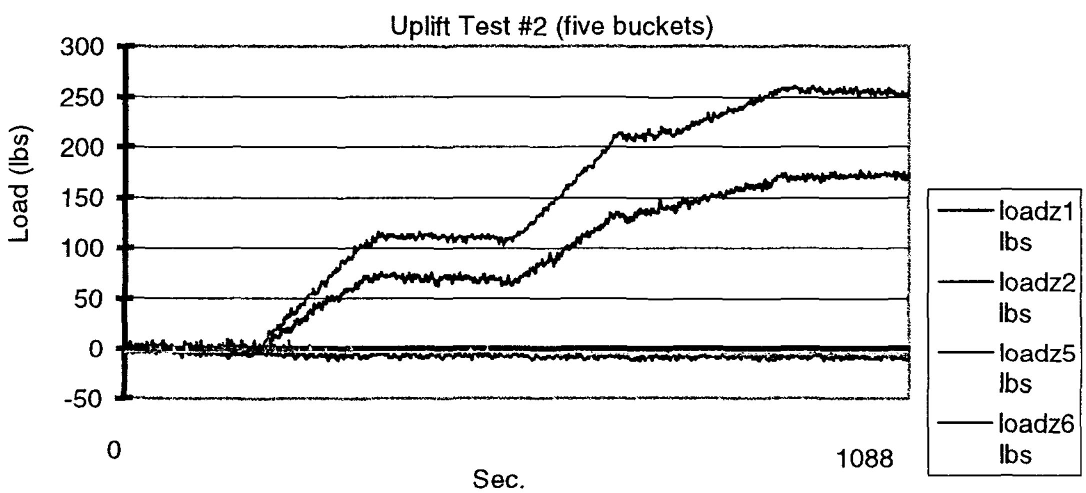

Figure 11.13 One level model uplift test with 5 buckets of water.

(b). Soft Footing Test

The soft footing test was setup to simulate a situation where certain shore legs of a slab-shoring system are supported on a comparatively softer base than the other shores of the slab-shoring system. The hypothesis was that the vertical force distribution of the shores would be changed by the presence of the soft footing. The results indicated that usually the presence of a soft shore would increase the loads in the shores near the shore with a soft footing, but that the load on the shore with the soft footing would decrease. The load distribution was found to be sensitive to load application sequence. The test data indicated that the maximum force of the shoring system when loaded asymmetrically was about 20% greater than that seen when the system was loaded symmetrically.

11.4 Lateral Stability Test of Slab and Shoring System

11.4.1 Introduction

Since most failures of reinforced concrete structures occur during construction, it is important to understand the mechanics of slab shoring systems, in particular the issues related to stability. The slab shoring system can become dangerously unstable in overloading conditions. It can become laterally unstable with the combination of construction loads, wind loads, uneven live loads, etc. Lateral tilt and deformation often precede these lateral instabilities. If the tilts and loads experienced by the slab shoring system are monitored, then it may be possible to prevent failures by providing an early warning when changes in the loads or the tilt angle of the system members exceed certain levels.

One of the key issues in designing a slab shore monitoring system is to determine what loads and tilt angles are critical indicators to the structure's stability. To this end, a shoring system model was built and tested to failure. The system was designed to model closely the way that an actual shoring system and structure behaves. As in a slab system, the applied load must be able to move with the structure. This rules out using any sort of press type of system to apply the load. This is because in a press type of system, the load could be applied at a constant rate until the model system begins to deform, and when the system deforms the load applied by the press will decrease. In order to get around this problem it was decided to use a system where the load was placed directly on the model system with gravity by using weights.

11.4.2 Experimental Description

For simplicity a single slab with four shoring members was tested. The design was constrained by a few specific parameters. A principal constraint was the available load cells. These were Hitec load cells, which can take measurements in three directions. In deciding how to best use the Hitec load cells, consideration was given to their sensitivity, and how much applied load would be necessary to obtain accurate measurements from the load cell. It was concluded that the model system must be capable of holding loads up to at least 1600 pounds. Another constraint was the amount of weight that could safely be applied to the model. The steel weights were used to simulate the weight of the concrete. With these considerations, a steel frame was constructed to model a concrete slab, and a sheet of plywood was fitted onto the frame to provide a platform on which the weights could be placed.

The selection of the model-shoring member was somewhat more complicated. The first concept considered would have used PVC tubing to simulate a steel tubing type of shoring member. However, PVC was found to be too flexible and tended to shatter after a certain amount of deflection. It was also found that a bracket was necessary to keep the PVC tube in place so that the model structure would stand on its own. Some other ideas included wooden dowels, steel pipe, or rebar. After completing testing with each type of model, it was decided that a shoring member made of reinforcing bar would best simulate the situation in a repeatable and controllable manner. In order to monitor the loads and tilt angles of these shoring members, data from the load cells and tilt sensors was collected using two data acquisition systems. One data acquisition system, the Megadac, was used to record data from the load cells beneath each of the shoring members and a tilt sensor mounted on one of the shoring members. The second data acquisition system was a wireless system from Fluke. It was used to record the weight of the applied load and the tilt in a shoring member opposite the first one.

A chain hoist raised and lowered the weight on and off of the model slab. The hoist was mounted on a trolley that rode on a large steel I-beam. The I-beam was used to support the entire model system in the case of collapse, as the safety cables were all attached to the beam.

Once set up, the model slab was attached to steel cables hanging from the ceiling so that if the system collapsed, the slab would not fall all the way to the floor, but rather would be caught by these "safety cables" a few inches before it hit the ground (see Figure 11.14). The primary reason for using the cables was for safety purposes. The cable system also prevented damage to the slab system or the load cells. The basket that contained the loading weights was also attached to safety cables so as to prevent all the weights from falling to the ground uncontrollably, but also allowed enough cable length for the weight basket to follow the slab until the collapse was well underway.

The weight basket was designed to contain the weights as well as the remote acquisition part of the Fluke wireless logger. There was a load cell mounted to the bottom of the weight basket that fed a signal into the remote system. The signal from a tilt sensor was also fed into the remote system. The tilt sensor was attached to one of the shoring legs. The reason for using this remote system was to show that it would be possible to monitor a shoring system with a wireless data acquisition system. If this approach was successful, the sensing units could be mounted on different shoring members and the data could be sent via telemetry to a base computer which would monitor all the units for unsafe conditions. Using a wireless system would prevent data loss due to cable damage, and reduce the labor required to install the system.

In the following figures, the different models used for testing are shown. In the first model, Figure 11.14, the four shores were inserted into brackets that were constructed specifically for this test. When inserted into these brackets (see Figure 11.15), the shores were essentially cantilevered at both the top and bottom. The effective length of the shores in this model is 30 inches. This type of model does not simulate the end conditions of an actual shore very well. The second type model is shown in Figure 11.16. Steel plates were welded to each end of the four shores (rebar). New inserts were made for the previously used brackets, with plates welded on the top of them. This allowed for the plates on the shores to match up directly with the plates on the inserts and the plates could be bolted together (see Figure 11.17 Config. A). After running a few tests with the plates bolted together, it was decided that this was actually just simulating the same cantilevered situation as in the first set up. In order to model a real shore more accurately, it was decided just to pin the plates together loosely (see Figure 11.17 Config.

B). After doing some testing with this set up, diagonals were also added to the model structure (see Figure 11.18).

The two-story model is shown in Figure 11.18. Simply adding another level on top of the first one created this model. Four more load cells were placed under the shores on the upper level, and one of the tilt sensors was moved up to the second level. Note that this model is shown with diagonals installed on each level. The diagonals provide the system with much more lateral stability and simulate a shore system in which diagonal bracing exists. The length of the rebar shores is shortened slightly to 25 inches for the two-story structure, as shorter legs will provide a little more stability. Several tests were performed in which the diagonals were in place. In order to establish the effectiveness of the diagonals, testing was also done while diagonal bracing was only partially installed, and when there was no diagonal bracing at all.

Each of the different model systems described previously was tested extensively under different loading situations. Tests were performed on each model in which:

1.) A known vertical load was placed on the model slab by lowering the weight basket onto the slab and putting enough slack in the chain and the safety cables so that when the system collapsed, the weight would be part of the system. Once the weight was at rest on the slab, a small side load was applied to the system. Adding 5 or 10 pound plates to the side load basket then increased this side load. The side load was increased gradually until the system collapsed.

2.) A known side load was applied to the model system, and then a vertical load was added to the system and stepped up by adding plates until the system collapsed. Adding 5, 10, and 45-pound plates to the exterior weight studs on the weight basket increased the vertical load. During each test, all of the acquisition equipment was recording data. Most of the tests were also video taped.

3.) Tests were also performed with the diagonal bracing in place. For this case, the system was not loaded to collapse, as this would have taken a great deal more weight than was available.

4.) An offset load was applied for a few of the tests, so that any changes in the loads and tilts could be observed.

5.) Most of these tests were also performed on the two-story structure. The only other variation that was added was that the side load was applied at two different places. For half of the testing with the two-story structure, the side load was applied at the slab on the first level. For the other half of the tests, the load was applied at the slab on the top level. Note that no tests were performed on the two-story structure when no diagonals were present. The situation with no diagonals on the two-story structure is too unstable and too dangerous for this type of testing.

6.) One other test that was performed was a test in which the failure of a single shoring member was simulated. This was done by shortening one of the shores and then placing an aluminum soda can under that shore. This test was done in order to demonstrate the shifting of loads and tilts in the case of a shore failure.

11.4.3 Results

The results obtained from these tests were quite consistent throughout. This was independent of whether the vertical load was applied first or the side load was applied first, and then varied with either the vertical load, or the horizontal load. The data and test matrix are summarized in Tables 11.4 – 11.6

Figure 11.19 is a sample of the data obtained from a one-story model system, with plates welded to the shores and pinned to the brackets for feet. Figures 11.20 – 11.25 are samples of data from other configurations. For figure 11.19 sharp changes in the data occur at time ~274 seconds, this is the point where the structure collapsed. As can be seen by examining the graph of the tilt sensor data, the critical angle of collapse was about 5.5 degrees. But 5.5 degrees would not be the angle at which a warning would be issued. A danger warning would have to be issued much earlier than this in order to allow time for both finding and fixing the problem, or evacuating the structure. Therefore a warning signal would have to be sent at a very small tilt angle such as 1 or 2 degrees.

A factor that becomes quite obvious when the diagonal supports are added to the structure is that it causes a shift in the distribution of the loads as the system is loaded. When a side load is applied to a shoring system with diagonals present, the vertical loads on the shoring member's shift to the members positioned closest to where the side load is being applied. This suggests that there are in fact two conditions that should be monitored: 1. any major *shifts in loads*, or 2. any *shifts in the tilt angles*. Also noteworthy in Tilt/Collapse Test #42, is the fact that even with the diagonals present there is a noticeable, though small, change in the tilt angles of the shoring members as the system is loaded.

The pictures in Figures 11.26 – 11.31 show the process of collapse. Figure 11.26 shows a one-story system without diagonals, in the process of collapsing. Figure 11.27 shows a case of offset loading on the single story structure with diagonals. Figures 11.28-11.31 show the two-story system. As the system collapsed, frames were taken to show how the structure behaved as it collapsed. Note that as the system collapsed, the upper level shifted to the right as the load was pulling it that way, while the lower level shifted to the left.

An examination of different critical tilt angles for different test set-ups and loading situations indicates that the data are quite consistent for similar testing situations. For the case in which the pinned joint is used, the joint that best represents actual shoring, the system collapses at a tilt angle of around 4 degrees. But for the case in which diagonals are present, the structure does not collapse. If the system were loaded to collapse for the case with diagonals, there would not be a lot of change in the tilt angle before collapse because the diagonals would not deform very much before they failed in tension. For the case of a two story structure, the few times it was brought to collapse, the critical angle was right around 5 degrees.

For the other set up in which the joints were representative of a cantilevered beam, both with the bolted plates, and the bracket inserts, the critical angle was repeatedly around 7 degrees. This indicates that for similar structures, the critical angles of collapse may be similar.

11.4.4 Discussion and Conclusions

In an attempt to better understand the mechanics of a slab shoring system and the issues related to stability in particular, a model system was designed for testing purposes. The model system allowed for variations in loading conditions and was designed to model several different shoring situations. Shoring situations modeled included: a. A single story shoring system, b. A two story shoring system, c. A shoring system in which diagonals are present, d. A shoring system in which there are no existing diagonals. Sensors were included in the system so that the loads existing on each shoring member could be monitored and the tilt angles of two representative shores were also monitored. The model system was then loaded to collapse so that critical loads and tilt angles could be determined for the point at which the system became unstable.

As would be expected, the testing showed that a system that includes diagonal supports was much more stable than a system without diagonals. Diagonals may, however, mask the critical tilt angles of a system because the diagonals prevent tilt unless the diagonals yield or buckle, therefore making the monitoring of the loads more important. In the case where diagonals were used, a large shift in the vertical loads on the system was observed. This suggests that a dangerous situation was occurring. For a slab shoring system with diagonals present, monitoring the loads on the shores would be useful in providing an early warning for dangerous situations.

For a slab shoring system which does not include diagonals, monitoring the tilt angles of the shores could be useful in providing an early warning for dangerous situations. Something that is not completely clear from this testing however, is the critical tilt angle of a shoring member at which the system becomes unstable or dangerous. As can be seen in the results, the angle at which the system collapses is fairly repeatable, but it is at some angle before that, that the system becomes unstable. This may be an area of interest that could be further researched.

As shown in the results of this testing, the monitoring of tilts and loads experienced by the slab shoring system would in fact be helpful in preventing failures by providing an early warning system when changes in the loads, or tilt angles of the system members exceed certain limits.

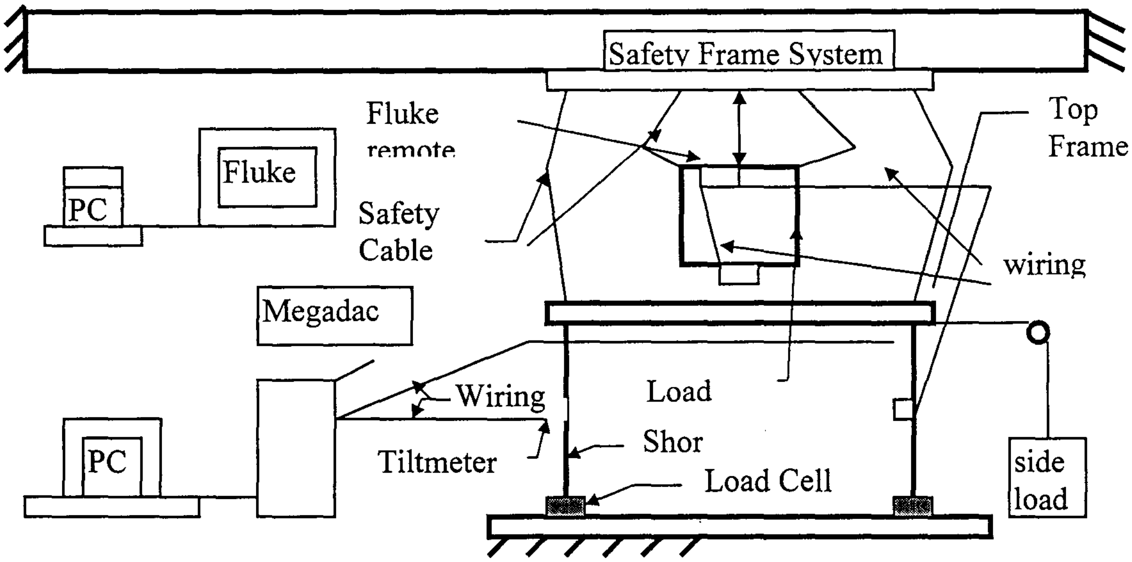

Figure 11.14 One story model shoring system.

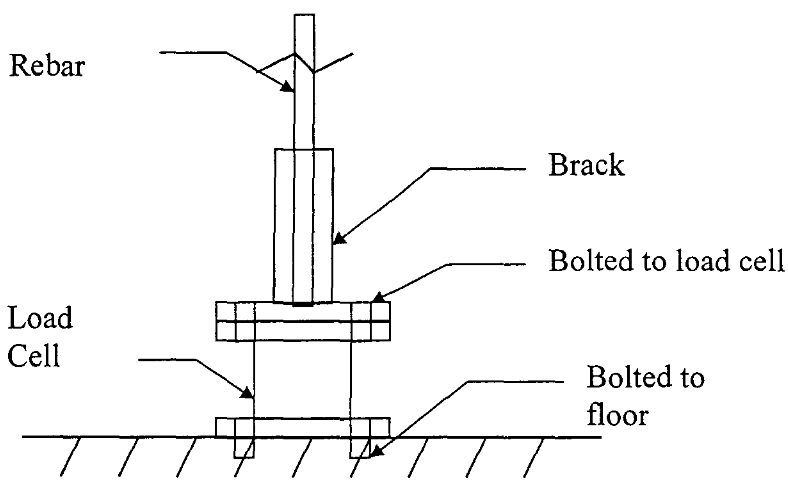

Figure 11.15 Illustration of shore in cantilevered type bracket.

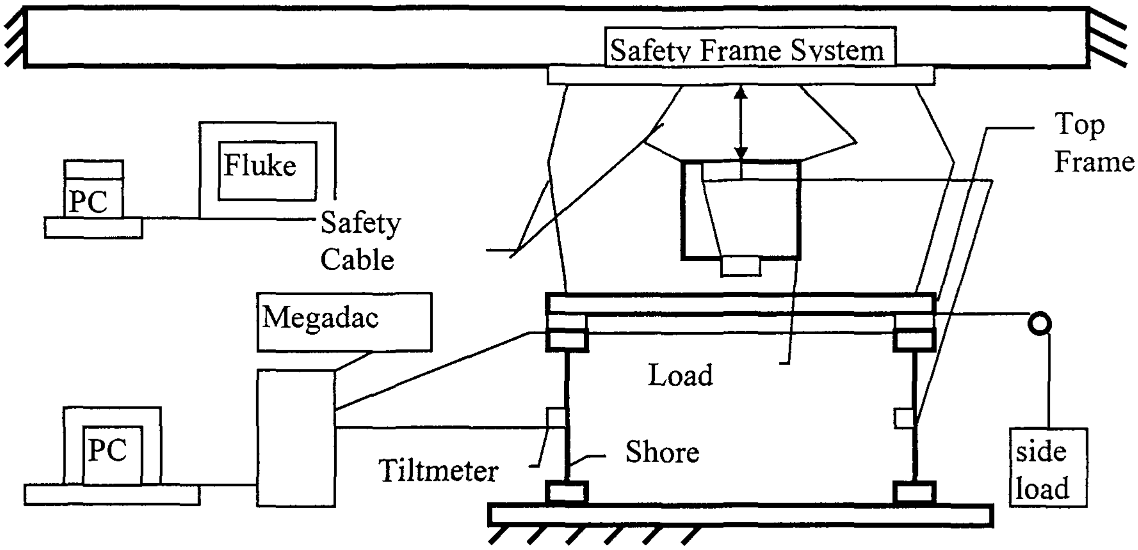

Figure 11.16 One level shoring system with plates welded on ends of the shores as feet.

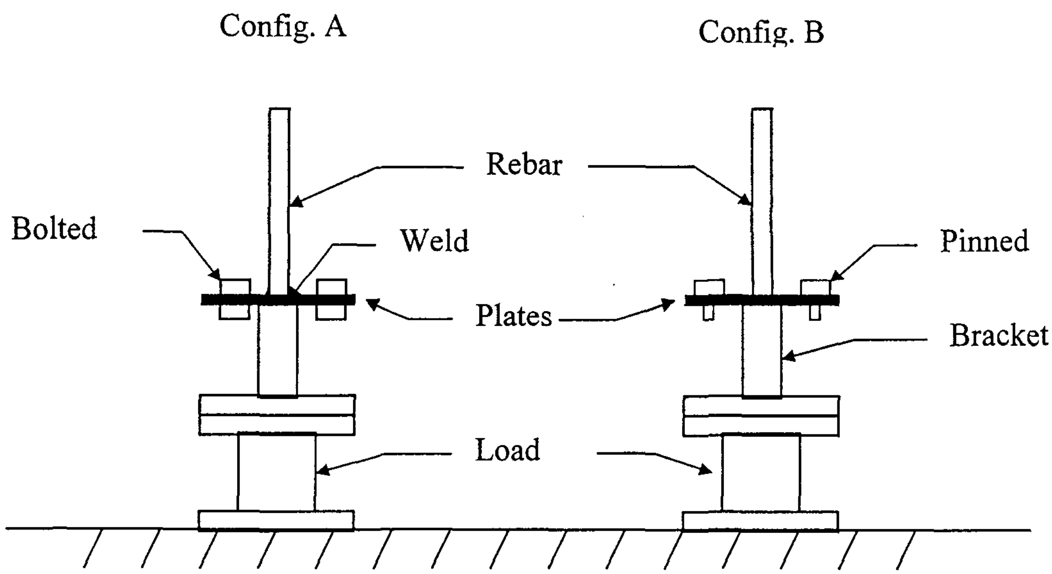

Figures 11.17 Different bracket configurations. Configuration A is bolted. Configuration B is pinned.

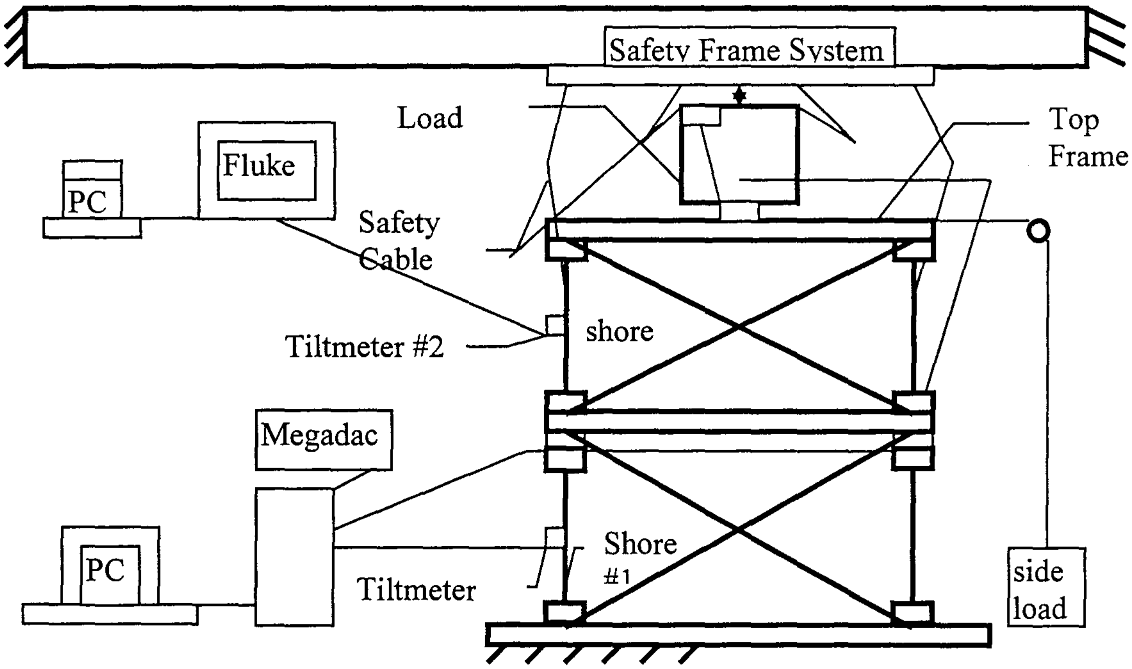

Figure 11.18 Model shoring with two levels with sixteen diagonal braces and eight shores

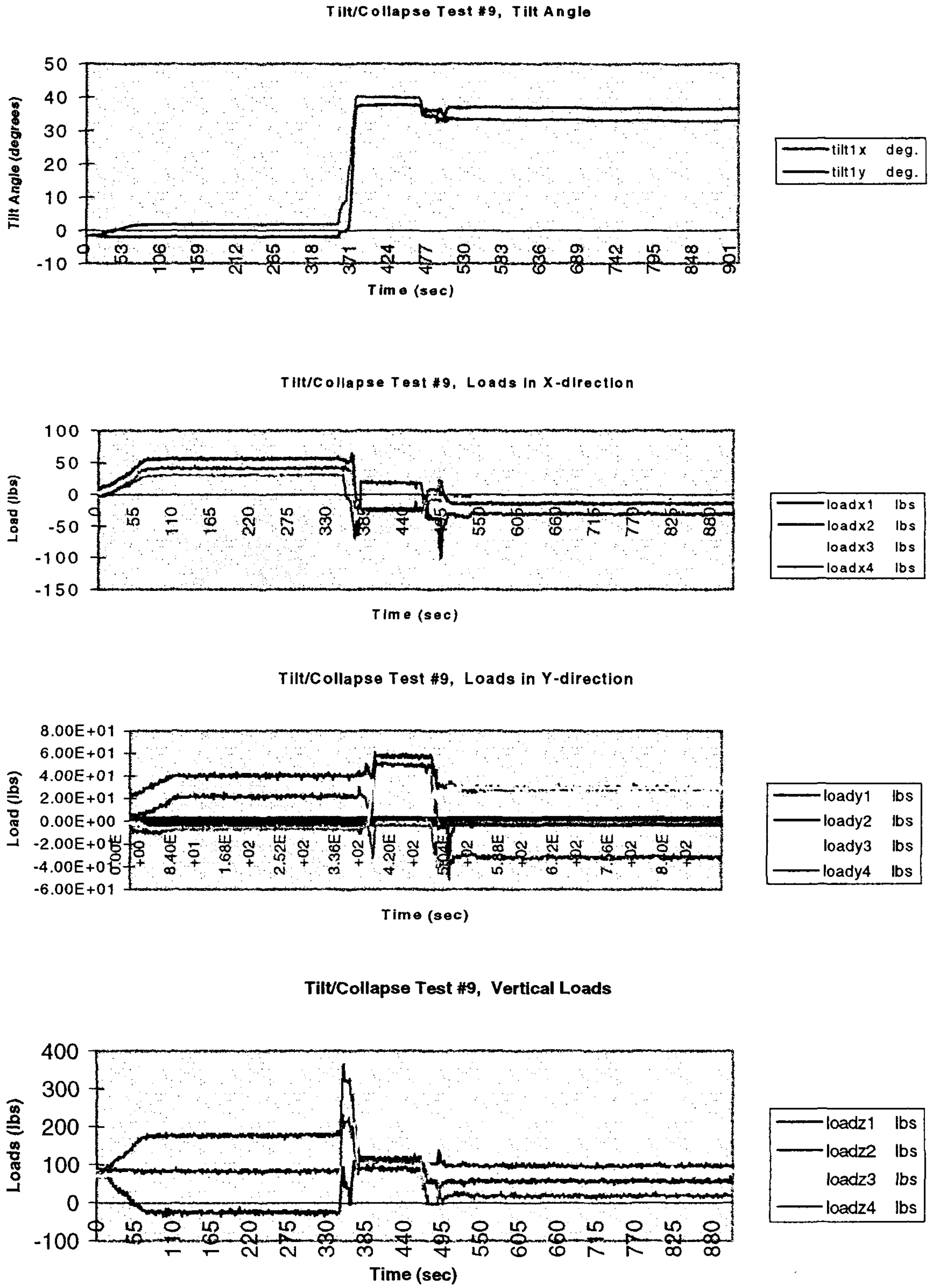

Figure 11.19 One level model with fixed end shores with vertical load 1500 lb. & side load 65 lb.

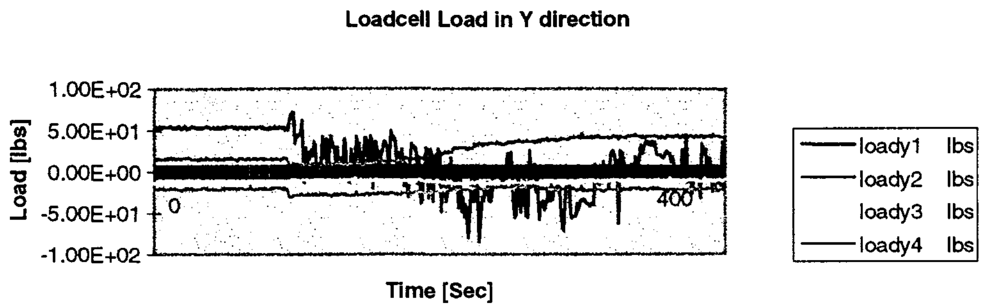

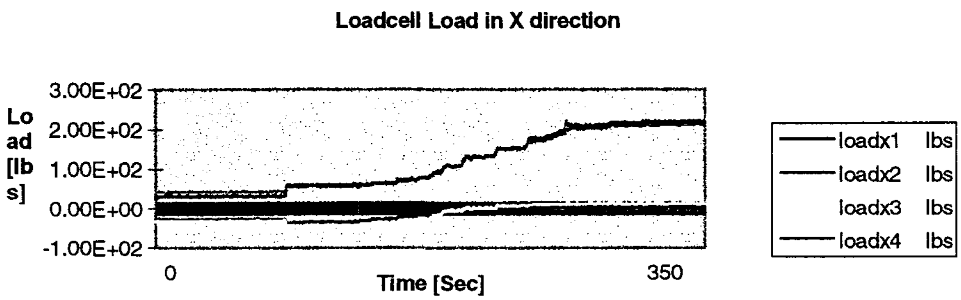

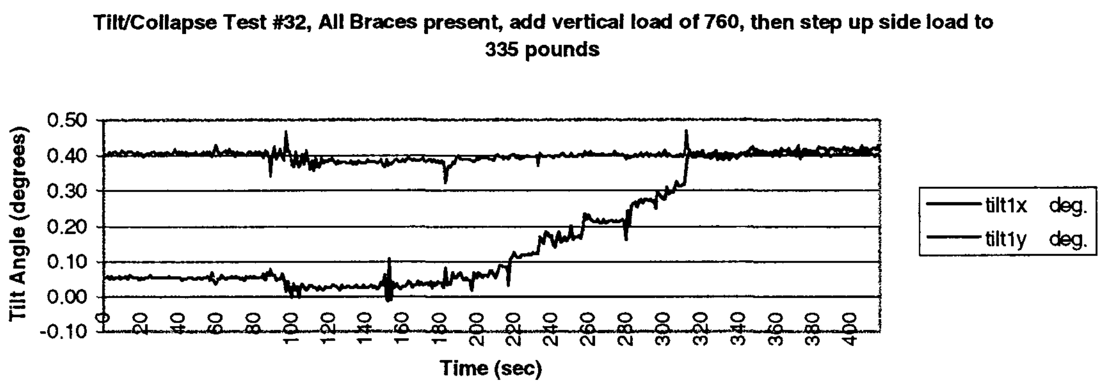

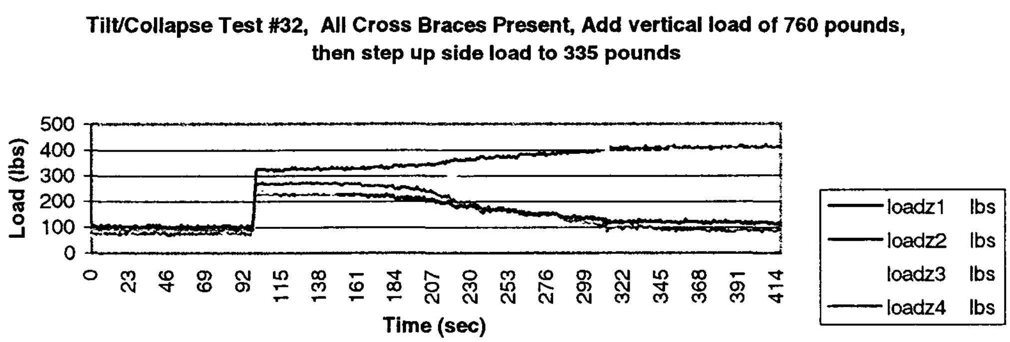

Figure 11.20 One level model with diagonal bars with vertical load 760 lb. and side load 335 lb.

Tilt/Collapse Test #34, Loads in Y-direction, One Story Structure, No Cross Braces Present, Loaded vertically with 760 lbs, then side load stepped up until collapse

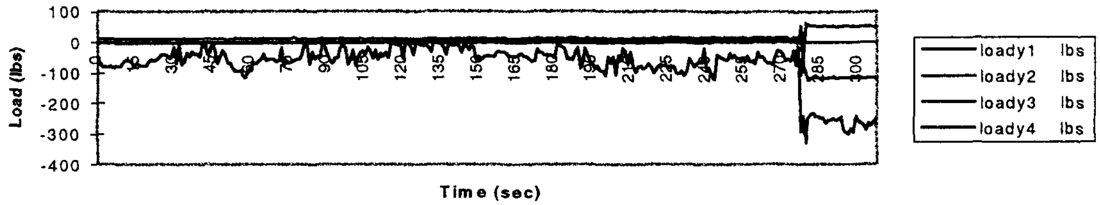

Tilt/Collapse Test #34, Welded feet, No Braces, Loaded vertically with 760 pounds, then applied side load until collapse

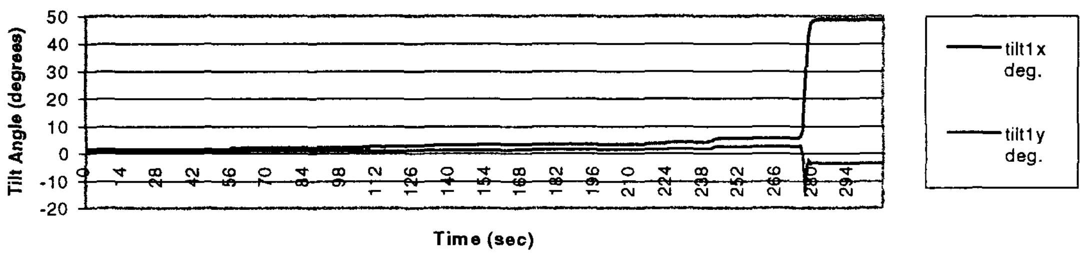

Tilt/Collapse Test #34, No cross bracing present, load vertically with 760 pounds, add side load until collapse

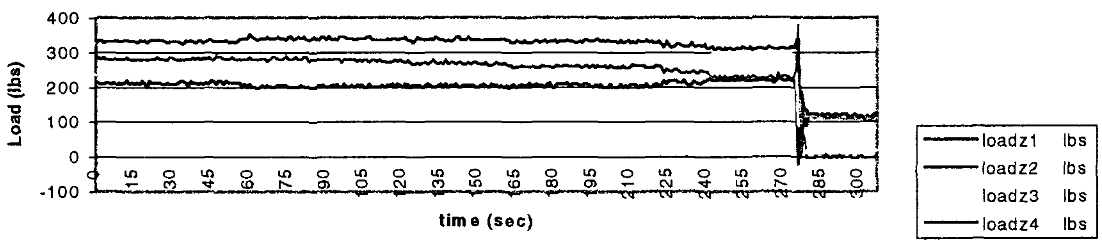

Tilt/Collapse Test #34, Loads in X-direction, One Story Structure, No Cross Braces Present, Loaded vertically with 760 lbs, then side load applied and stepped up until collapse, Final *side load = 60 lbs.*

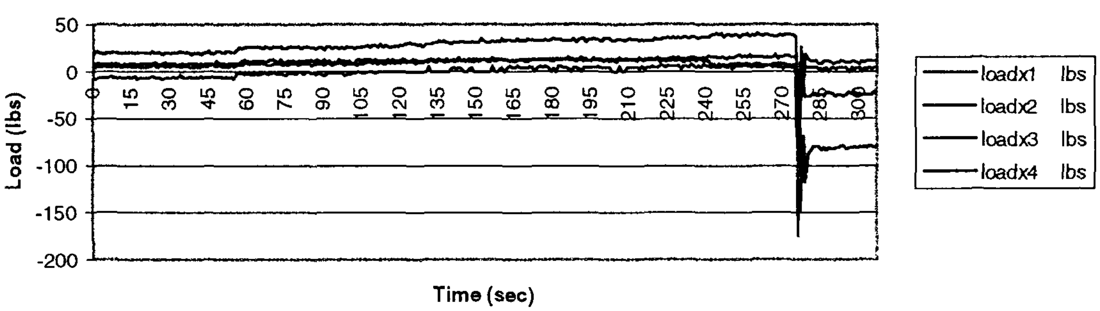

Figure 11.21 One level model without any diagonal bars with vertical load 760 lb. and side load 60 lb.

Tilt/Collapse Test #42, Two Story Structure, All Cross Braces Present, Loaded vertically first, then side load applied at upper level and stepped up to 225 lbs

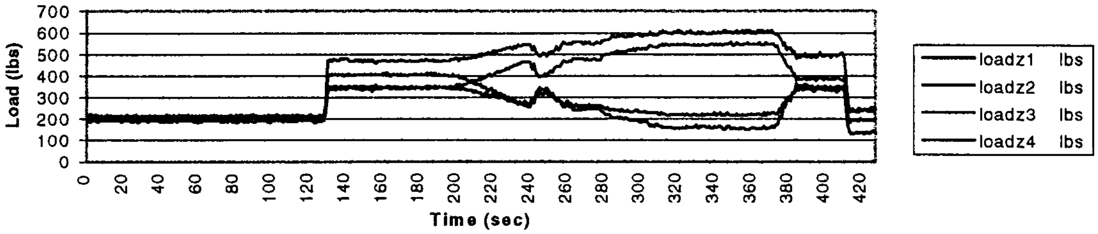

Tilt/Collapse Test #42, Loads in X-direction (lower level), Two Story Structure, All Cross Braces Present, Loaded vertically first, then side load applied at upper level and stepped up to 225 lbs.

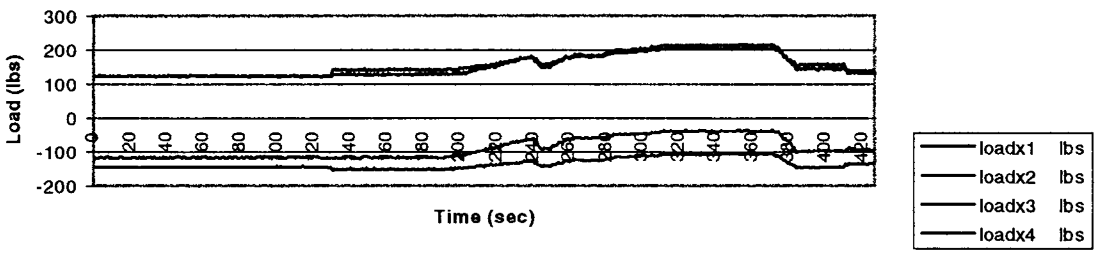

Tilt/Collapse Test #42, Loads in Y-direction (lower level), Two Story Structure, All Cross Braces Present, Loaded vertically first, then side load applied at upper level and stepped up to 225 lbs

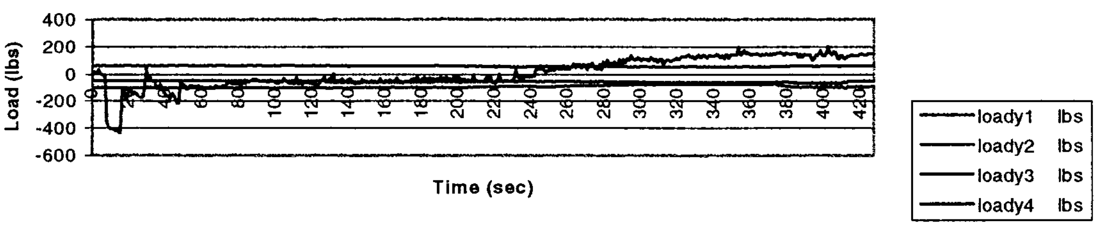

Tilt/Collapse Test #42, Tilt Angle of leg #1, Two Story Structure, All Cross Braces Present, Loaded vertically first, then side load applied at upper level and stepped up to 225 lbs

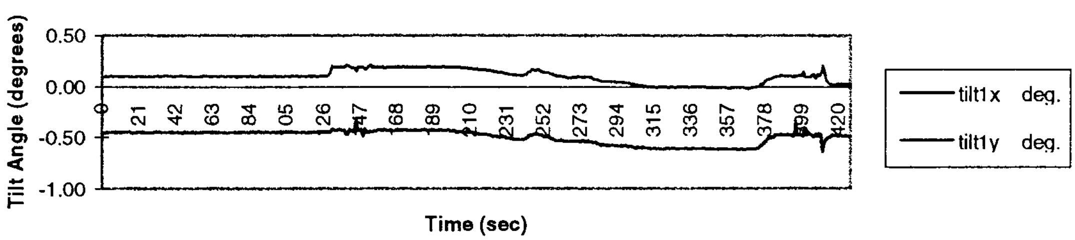

Figure 11.22 Two level model with sixteen diagonal bars with vertical load 760 lb. and side load 225 lb.

Tilt/Collapse Test #42, Loads in X-direction (upper level), Two Story Structure, All Cross Braces Present, Loaded vertically first, then side load applied at upper level and stepped up to 225 lbs.

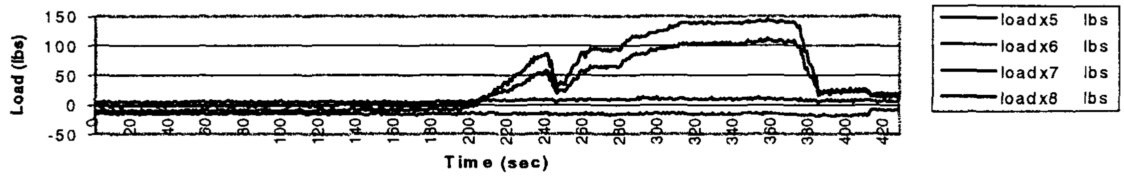

Tilt/Collapse Test #42, Loads in Y-direction (upper level), Two Story Structure, All Cross Braces Present, Loaded vertically first, then side load applied at upper level and stepped up to 225 lbs

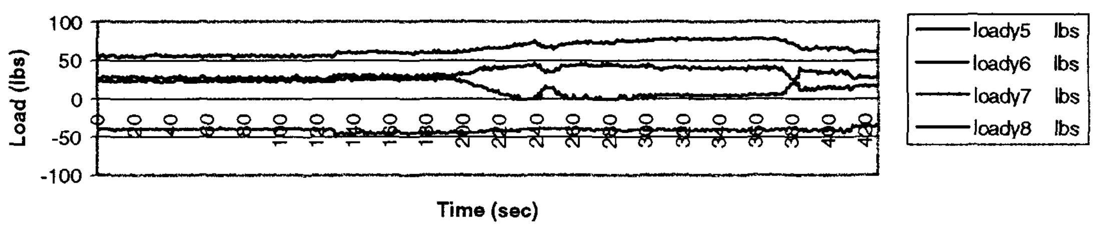

Tilt/Collapse Test #42, Tilt of Leg #5, Two Story Structure, All Cross Braces Present, Loaded Vertically first, Then side load applied at upper level and stepped up to 225 lbs.

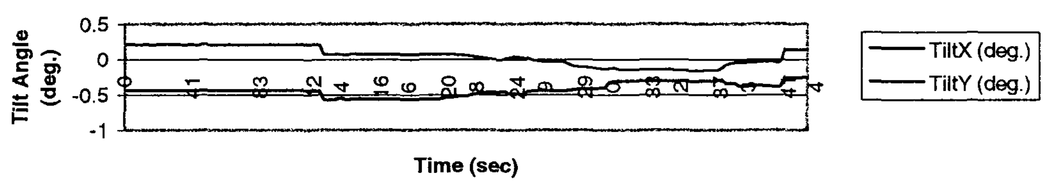

Tilt/Collapse Test #42, Vertical loads (upper level), Two Story Structure, All Cross Braces Present, Loaded vertically first, then side load applied at upper level and stepped up to 225 lbs

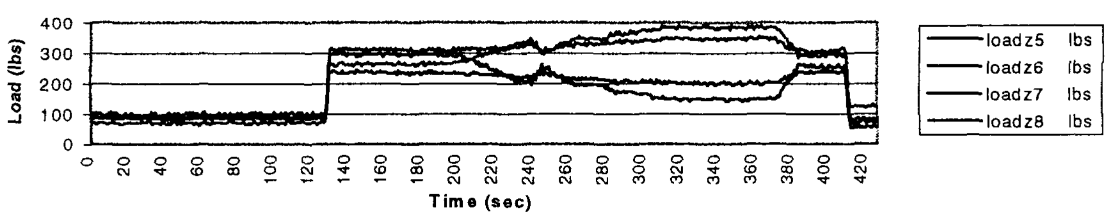

Figure 11.23 Two level model with diagonals and with vertical load 760 lb. (top level) and 360 lb. (lower level) and side load 225 lbs.

Tilt/Collapse Test #48, No braces on upper level, No long braces on lower level, (only braces present are on ends of lower level, Side load applied on upper level, final side load applied = 80 lbs

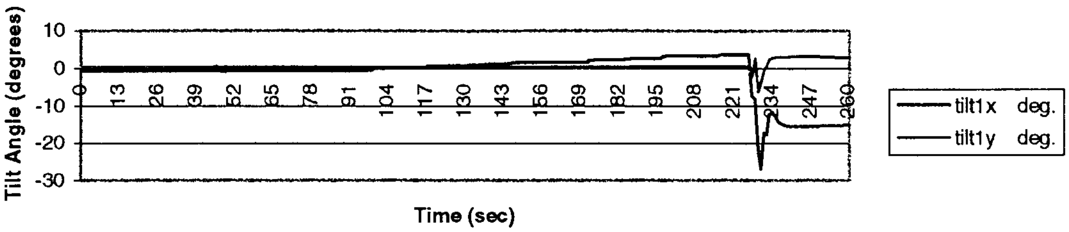

Tilt/Collapse Test #48, No Braces on Top level, No long braces on lower level (only braces present are on ends of lower level), Side load applied at upper level, final side load applied = 80 lbs

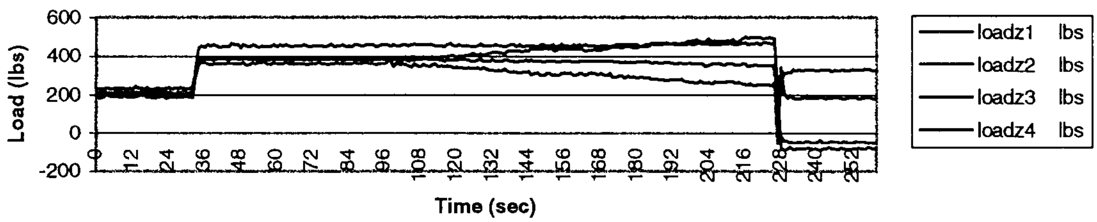

Tilt/Collapse Test #48, No braces on upper level, no long braces on lower level (only braces present are on ends of lower level), Side load applied at upper level, final side load applied = 80 lbs

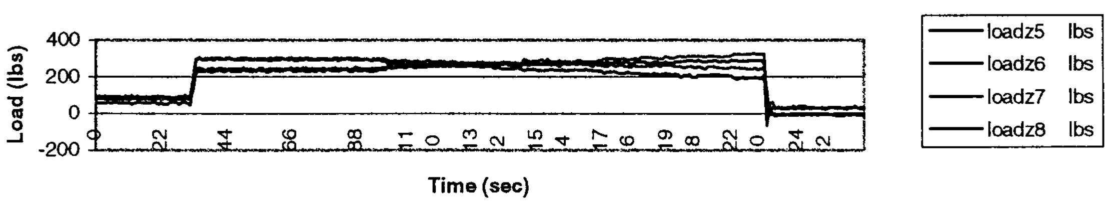

Tilt/Collapse Test #48, Loads in X-direction (lower level), No braces on upper level, No long braces on lower level (only braces present are on ends of lower level), Side load applied at upper level, final side load applied = 80 lbs

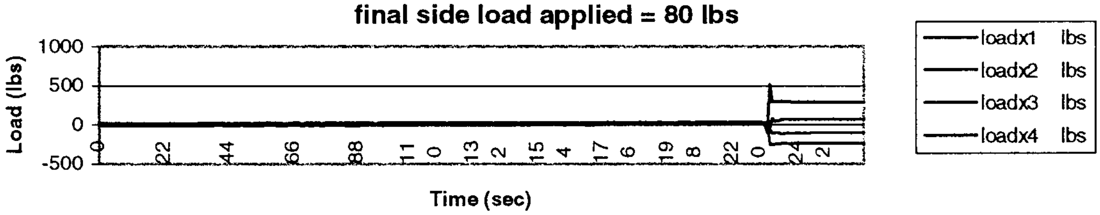

Figure 11.24 Two level model without any diagonal bars with vertical load top level 760 lb. & lower level 360 lb. and side load 80 lb., top level collapse to the right and the lower level to the left.

Tilt/Collapse Test #48, Loads in X-direction (upper level), No braces on upper level, No long braces on lower level (only braces present are on ends of lower level), Side load applied at upper level, final side load applied = 80 lbs

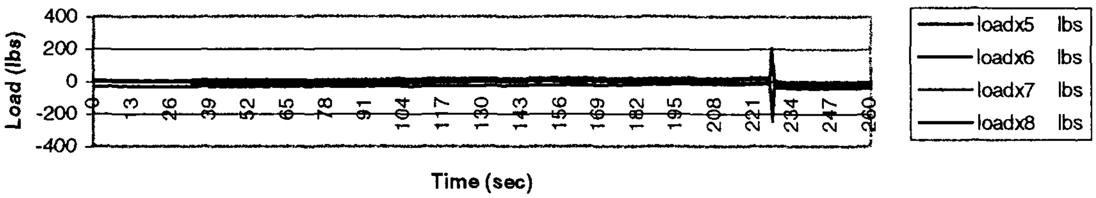

Tilt/Collapse Test #48, Loads in Y-direction (lower level), Two Story Structure, No Braces on upper level, No long braces on lower level, (only braces present are on ends of lower level), Side load applied on upper level, final side load applied = 80 lbs

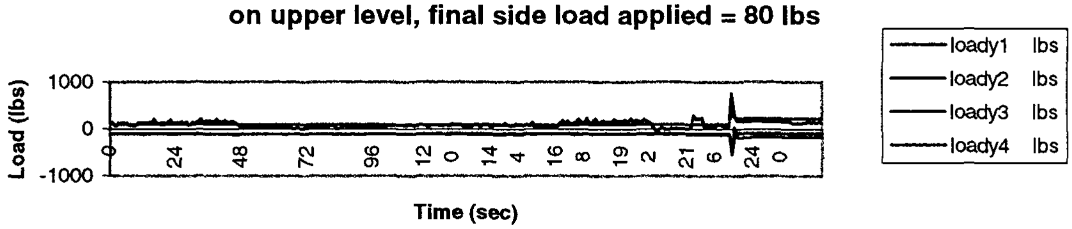

Tilt/Collapse Test #48, Loads in Y-direction (upper level), Two Story Structure, No Braces on upper level, No long braces on lower level, (only braces present are on ends of lower level), Side load applied on upper level, final side load applied = 80 lbs

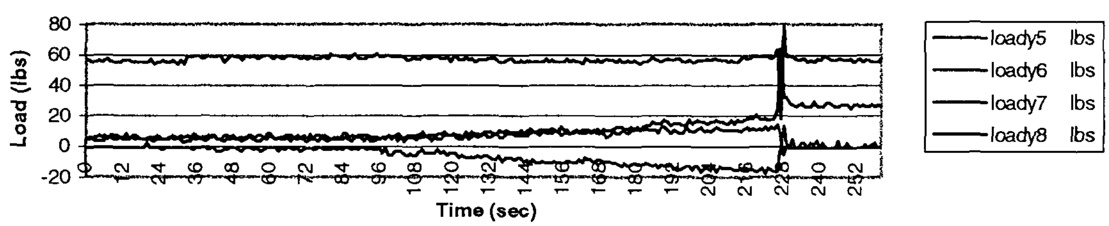

Tilt/Collapse Test #48, Tilt Angle of Leg #5, No Braces on upper level, no long braces on lower level, (only braces present are on ends of lower level), Side load applied at upper level, final side load applied = 80 lbs

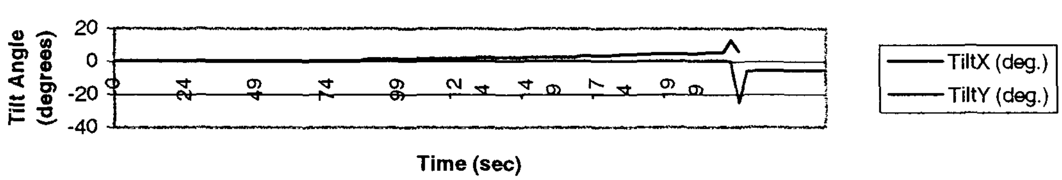

Figure 11.25 Two level model without any diagonal bars with vertical load top level 760 lb. & lower level 360 lb. and side load 80 lb., top level collapse to the right and the lower level to the left.

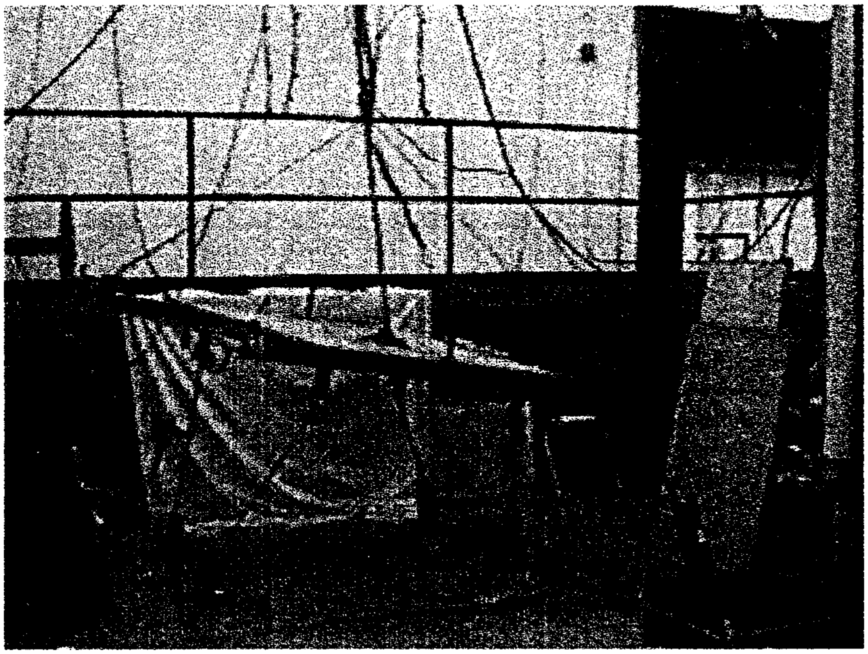

Figure 11.26 Collapse of one-story system with pinned ends.

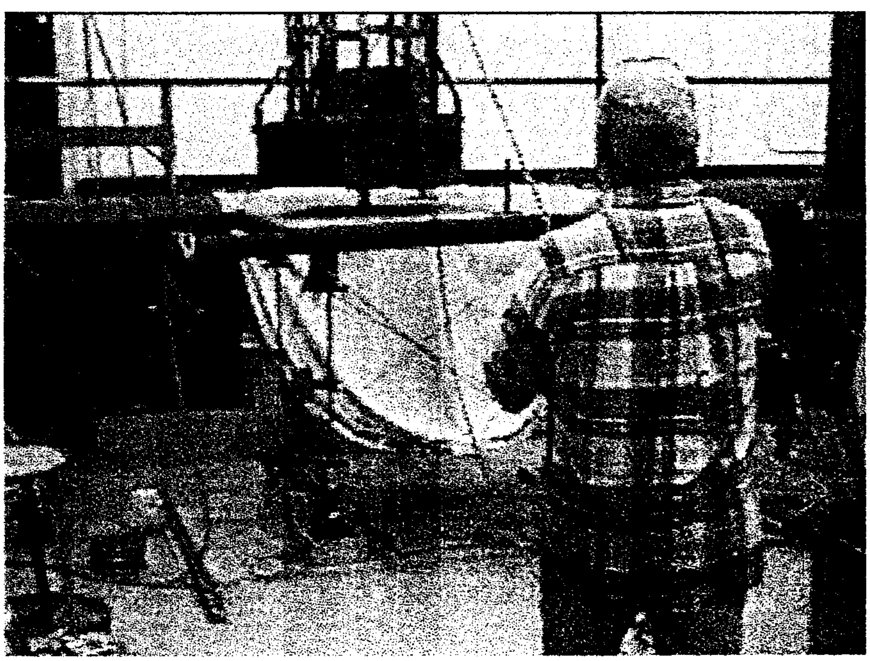

Figure 11.27 Applying vertical load to one story shoring system.

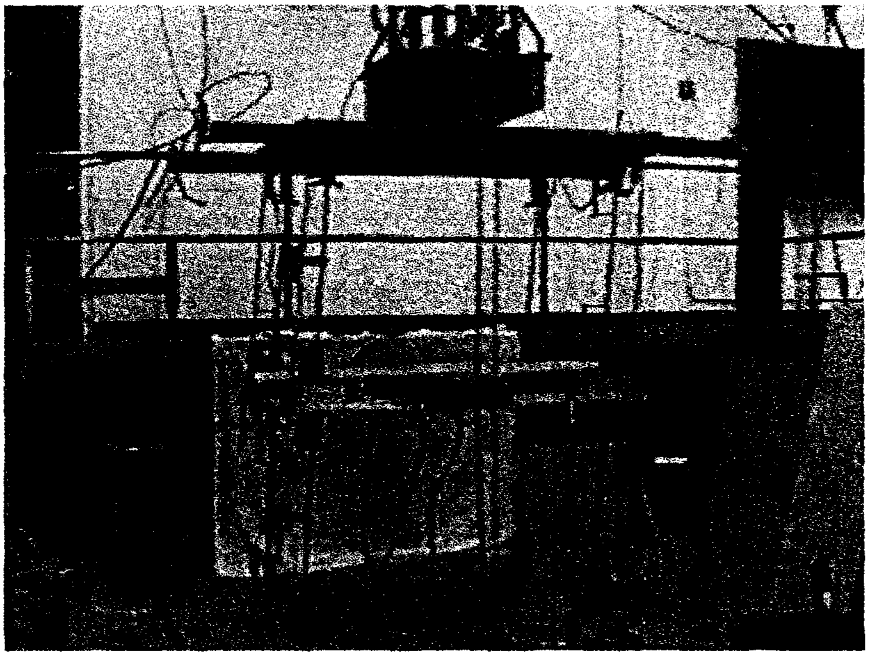

Figure 11.28 Impending collapse of two story shoring system.

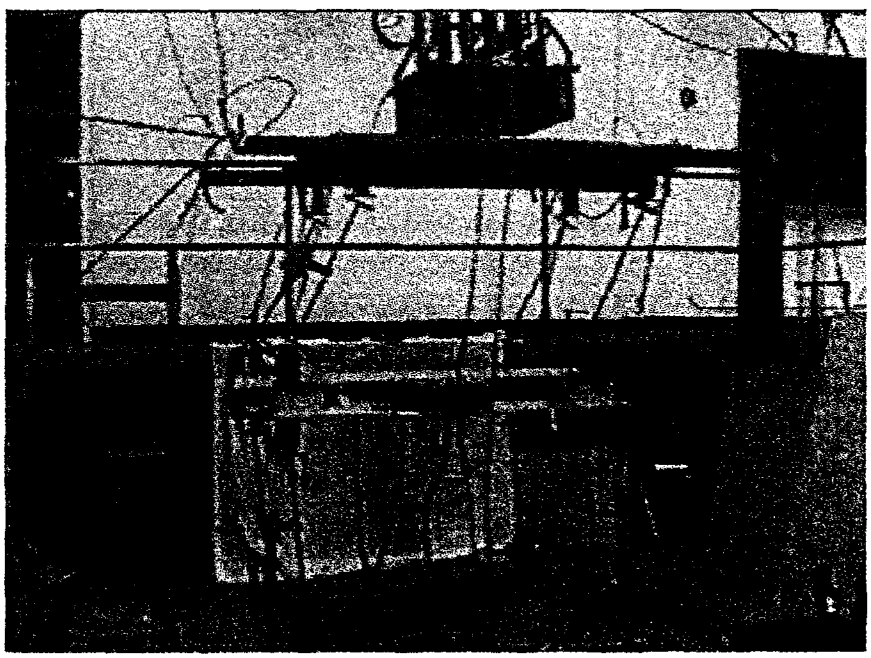

Figure 11.29 Start of collapse of two story shoring system.

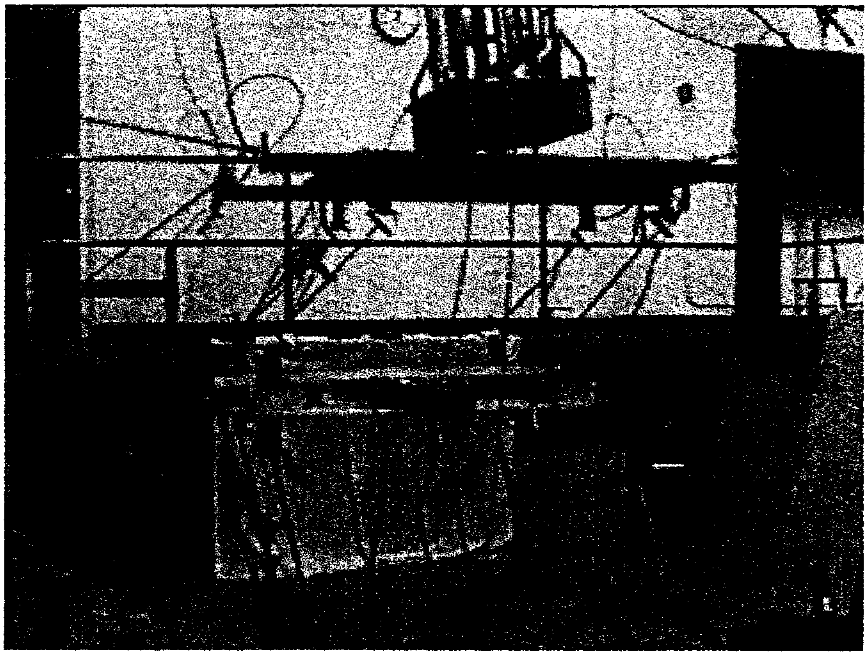

Figure 11.30 Continuation of lateral collapse of two story shoring system.

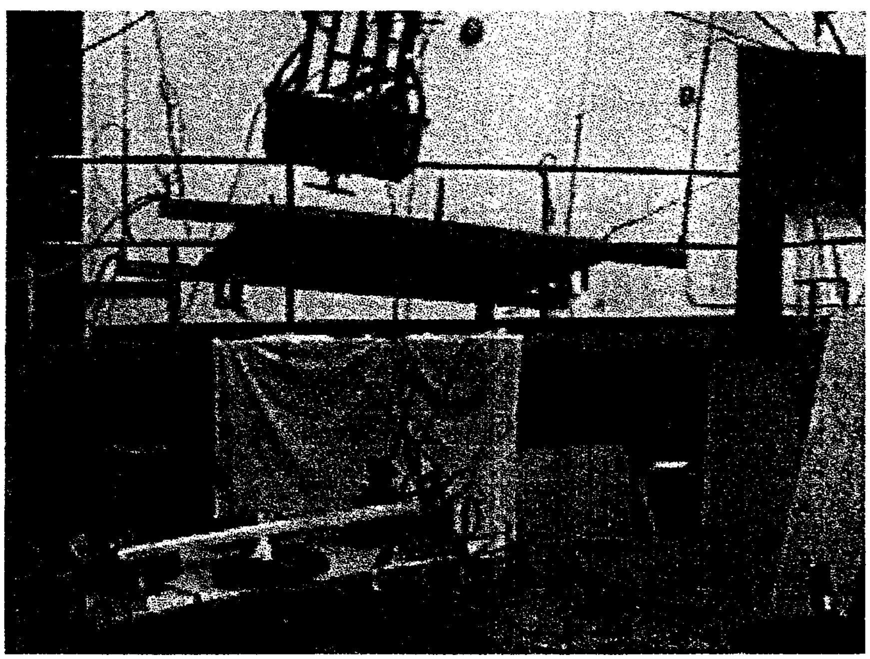

Figure 11.31 Two story shoring system collapses. Safety system restrains loading weights.

12. Beckley WV Building Test

The first site at which shore load measurements were taken was at a Federal prison under construction in Beckley WV, Figure 12.1. The Beckley prison is a fairly large complex consisting of a series of low-rise 5-story reinforced concrete structures that contained approximately 48 2-person cells and open-bay rooms. One of these buildings was chosen for the testing. The choice of building was based primarily on the timing and availability of the structure.

Since the Beckley site was the first site to be visited, all of the test equipment had to be acquired, tested and configured prior to the tests. The main pieces of equipment that were acquired were the load cells, the data acquisition system, and the associated cabling and hardware.

The load cells were 3-axis ring-type load cells that were custom manufactured by Hitec Corp. of Westford, MA. The load cells were nominally configured to have a range of +/- 20,000 lb. (88,900 N) in the vertical or Z-direction, and +/- 10,000 lb. (44,500 N) in the horizontal or X and Y-directions. Six threaded 3/16 in dia. holes were placed in each end of the load cells for the attachment of mounting hardware. Figure 12.2 shows a Hitec load cell undergoing a lateral load calibration check in the laboratory.

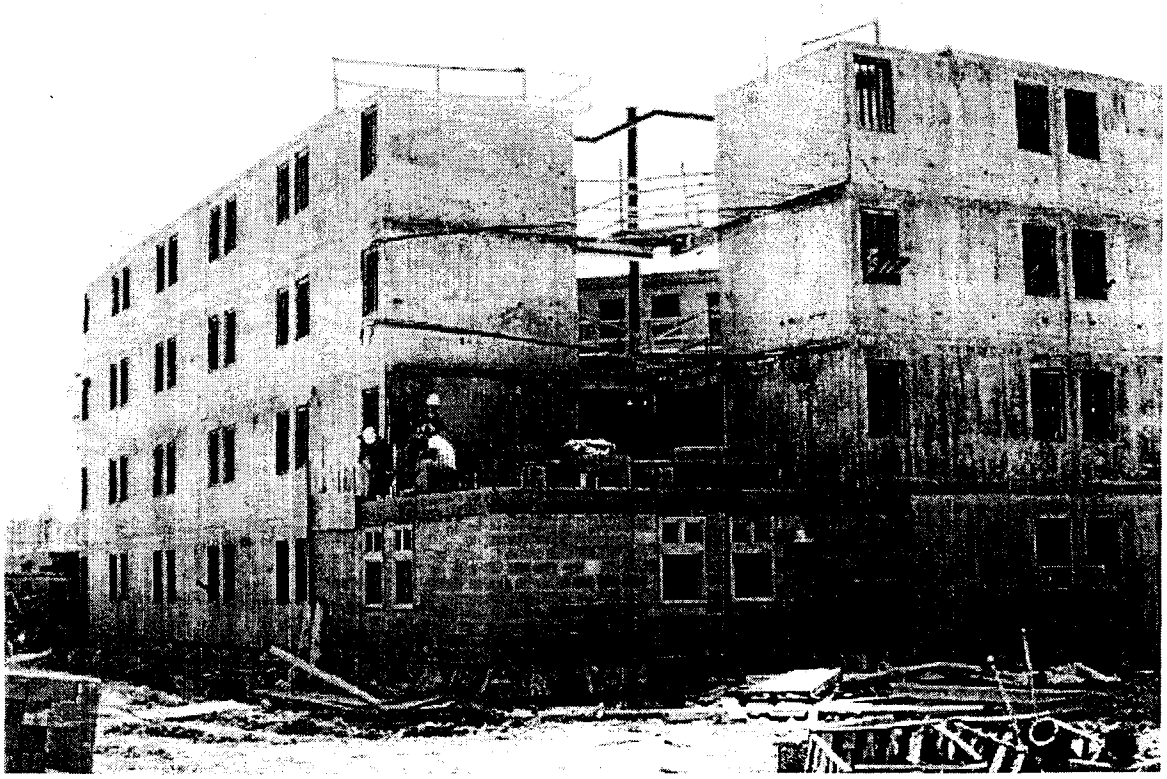

Figure 12.1 Beckley WV federal prison building under construction.

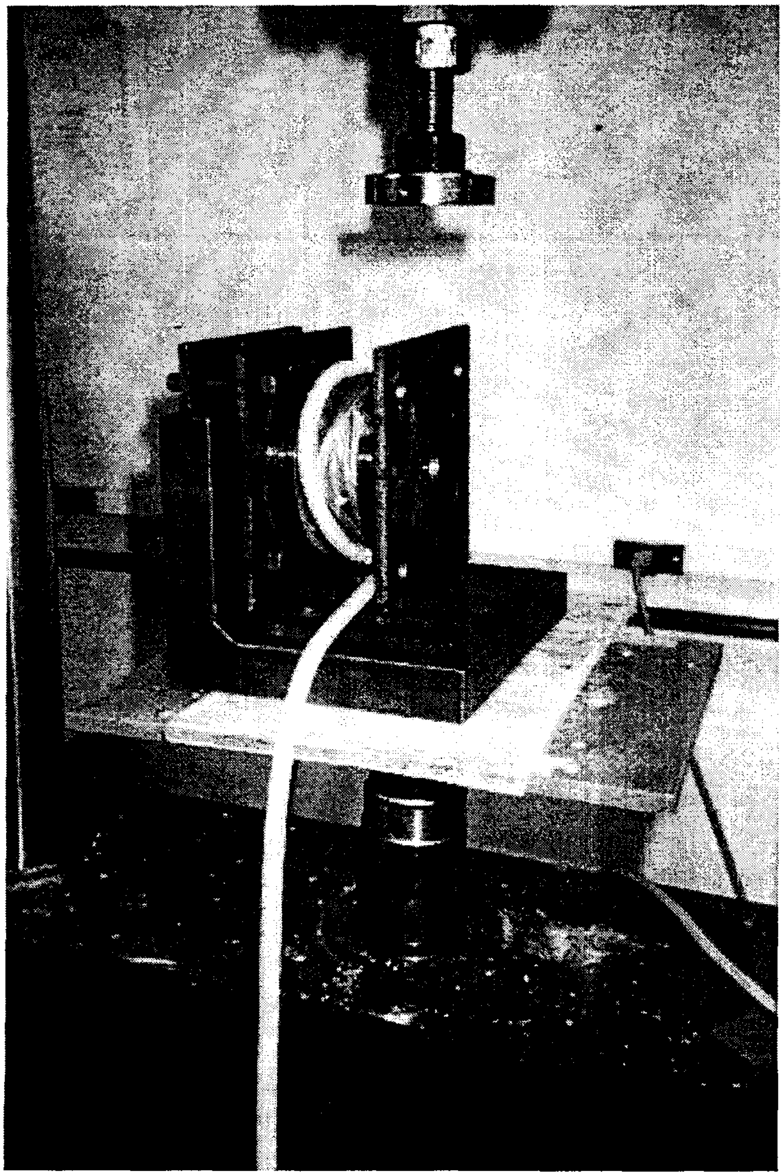

Figure 12.2 Hitec load cell undergoing horizontal axis calibration testing in the laboratory.

The data acquisition system was a Megadac digital data acquisition system from Optim Electronics with the following options: 1. A 3008AC mainframe; 2. four AD 885D 8-channel analog input modules; 3. Three STB 884/SCV 8-channel screw terminals; 4. A 3008 SCSI interface; and 5. A PL2070 external rewritable laser disc. The system was controlled with a Winbook 75 MHz 486DX laptop computer via a National Instruments PCMCIA GPIB card. A Colorado Trakker 250 external tape drive provided redundant data backup. Reliable electric power was provided with an uninterruptible power supply from

TrippLite Model No. BC900LAN with a rating of 900 VA and 650W. Figure 12.3 shows the Megadac data acquisition system.

Additional hardware was required for the field-testing. This consisted of rugged weatherproof shielded 14-conductor cable to run from the Megadac to the load cells. Military style (Bendix) connectors were used to make the external connections. The cables were strain-relieved and covered for waterproofing at both ends. Square steel mounting plates with countersunk holes were attached to both ends of the load cells. A fairly weatherproof metal box housed the entire data acquisition system.

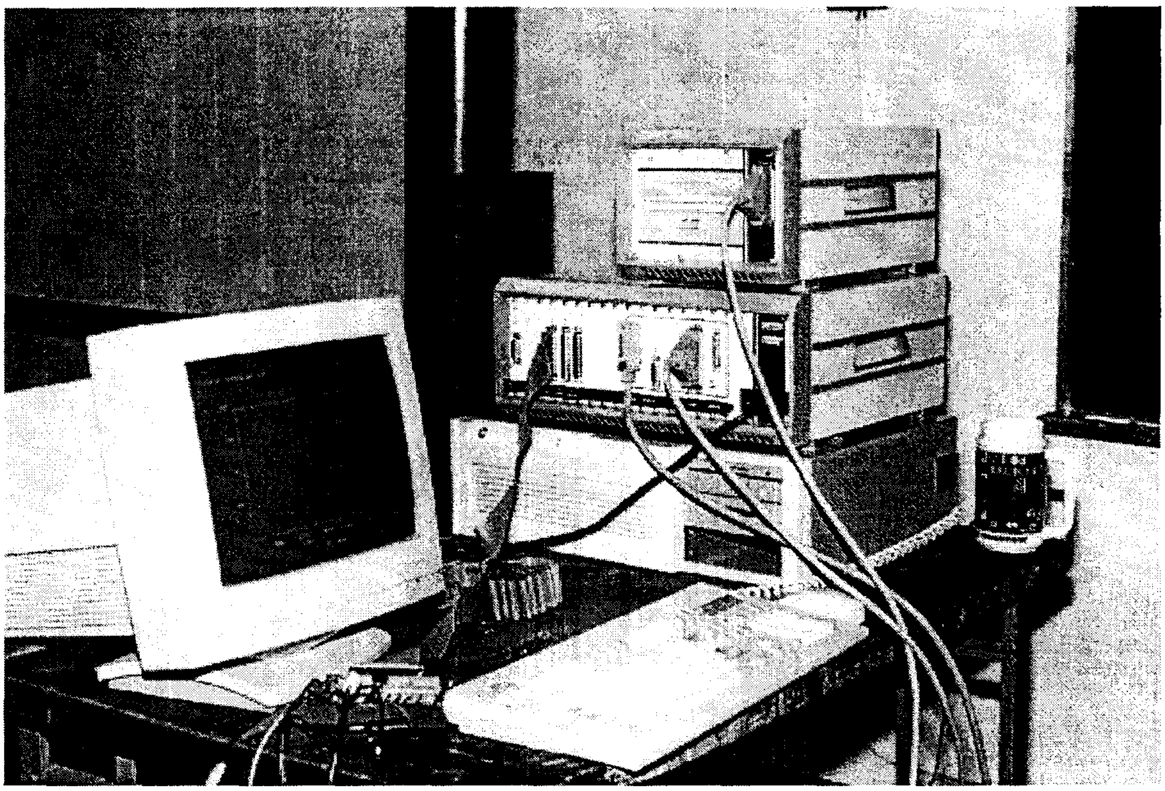

Figure 12.3 Megadac data acquisition system.

Assembling the equipment took most of the summer of 1994. The last pieces to arrive were the Hitec load cells. Once the equipment was assembled, it was loaded into a rented van and driven 14 hours to the Beckley WV site.

Data were collected from September 9 to 19, 1994. Two specific locations were instrumented and loads were monitored prior to placement of the concrete slab, during concrete placement, and after the slab was completed. Only shoring data were collected since reshores were not used. Two small pour areas were instrumented at the Beckley site. These areas, shown in Figure 1, were identical 0.2-m (8-in.) thick slabs with pour areas of approximately 9.4 m^2 (87 ft^2). Since these areas were small, only four steel shores were used for vertical support during the pours. All four shores were instrumented for each of the small pour areas. Two steel I-beams were used to support the forms in each of the small pour areas. These I-beams spanned from shores 1/5 to shores 3/8 and from shores 2/7 to shores 4/6 (see Figure 12.4 and 12.5). The steel I-beams supported wooden stringers, which in turn supported the plywood forms. The large pour area was approximately 51.28 m^2 (552 ft^2). Sixteen steel shores supplied vertical support. The slab thickness was 0.2 m (8 in.) and 0.4 m (16 ' .), as shown in Figure 12.5. Steel I-beams were used as the primary support for the 0.4-m (16-in.) slab thickness section. Four I-beams were used to span between shores 1-2, 3-4, 5-6, and 7-8 (see Figure 12.5). The I-beams supported aluminum I-beams which spanned the 7.32 m (24 ft.) length of the large pour area. Aluminum I-beams were also used to span from these members to two exterior steel I-beams also spanning the 7.32 m (24 ft.) length, thereby providing support for the 0.2 m (8 in.) thick slab sections. Only those shores indicated in Figure 12.6 were instrumented during the large pour.

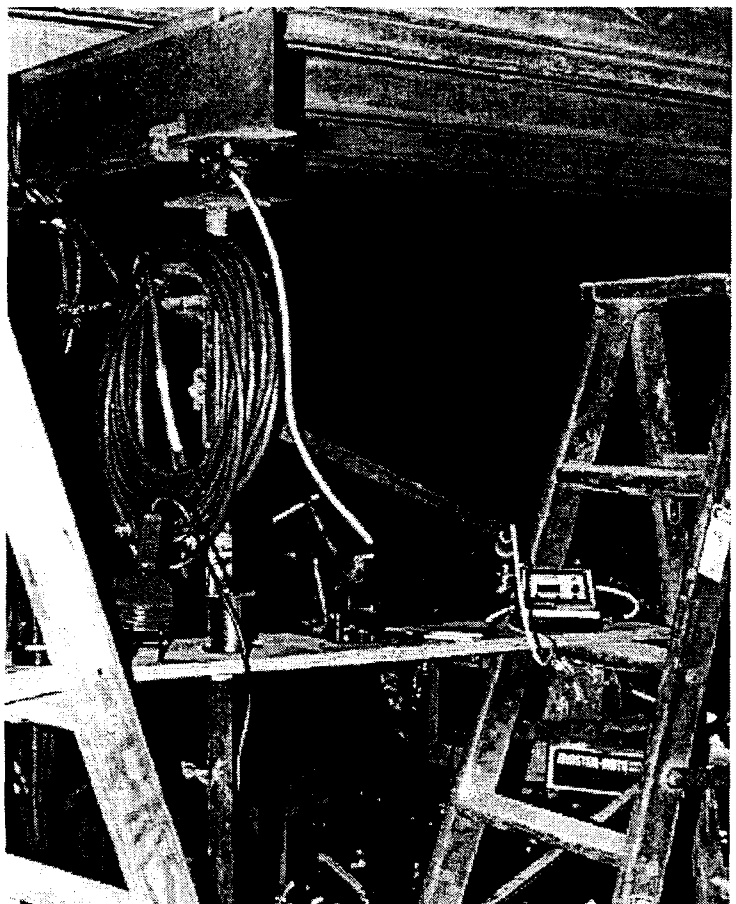

Figure 12.4 Load cell installed in the shoring system at the Beckley WV prison site.

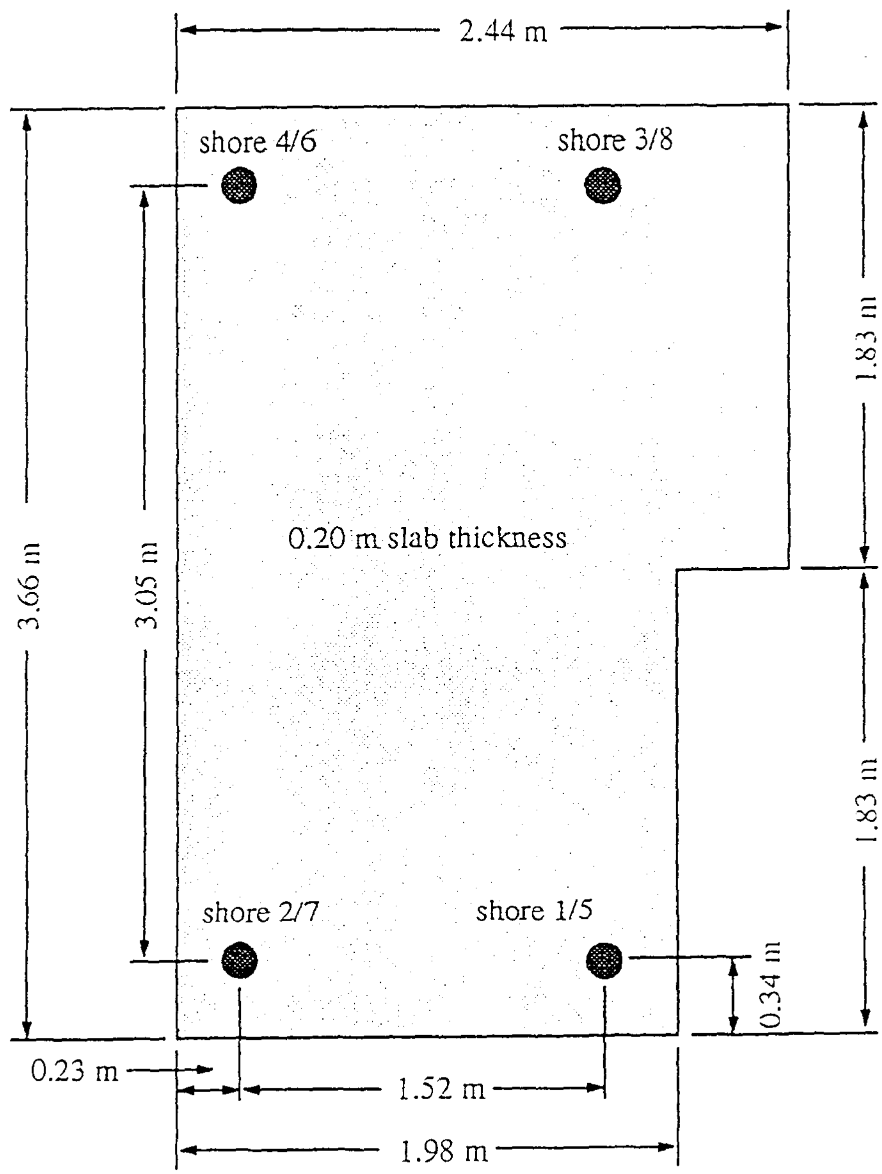

Figure 12.5 Layout of the small pour area at Beckley WV federal prison.

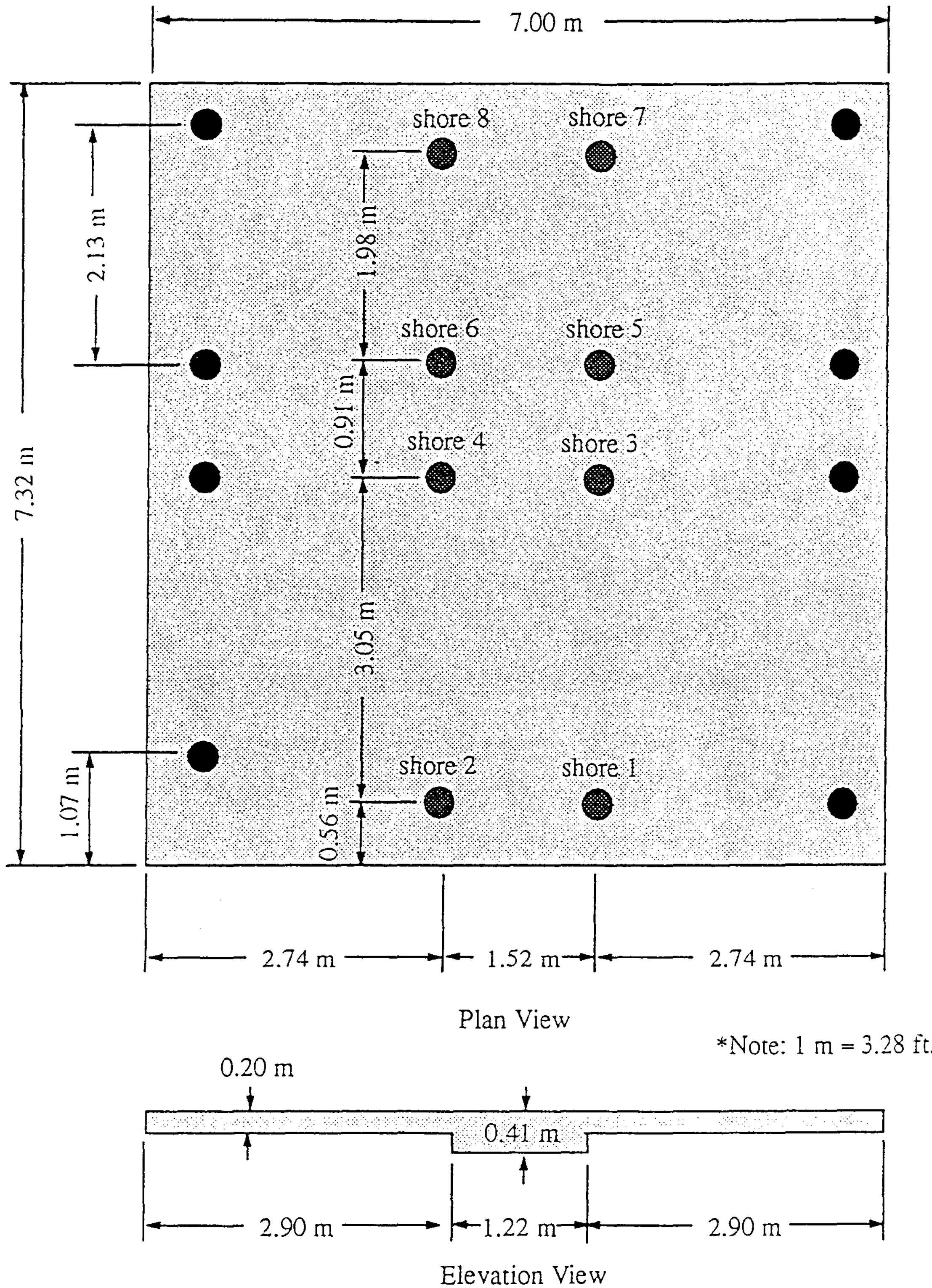

Figure 12.6 Layout of large pour area at Beckley, WV federal prison.

The shoring structure was loaded during pouring by a bucket dumping operation, Figure 12.7. The location of individual bucket dumps was recorded, Figure 12.8. During curing, live loads were imposed on the structure, such as the storage of equipment and construction materials, Figure 12.9.

Figure 12.7 Bucket dumping operation during pouring at Beckley WV.

Pouring Sequence for the Second Pour

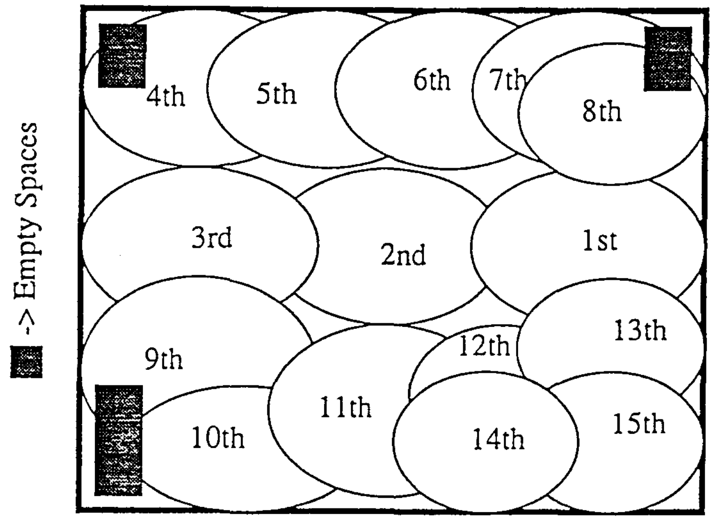

Figure 12.8 Location of individual bucket dumps for large pour area at Beckley WV.

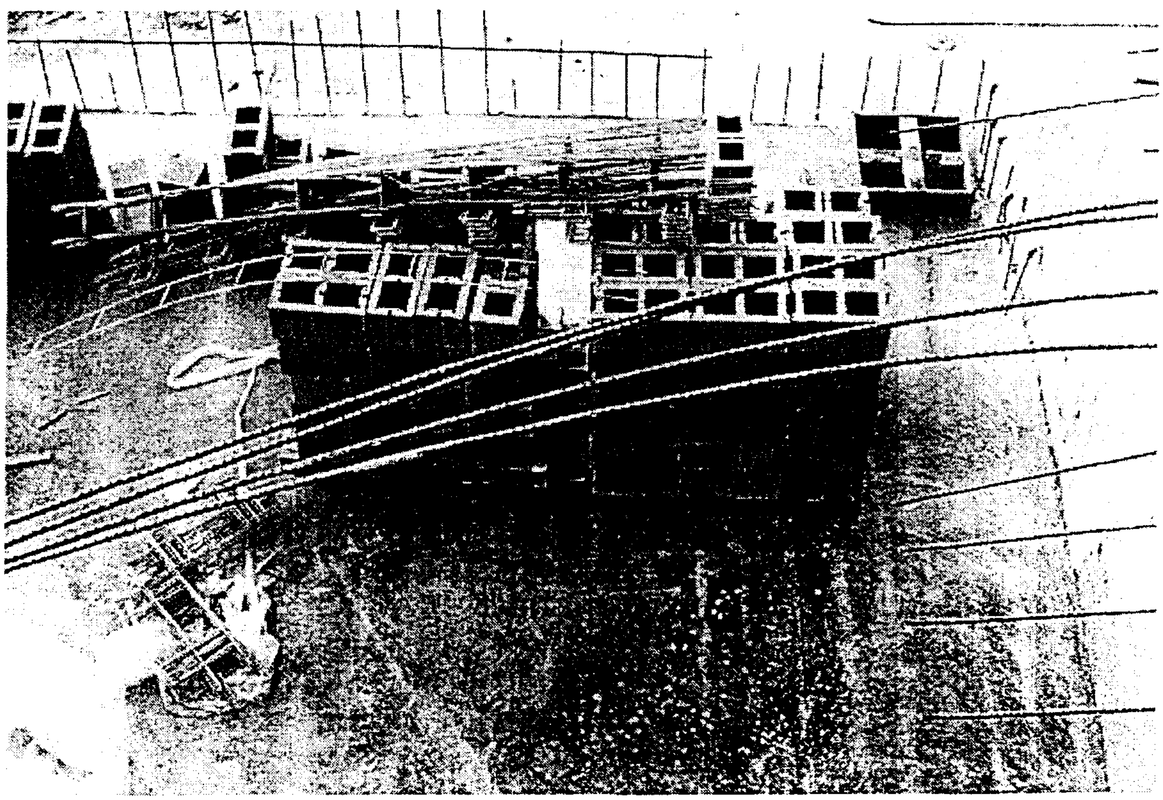

Figure 12.9 Storage of construction materials producing a live load at Beckley WV.

The data collected at the Beckley site included vertical and lateral shore load effects (one vertical and two lateral load channels per instrumented shore) during both the pouring and curing phases for each pour area. The sampling frequency for the pouring data was 100 Hz. This permitted the collection of sufficient data for later dynamic load analysis. Since the pour durations were several minutes, the data files were typically too large to be manipulated efficiently. For the purposes of data analyses, the data sets were reduced to more manageable sizes by stripping nine out of each ten points from the raw pour data. The effects of this data reduction were not noticeable during graphical comparisons (i.e., no load spikes were lost), however this information might need to be re-included for any dynamic analysis. Although the curing data were sampled at a lower frequency, similar reductions were per-formed to maximize efficiency during data analyses.

Figures 12.10 and 12.11 show the vertical and horizontal shore loads that were measured on a small bay at the Beckley WV site during pouring. Figures 12.12 and 12.13 show the vertical and horizontal shore loads that were measured on a large bay at the Beckley WV during pouring. Figures 12.14 and 12.15 show the vertical and horizontal shore loads that were measured on a large bay at the Beckley WV during curing. An analysis of the data appears in Section 16.

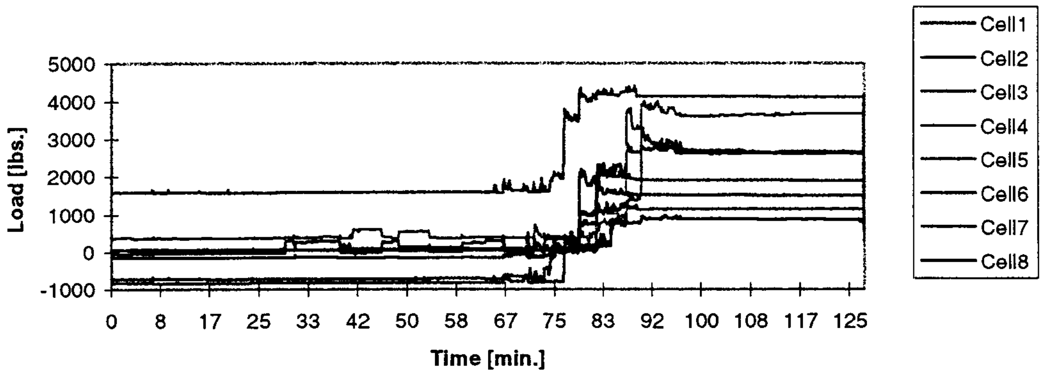

Figure 12.10 Vertical shore loads on small bay at Beckley WV during pouring.

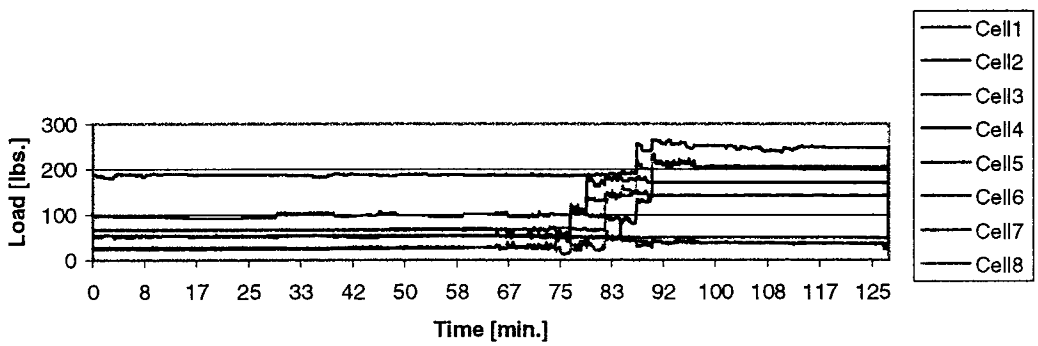

Figure 12.11 Horizontal shore loads on small bay at Beckley WV during pouring

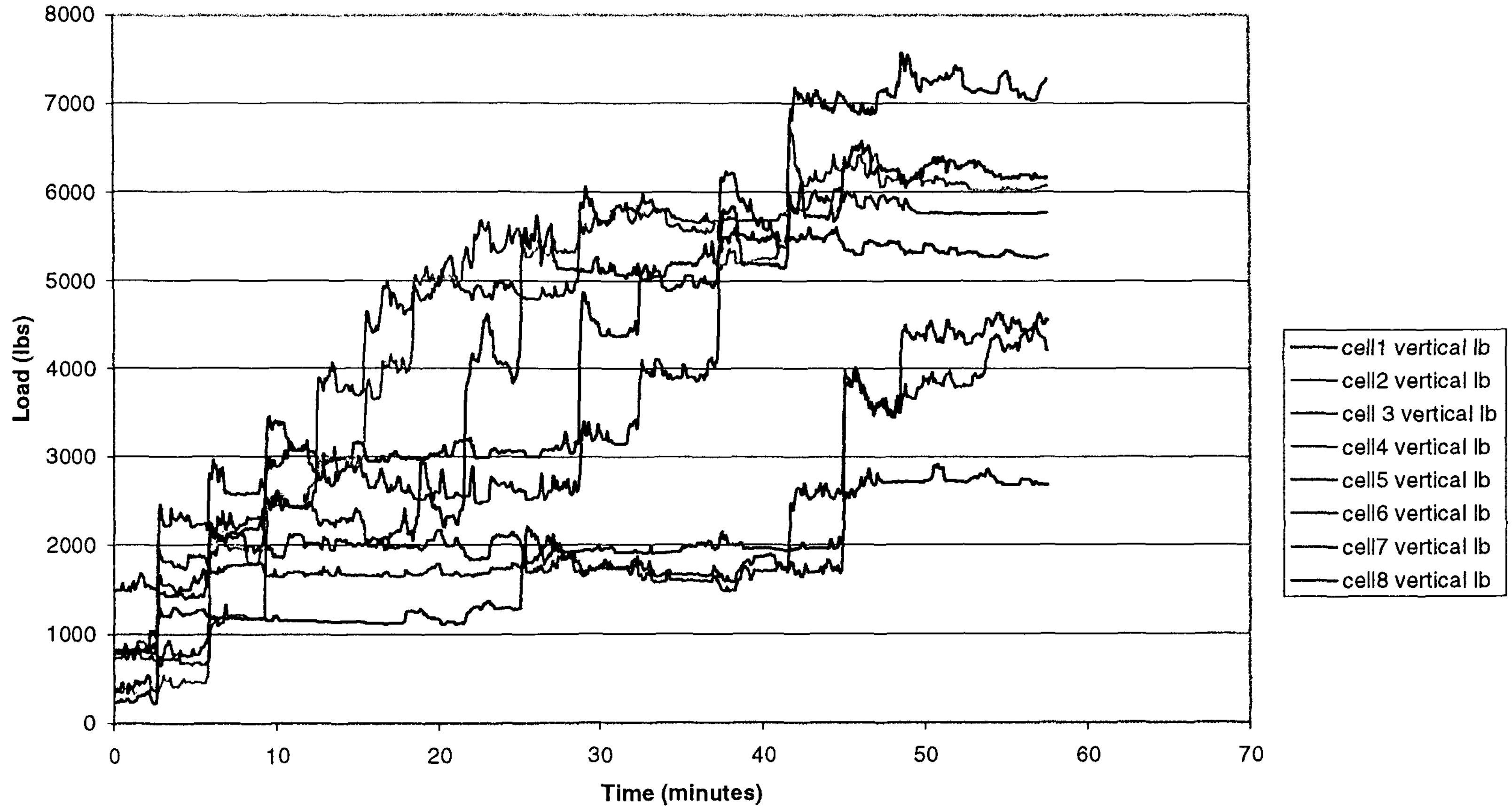

Figure 12.12 Vertical shore loads on large bay at Beckley WV during pouring.

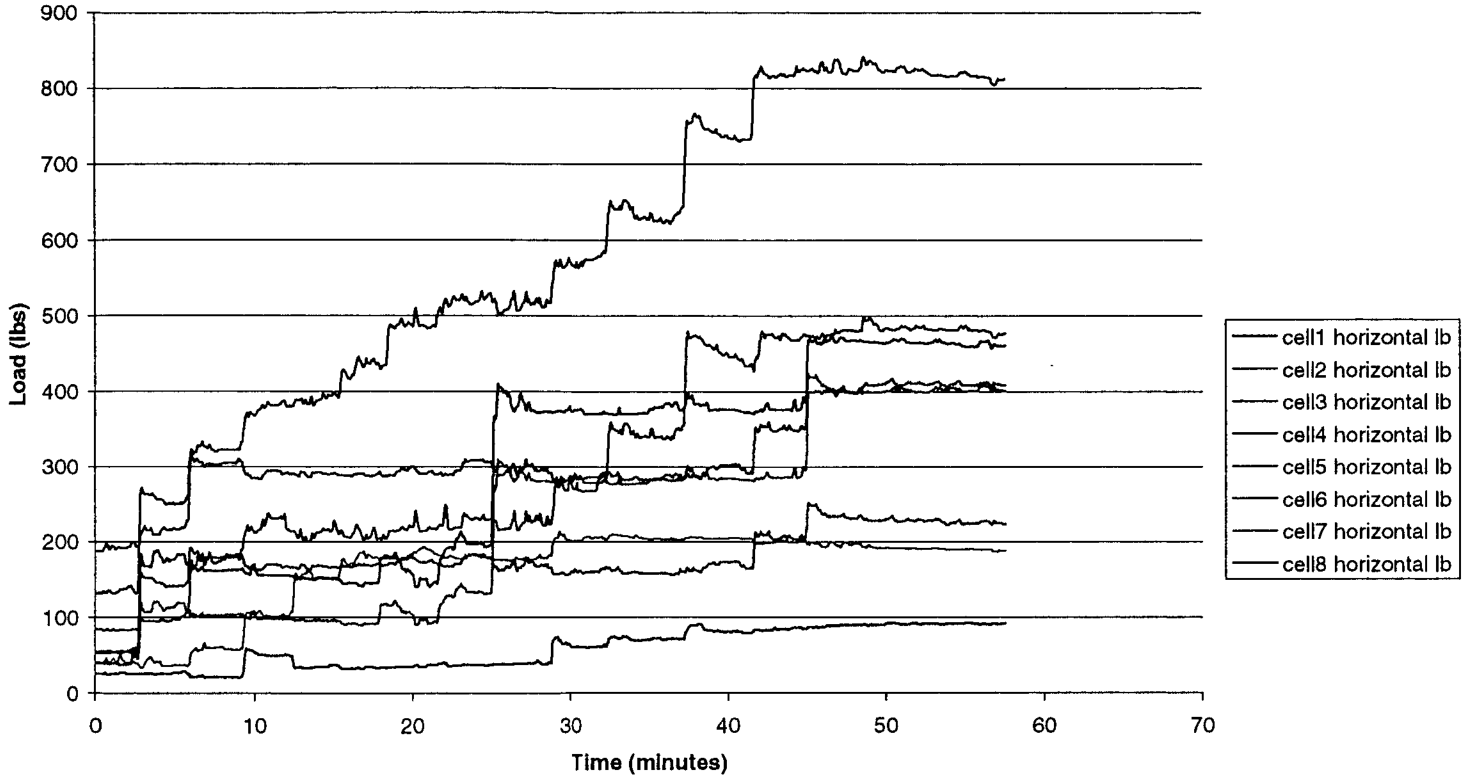

Figure 12.13 Horizontal shore loads on large bay at Beckley WV during pouring.

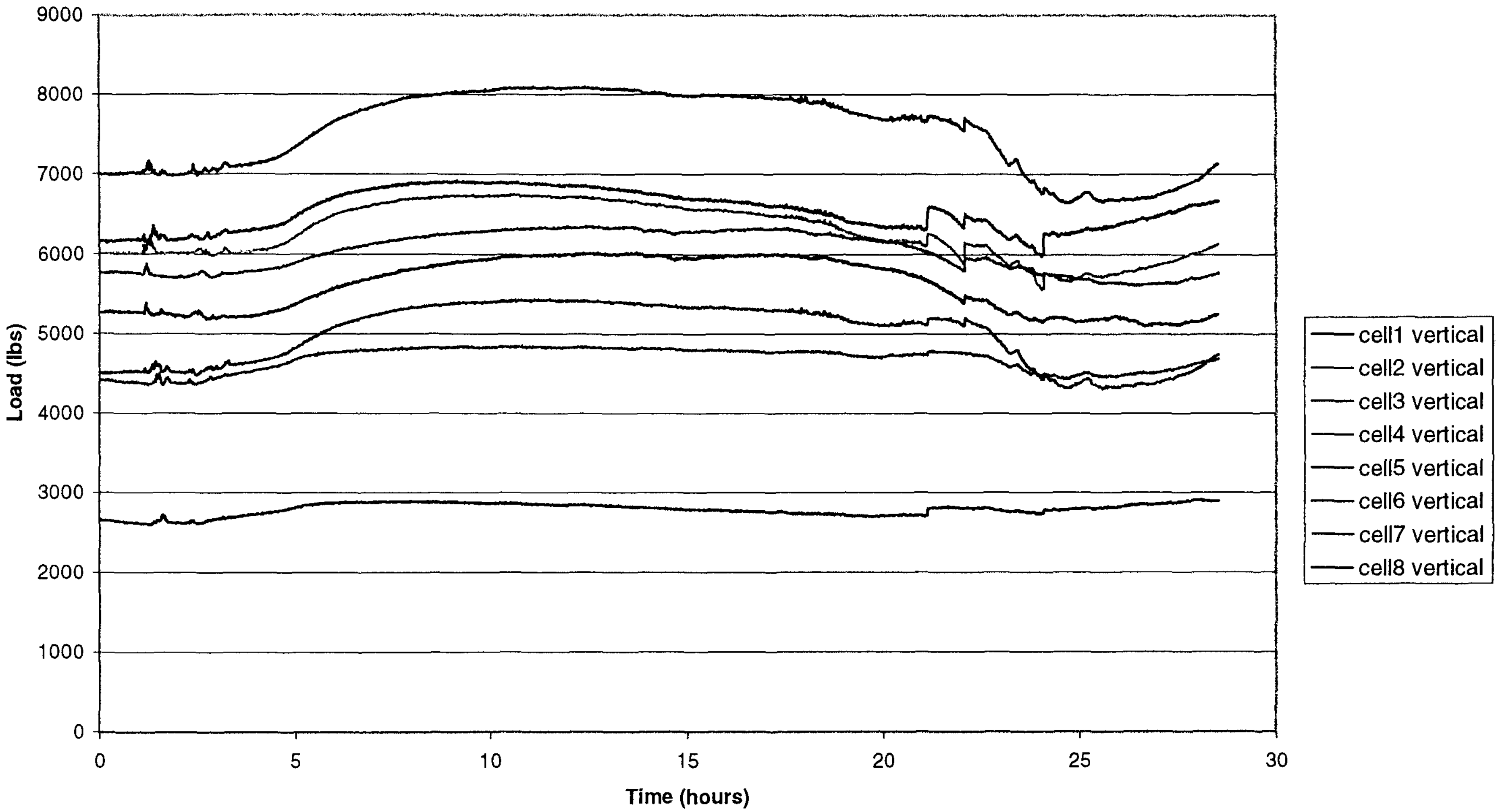

Figure 12.14 Vertical shore loads on large bay at Beckley WV during curing.

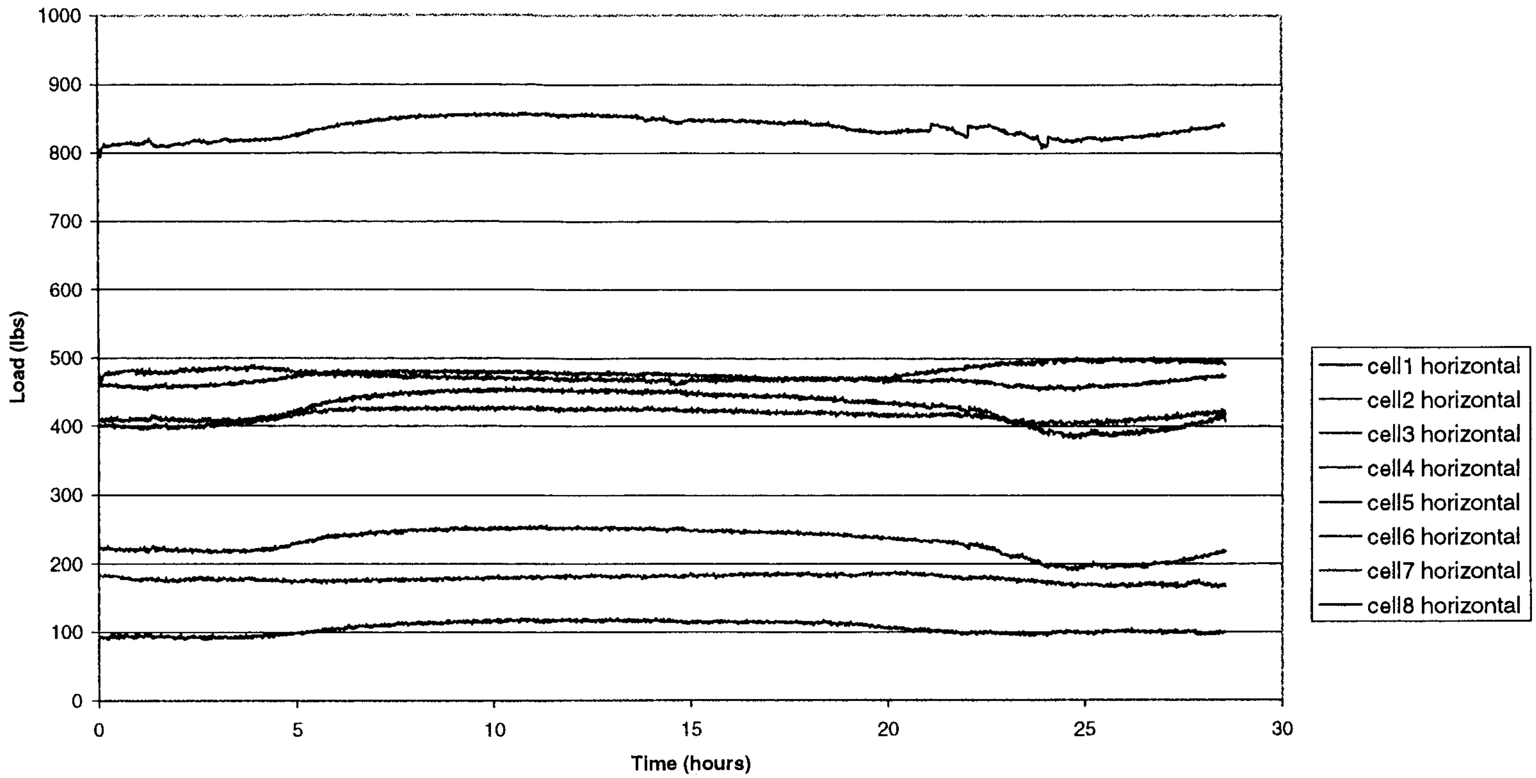

Figure 12.15 Horizontal shore loads on large bay at Beckley WV during curing

13. East Ave. VT Building Test

Following the data collection in Beckley WV, a building site became available almost immediately on the University of Vermont campus. This building was a library storage facility on East Ave. in Burlington, VT. The East Ave storage facility is a two-story low-rise structure with several fairly large bays. Data were collected at three locations for shoring that was placed between a concrete base floor and the first floor. Four-post scaffolding type shoring was used.

The data collection ran from September 30, 1994 to October 21, 1994. During this period, there was a series of torrential rainstorms that forced a stoppage of construction activities, and hampered data collection efforts. Nonetheless, data were collected successfully at 3 locations for both pours and cures. Figure 13.1 is a diagram of the floor plan and the data collection locations. Figure 13.2 is a photograph of the shoring at East Ave. Figures 13.3 and 13.4 are vertical and horizontal shore loads measured at East Ave. during pouring, respectively. Figures 13.5 and 13.6 are vertical and horizontal shore loads measured at East Ave. during curing.

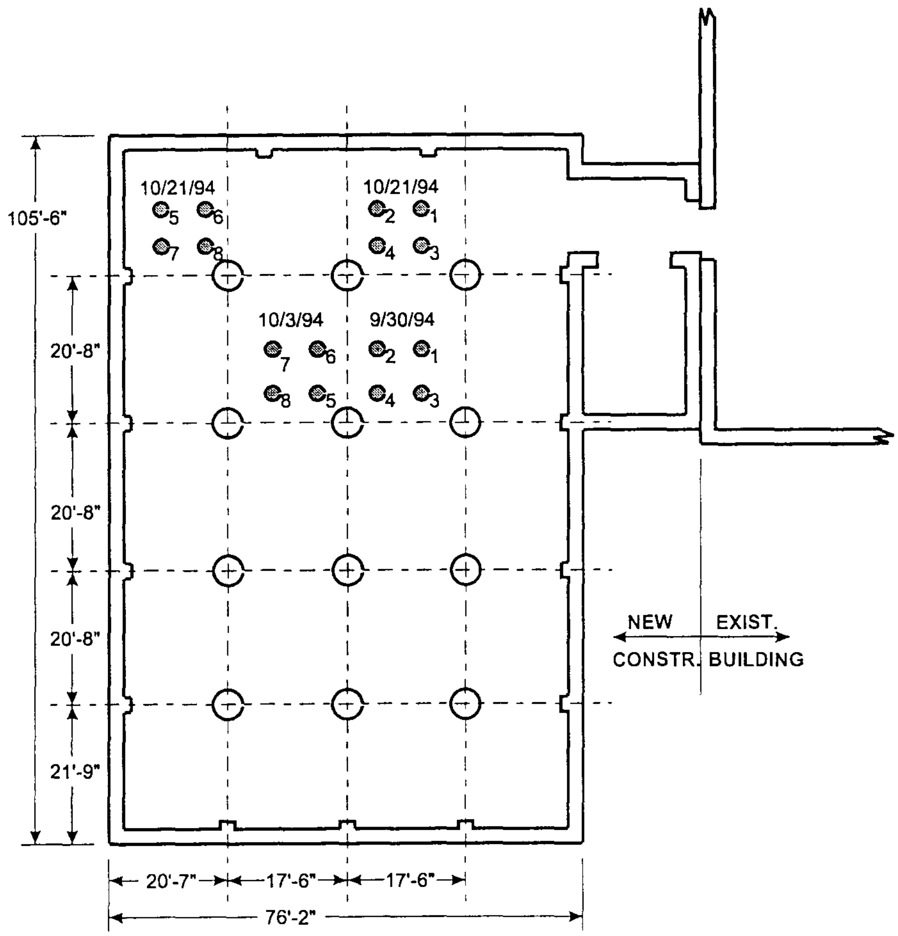

Figure 13.1 Floor plan and data collection locations for East Ave. Library storage facility.

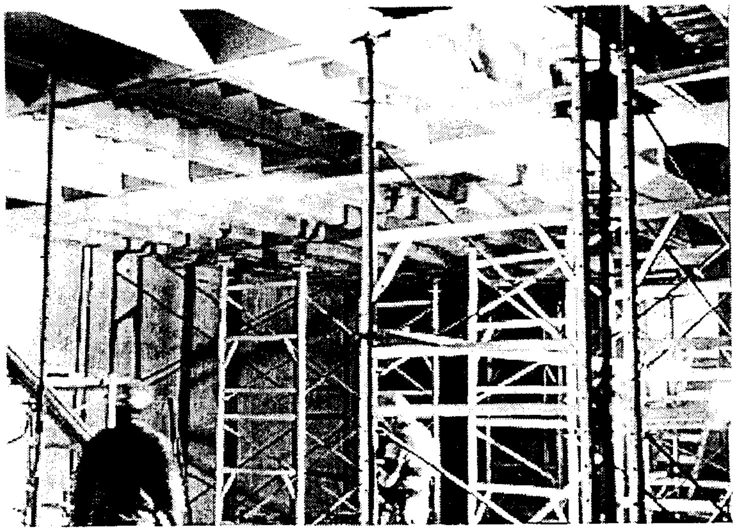

Figure 13.2 Shoring at the East Ave. Library Storage Facility.

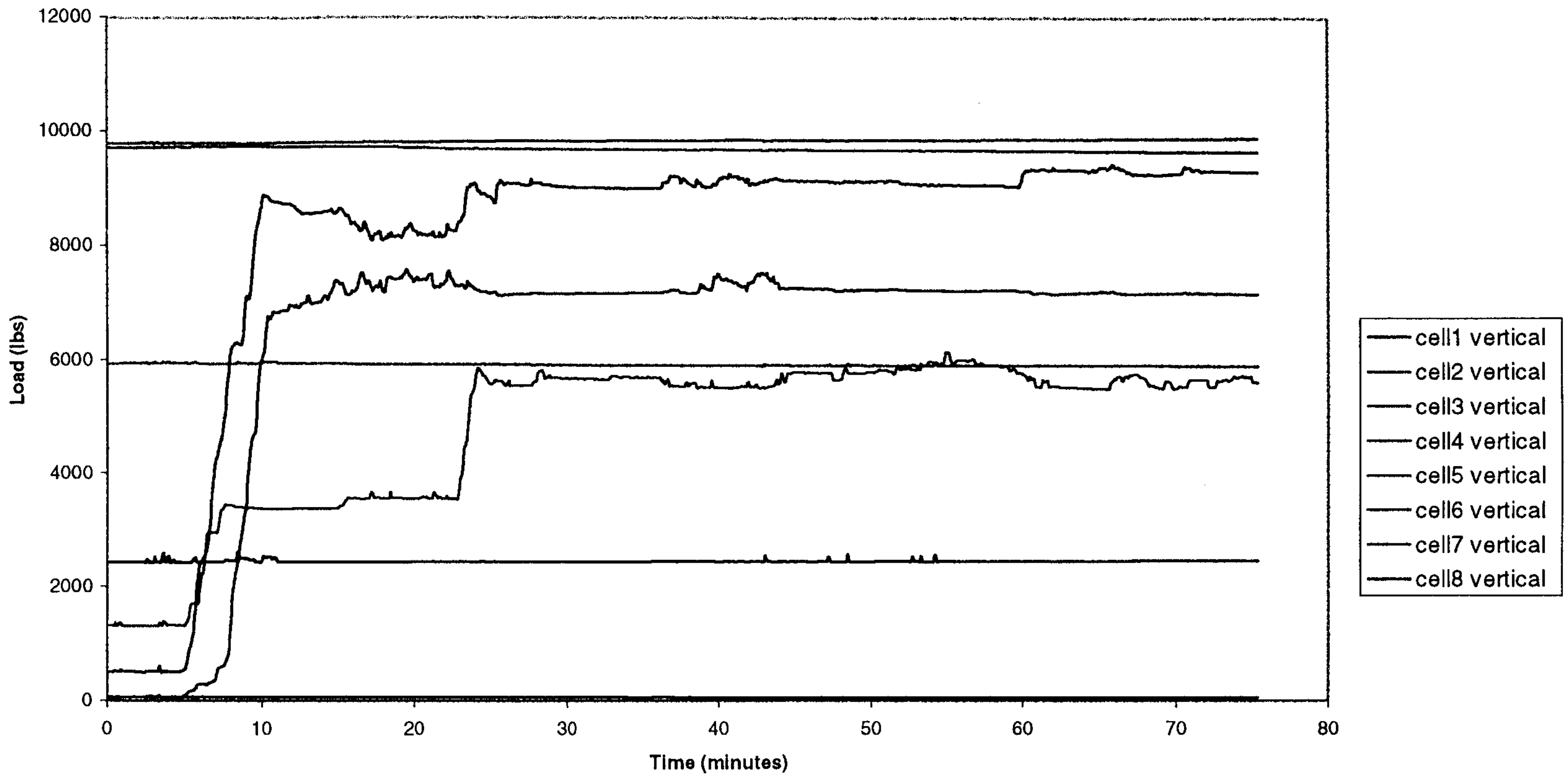

Figure 13.3 Vertical shore loads measured at East Ave. during pouring.

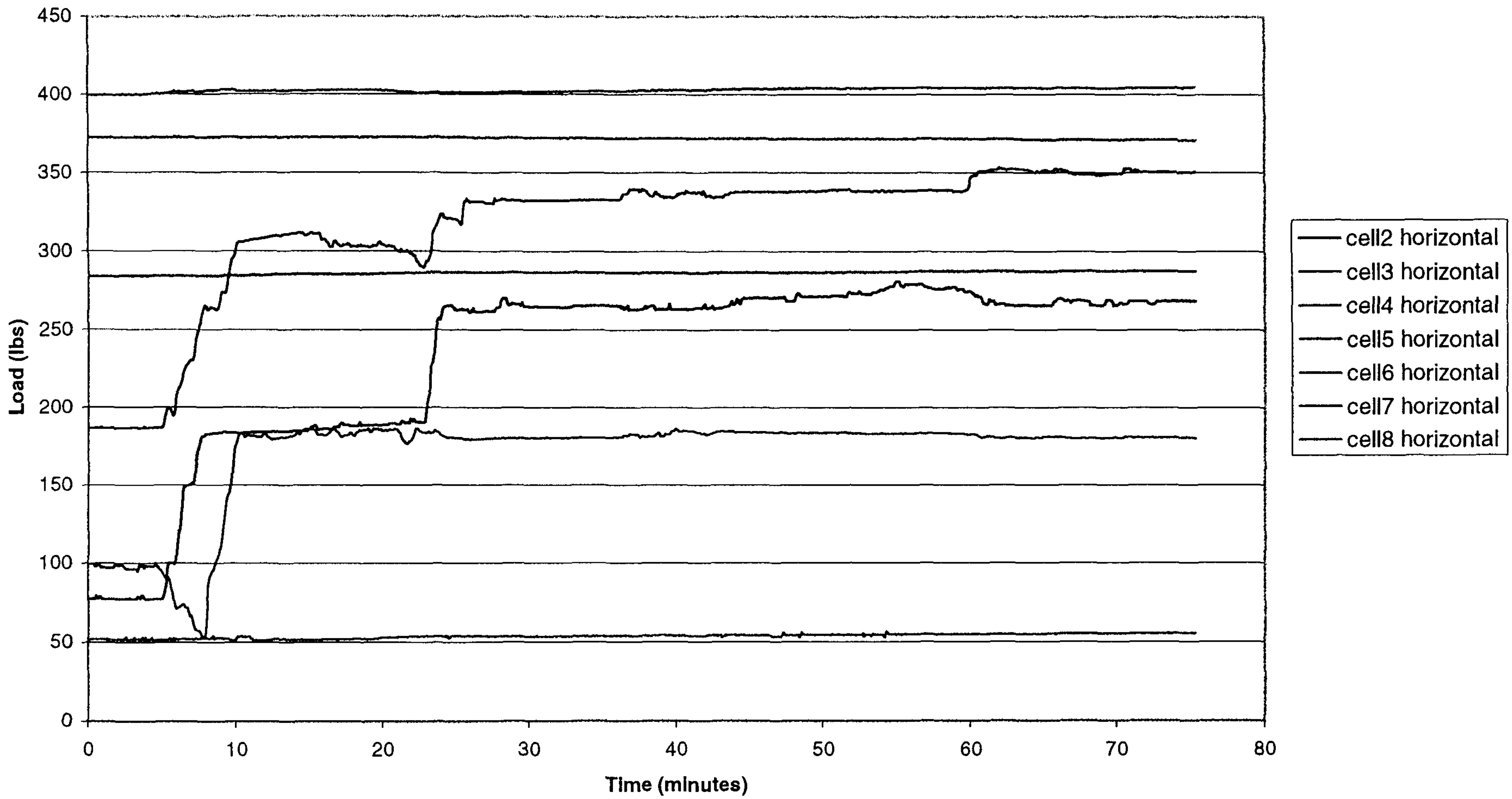

Figure 13.4 Horizontal shore loads measured at East Ave. during pouring

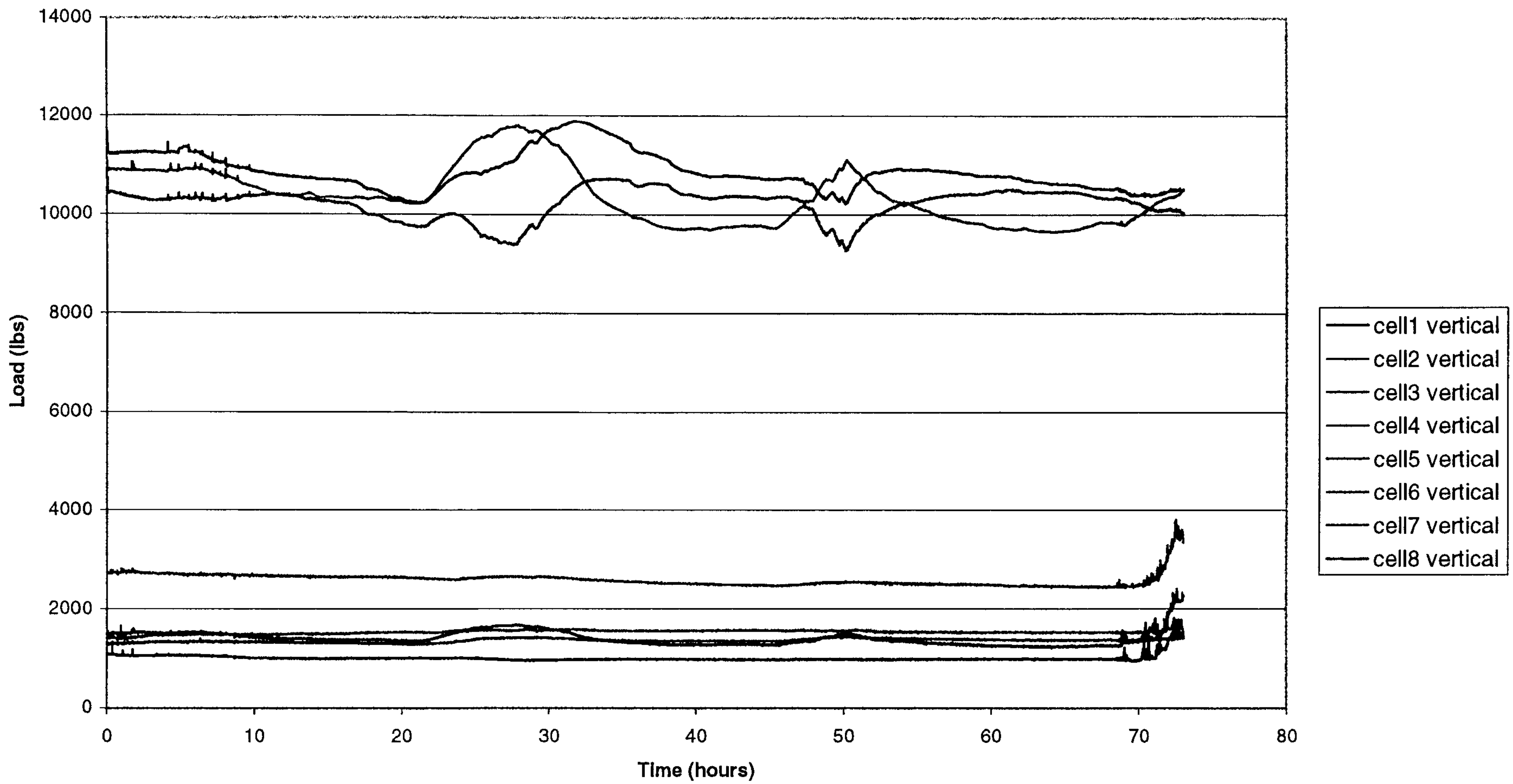

Figure 13.5 Vertical shore loads measured at East Ave. during curing

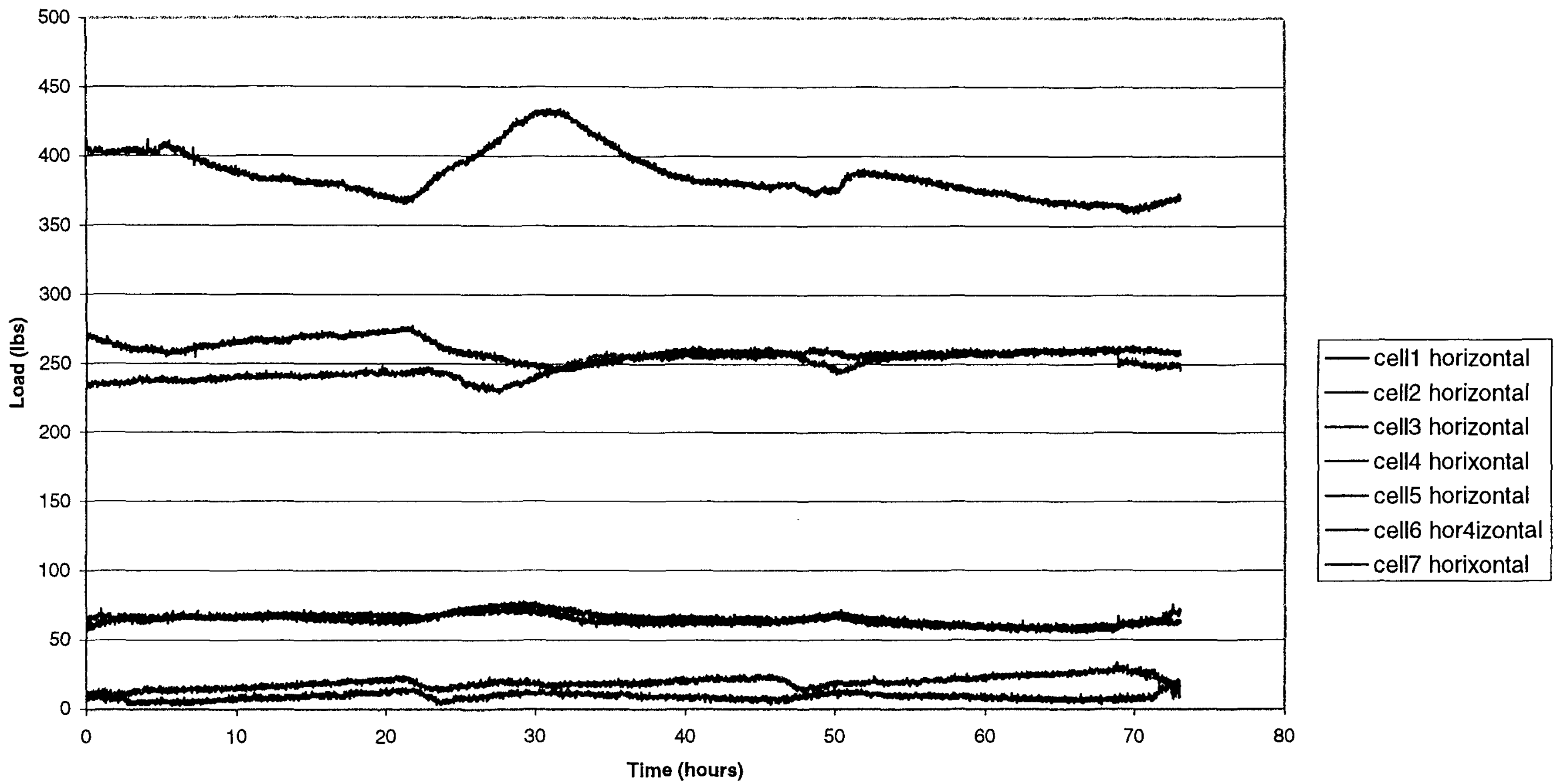

Figure 13.6 Horizontal shore loads measured at East Ave. during curing.

14. Pomeroy Hall VT Building Test

Following the completion of the data collection at the East Ave. site, finding a suitable building site became quite difficult. This was attributed to an overall lull in building construction in the Northeast and Midwest parts of the United States and due to the relative price of steel and concrete. During this period, steel was quite inexpensive and most buildings were being fabricated out of steel, rather than concrete. In order to maintain a stream of research during this lull between test sites laboratory and computational studies were conducted as described in Sections 10 and 11 of this report.

Eventually sites began to become available. The first site that became available was Pomeroy Hall on the University of Vermont campus. Pomeroy Hall is an old structure that was built in a series of steps starting in 1828 and ending around 1880. During the winter of 1997 the internal wood structure of Pomeroy Hall was gutted and replaced with a steel structure, while maintaining the external appearance of the building, Figure 14.1.

As part of the construction process vertical wood shores were used to support the roof structure. Load cells were placed in line with vertical shores. Figure 14.2 shows a floor plan and load cell locations. Based on prior experience at the Beckley and East Ave. sites, it was decided sample data at a much slower rate, once every fifteen minutes. The low sampling rate enabled the collection of static, but not dynamic data. It was assumed that there would not be many interesting dynamic loads for this shoring configuration.

Data were collected from January 9, 1997 to February 8, 1997. Figures 14.3 to 14.6 show the load data. The loads were not very large. However, the loads did show some large day to day variations. It was hypothesized that these variations were due to changes in thermal and snow loads. Figure 14.7 is a listing of the local weather conditions during this period as given by the Burlington Free Press.

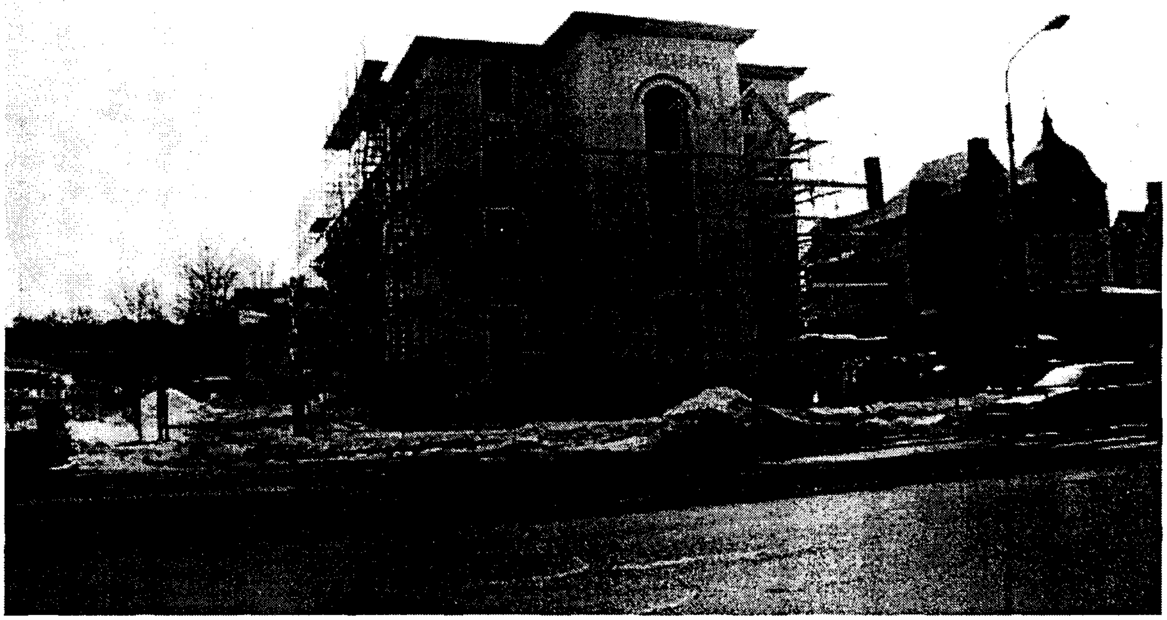

Figure 14.1 Pomeroy Hall at UVM under reconstruction.

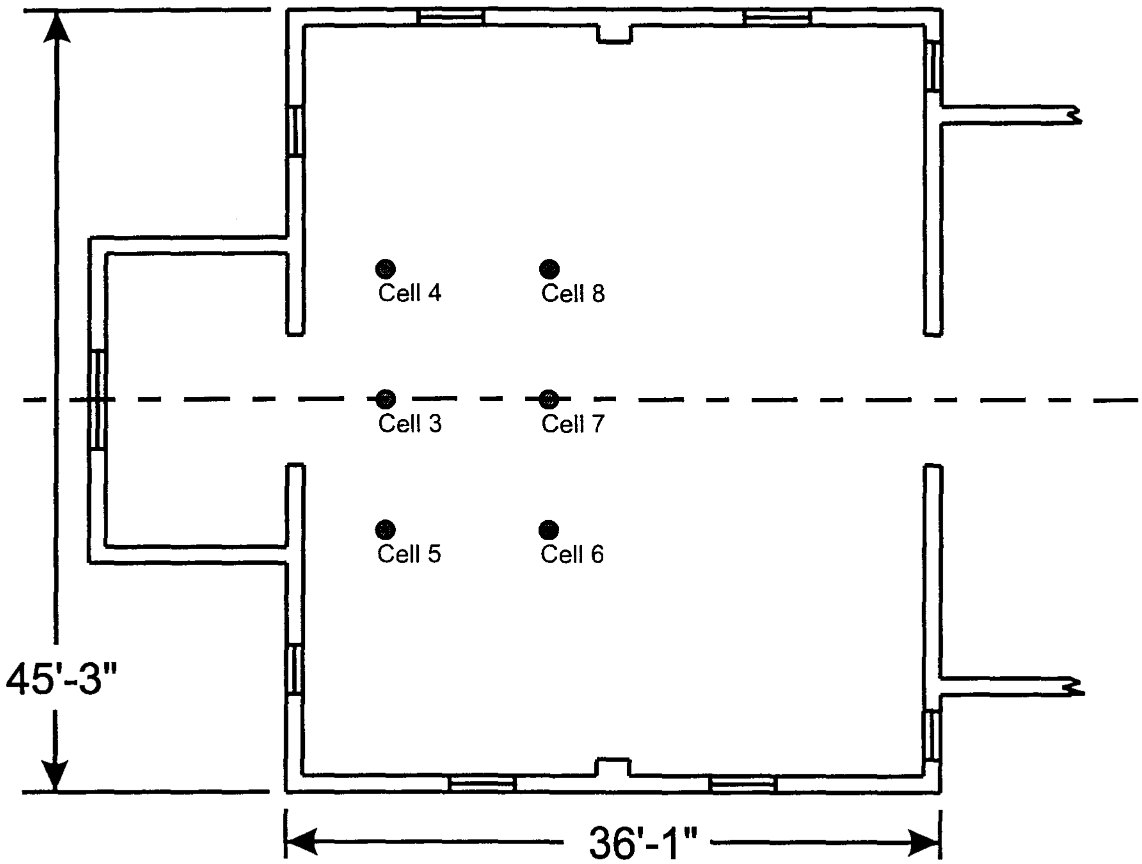

Figure 14.2 Floor plan of Pomeroy Hall and loadcell locations.

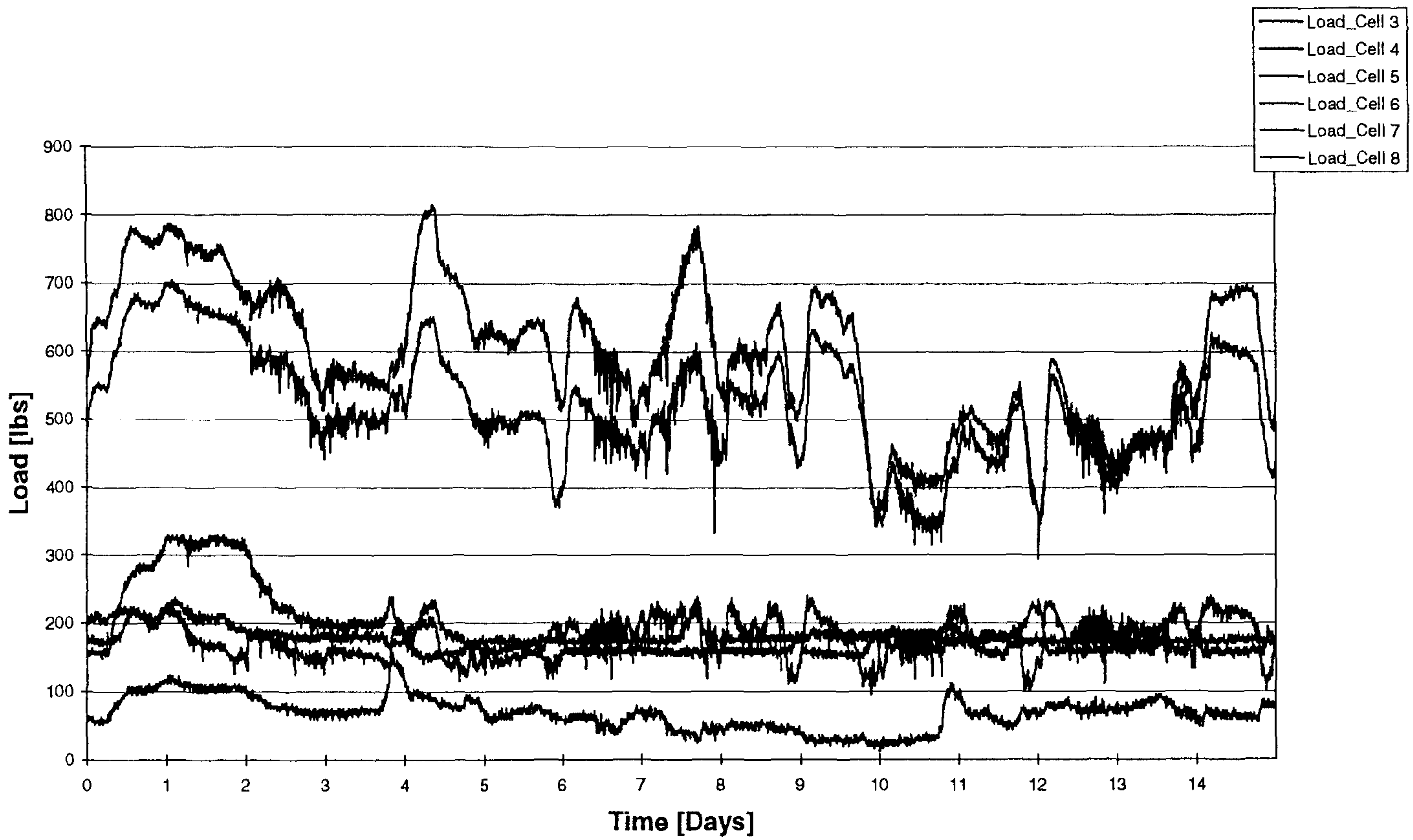

Figure 14.3 Vertical Shore Loads at Pomeroy Building
[from 1/9/97 to 1/24/97]

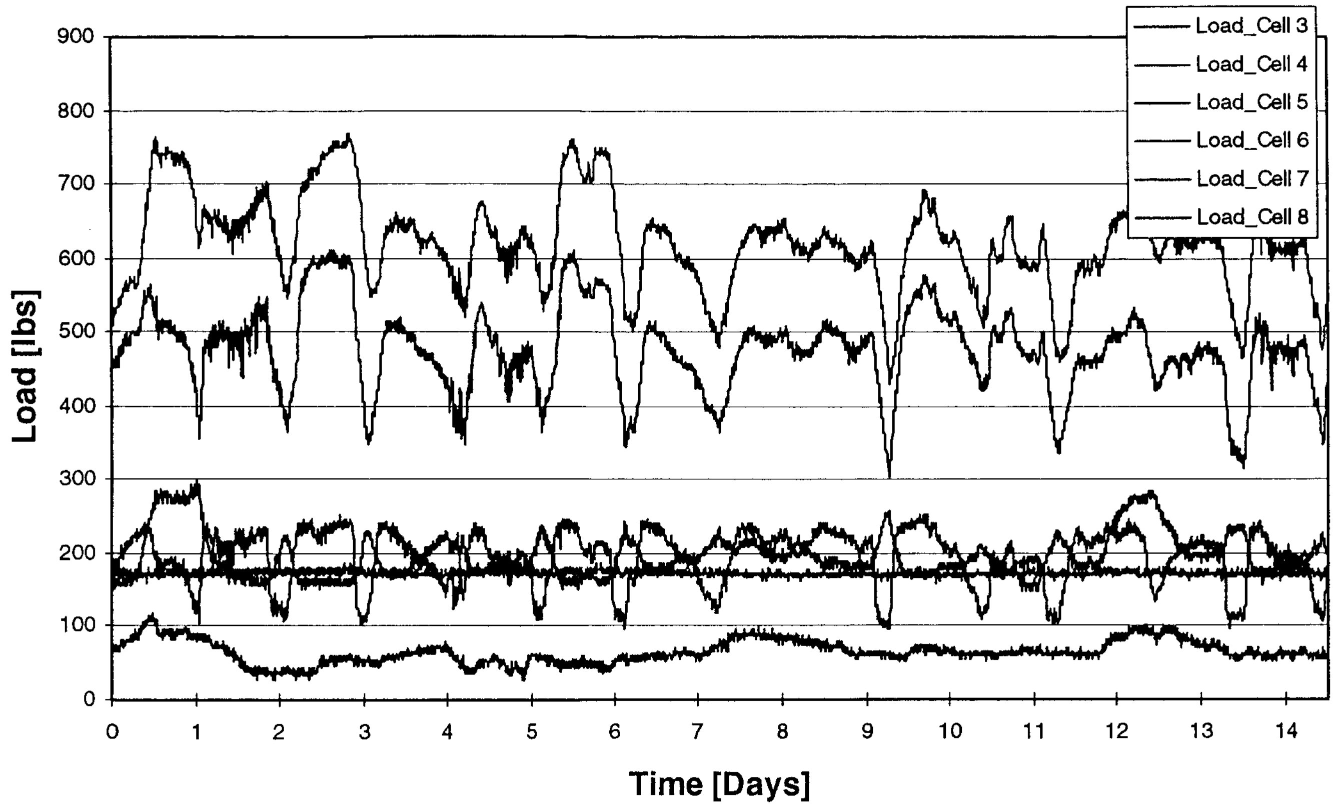

Figure 14.4Vertical Shore Loads at Pomeroy Building
[from 1/24/97 to 2/8/97]

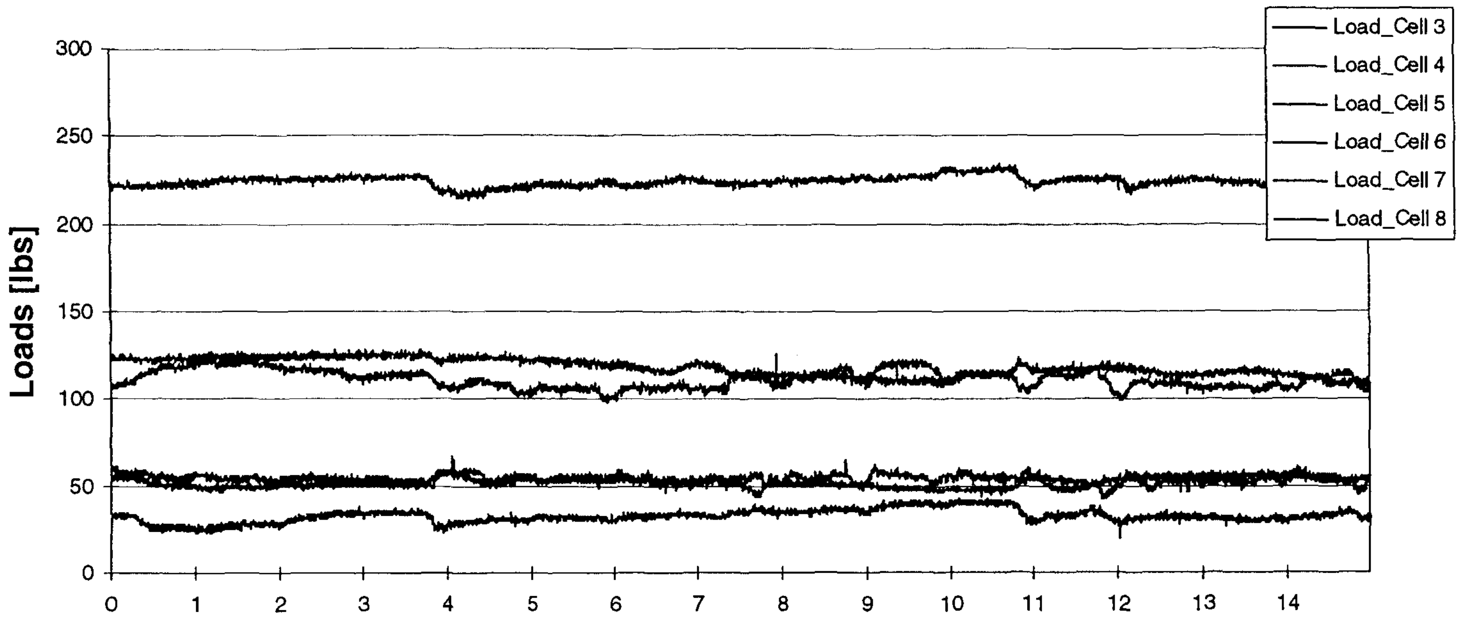

Figure 14.5 Horizontal Shore Loads at Pomeroy Building
[from 1/9/97 to 1/24/97]

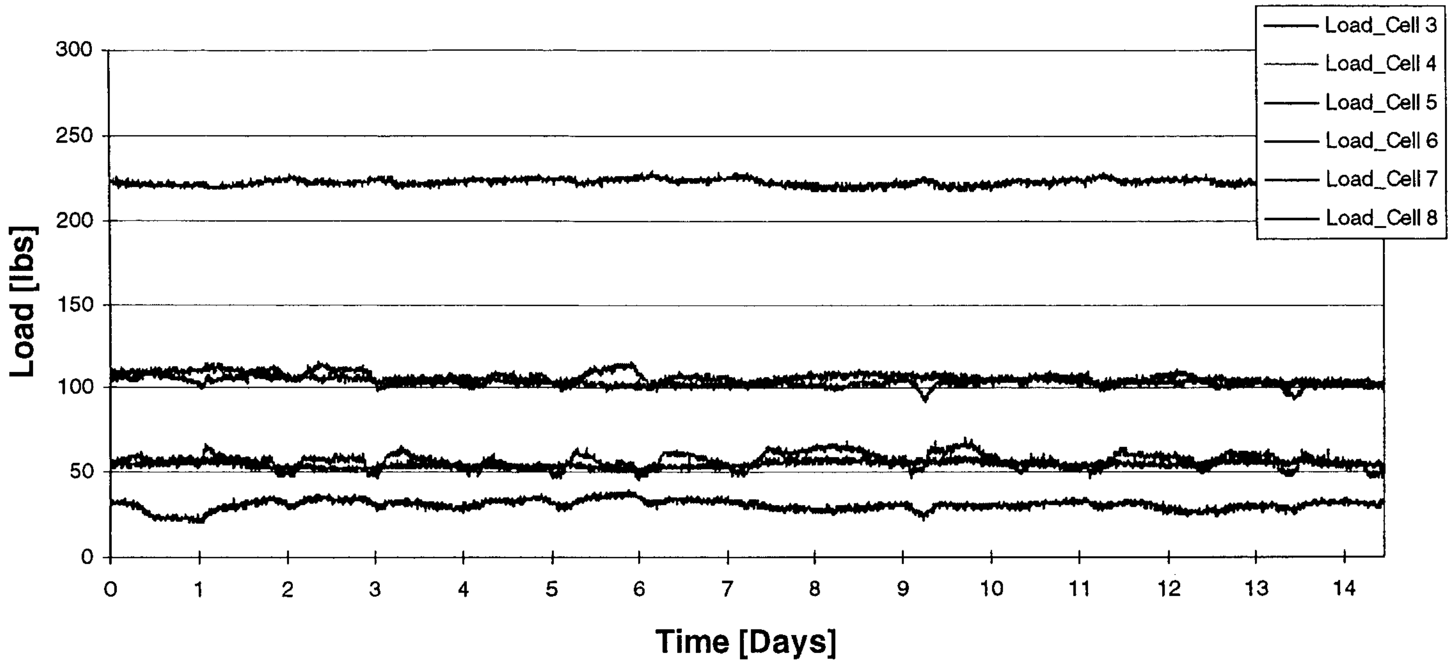

Figure 14.6 Horizontal Shore Loads at Pomeroy Building
[from 1/24/97 to 2/8/97]

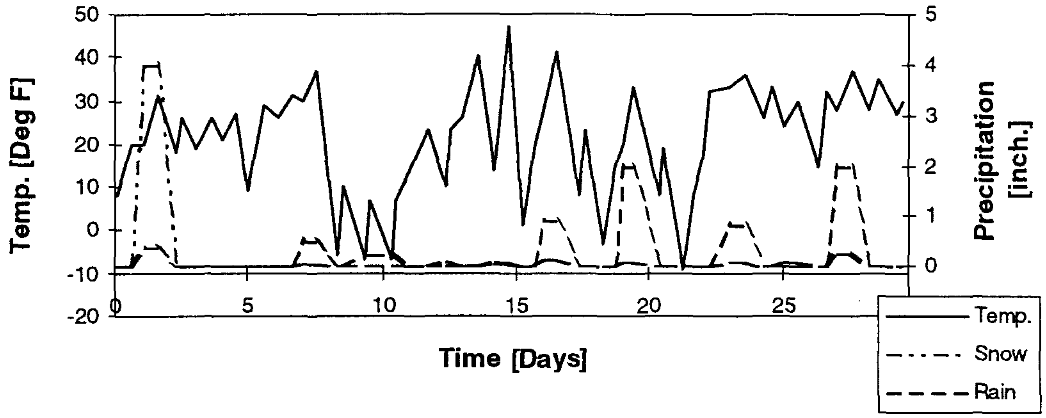

Figure 14.7 Weather Data in Burlington, VT

[Data obtained from the Burlington Free Press, 1/9/97 to 2/8/97]

15. Boston Museum Towers Building Test

15.1 Site Description

In the summer of 1997 a major concrete construction site in Cambridge, MA became available. This site, referred to in this report as the Boston Museum Towers, was a multiple building complex with two 25-story, one 5-story and one 7-story reinforced concrete buildings. Figure 15.1 shows one the Boston Museum Towers as it is about two thirds complete.

Figure 15.1 Boston Museum Tower under construction.

The lead structural engineering firm on this project was Weidlinger Associates of Cambridge, MA. Dr. Minhaj Kirmani, Suresh Babu, and Juan Pedro of Weidlinger provided a considerable amount of help during the project. The general contractor on the site was Beacon/Skanska Construction. Dr. James Becker and Walter Turgeon of Beacon also provided a considerable amount of assistance on the project.

Shore load data were taken during the construction of the South 25-story tower. This tower, as well as the North Tower, was constructed so that each story was virtually identical. The slabs were 8-in thick. In order to reduce costs and to avoid cold-weather concreting, the building was constructed at a fairly fast pace. A floor was poured every 4 or 5 working days. In order to sustain this pace without resorting to the use of rapidly curing concrete, a multilevel shoring system was used. It employed a rather unique drophead feature that enabled the removal of the formwork without requiring the removal the shores and a subsequent reshoring operation.

15.2 Data Collection

Data were taken at the site from June 2, 1997 to August 29, 1997. Since multilevel shoring was used, the load cell configuration was set up so as to measure the loads through cycles of multiple level shoring. For each floor, one of the large bays was selected for the placement of two load cells. Figure 15.2 is a photograph of a load cell installed in the shoring. Figure 15.3 is a photograph of a loadcell as it is wrapped in a water-resistant jacket. The location of the loadcells is indicated in Figures 15.4 and 15.5. A measurement cycle consisted of placing two load cells at locations A and B as indicated in Figure 15.5 and recording the data during pouring and curing operations on that floor. On the next floor two more load cells were placed on the shores at locations A and B directly above the shores for the shores for the two load cells below. This cycle was continued for up to five floors.

After the load cells were installed in a five-floor cycle, they were disconnected the data acquisition system moved, and the cycle restarted. The reason for using five floor cycles was twofold. One was that the shoring system used four and five stories per cycle. The other was that the load cell cables had finite length and had to be disconnected and the data acquisition system moved up to higher floors. The data acquisition system was housed in a very rugged steel crate. The crate required a crane to lift it up to the higher floors.

Load data were collected starting on the 8^{th} floor and continued up to the 22^{nd} floor. The data were collected fairly continuously over this time period. However, certain interruptions occurred. These were due to power losses, missed opportunities for load cell placement and the shorting of load cell cables when the load cells were hosed down with water during formwork preparation operations.

Even though the data acquisition rates were reduced to once every 10 minutes for the curing operations, and reduced to once every second during pouring, an enormous amount of data was collected. Reducing this data to meaningful information is a

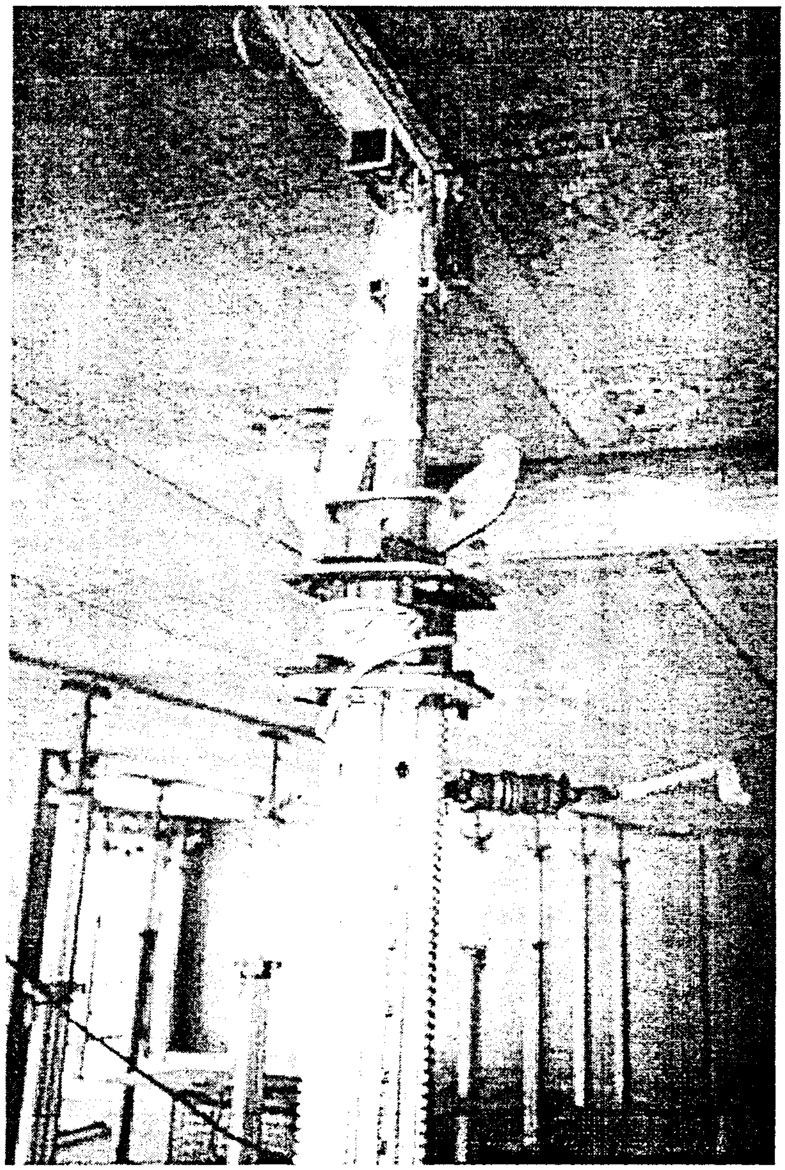

Figure 15.2 Load cell in the Boston Museum Towers shoring after the removal of the formwork.

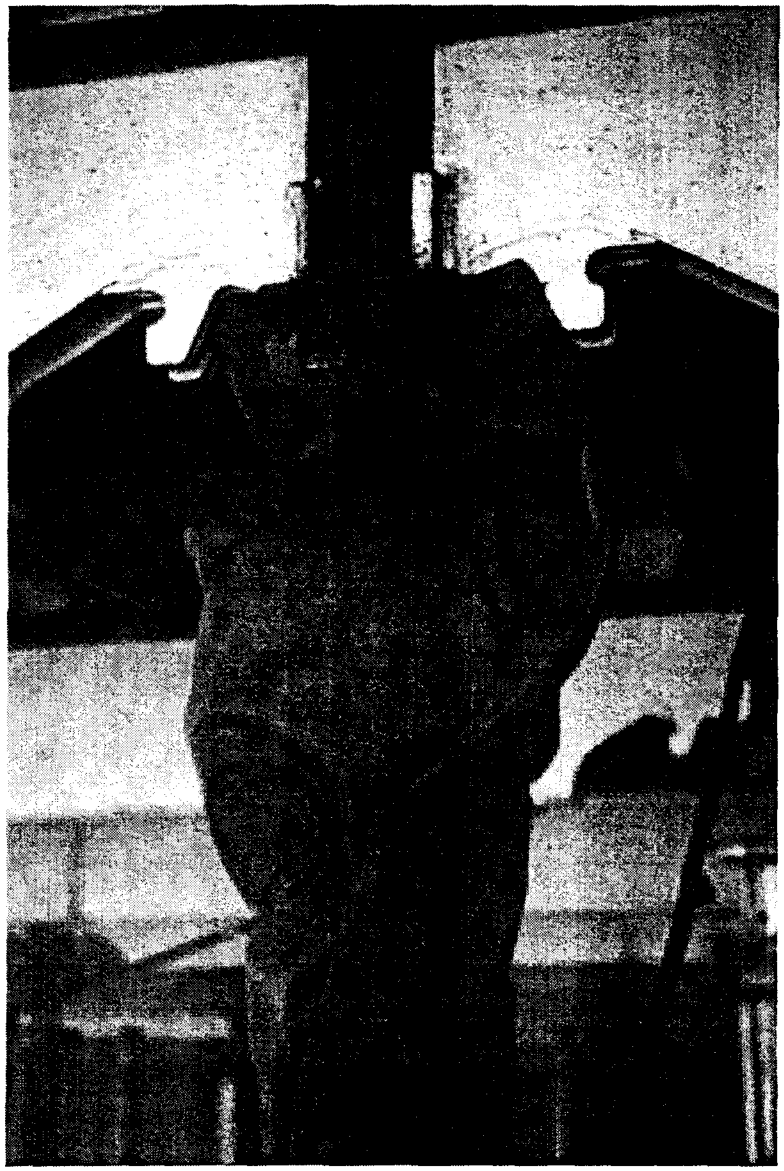

Figure 15.3 Load cell wrapped in water-resistant jacket.

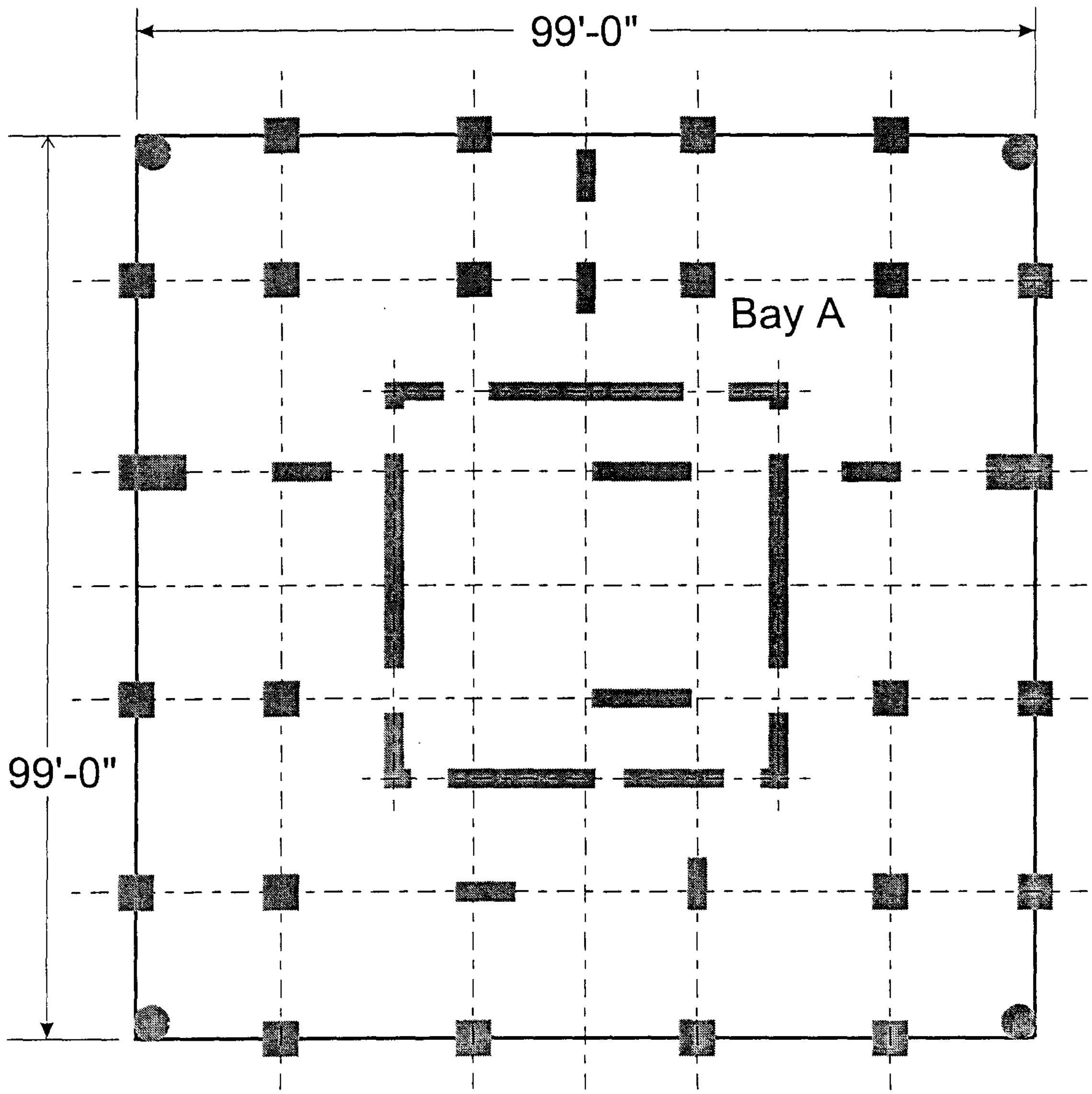

Figure 15.4 Floor plan at Boston Museum Towers and location of bay in which measurements were taken.

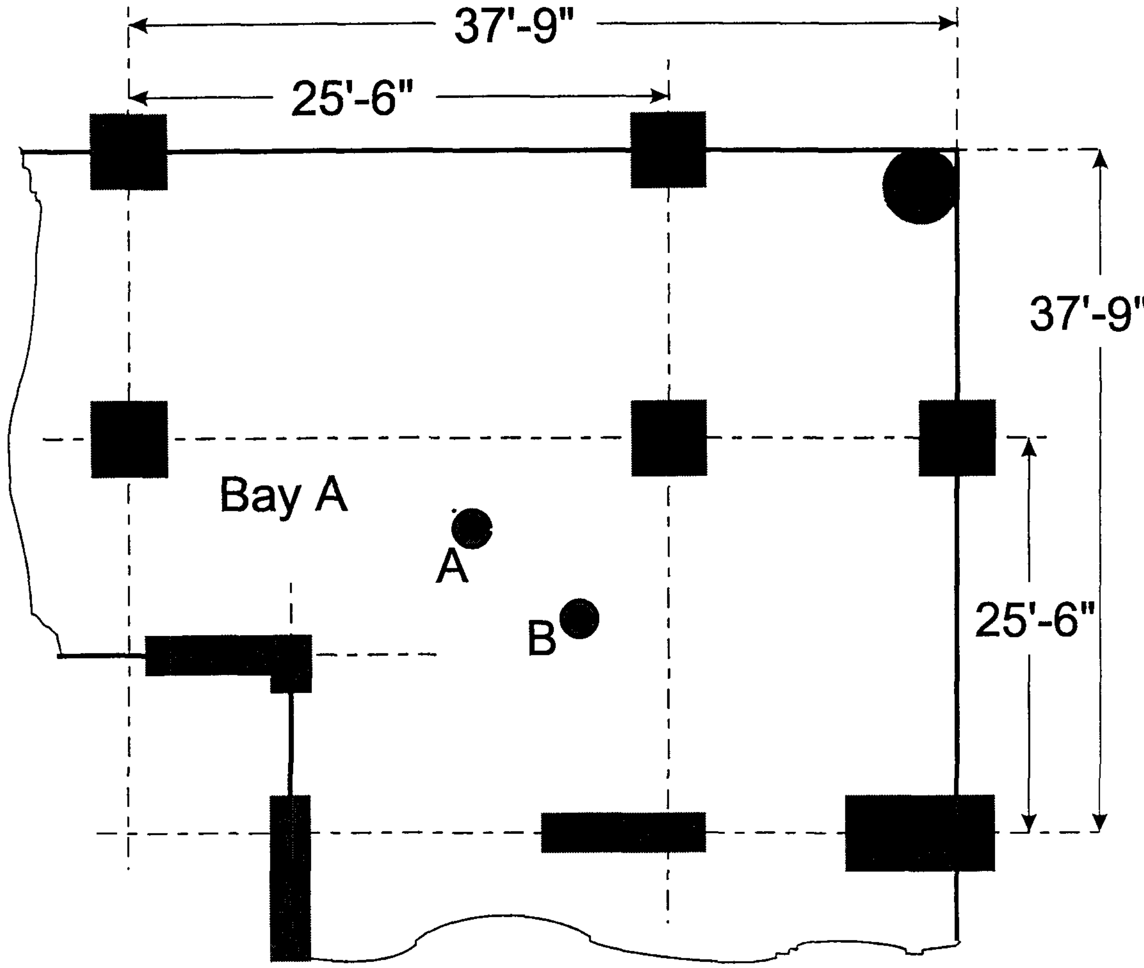

Figure 15.5 Location of shore load measurements at Boston Museum Towers.

daunting task that is still ongoing. The first pass at data analysis involved separating the data into 24-hour chunks that were of a more manageable size, and examining the data for any spurious signals. Spurious signals sometimes arose when the load cells were hosed down along with the forms before pouring. This would cause a shorting of the cables, which could be identified by wild full-scale swings in the recorded data. These traces were discarded. Appendix A1 contains the shore load data that were collected at the Boston Museum Towers for each 24-hour period during which data were collected. Appendix A2 shows the load cell configuration that corresponds to the data that appears in Appendix A1.

Each 24-hour period was then scanned for the maximum vertical and horizontal load on each load cell. Tables 15.1 through 15.9 show the 24-hour maximum vertical and horizontal loads for the months of June, July and August.

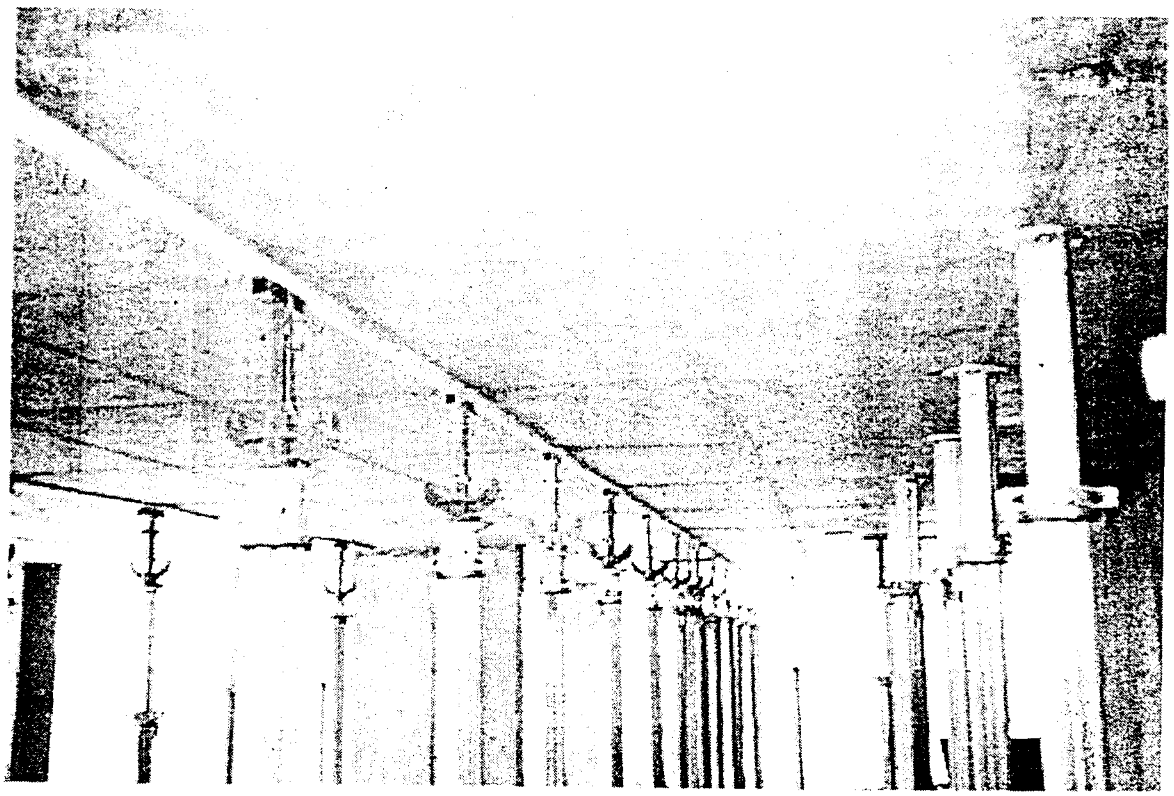

Figure 15.7 Peri shores with the formwork stripped from the dropheads.

Eliminating reshoring also allows a faster construction scheduled because the formwork can be stripped safely at an earlier time in the cure cycle. The use of drophead shoring may be one of those situations where the use of a new technology that promotes safety also is also a more economical technique. One of the disadvantages of using a drophead shoring system is that the system requires more individual pieces and increases the complexity of managing the inventory of shoring equipment on the construction site.

Date	Comments	1st story	2nd story	3rd story	4th story	5th story
6/2/97	8th Story Pouring					
6/5/97		3433				
6/6/97	9th Story Pouring	3425				
6/6/97		4066	5501	NA	NA	
6/7/97		4123	5964	NA	NA	
6/8/97		4304	6258	NA	NA	
6/9/97		4626	6772	NA	NA	
6/10/97		3415	4836	NA	NA	
6/11/97		2593	4096	NA	NA	
6/12/97	10th Story Pouring	2226	3566	NA	NA	
6/12/97		NA	3805	4331	NA	
6/16/97		2600	2957	7309	NA	
6/17/97		1463	2548	4806	NA	
6/18/97	11th Story Pouring	1478	2461	4716	NA	
6/18/97		NA	3485	3354	5387	
6/19/97		NA	NA	NA	NA	
6/20/97		4675	3025	3407	6827	
6/21/97		4946	3205	3657	7309	
6/25/97	12th Story Pouring	NA	NA	NA	NA	
6/30/97		2940	4460	2890	NA	NA

Table 15.1 Maximum Z-direction vertical loads (lb.) measured at Boston Museum Towers in June 1997. (NA = not available)

Date	Comments	1st story	2nd story	3rd story	4th story	5th story
6/2/97	8th Story Pouring					
6/5/97		-4				
6/6/97	9th Story Pouring	-4				
6/6/97		85	-8	NA	NA	
6/7/97		87	-10	NA	NA	
6/8/97		87	-12	NA	NA	
6/9/97		94	-16	NA	NA	
6/10/97		83	-17	NA	NA	
6/11/97		74	-17	NA	NA	
6/12/97	10th Story Pouring	66	-16	NA	NA	
6/12/97		NA	83	-13	NA	
6/16/97		107	77	18	NA	
6/17/97		113	75	7	NA	
6/18/97	11th Story Pouring	113	72	6	NA	
6/18/97		NA	156	78	12	
6/20/97		-53	155	81	22	
6/21/97		-55	157	83	25	
6/25/97	12th Story Pouring	NA	NA	NA	NA	
6/30/97		NA	-62	152	NA	-24

Table 15.2 Maximum X-direction horizontal loads (lb.) measured at Boston Museum Towers in June 1997. (NA = not available)

Date	Comments	1st story	2nd story	3rd story	4th story	5th story
6/2/97	8th Story Pouring					
6/5/97		174				
6/6/97	9th Story Pouring	176				
6/6/97		-126	222	NA	NA	
6/7/97		-129	231	NA	NA	
6/8/97		-130	237	NA	NA	
6/9/97		-142	248	NA	NA	
6/10/97		-110	240	NA	NA	
6/11/97		-71	269	NA	NA	
6/12/97	10th Story Pouring	-59	279	NA	NA	
6/12/97		NA	-63	302	NA	
6/16/97		70	-69	355	NA	
6/17/97		-56	-60	416	NA	
6/18/97	11th Story Pouring	-52	-57	452	NA	
6/18/97		NA	-16	-59	539	
6/20/97		54	-21	-77	706	
6/21/97		53	-21	-81	784	
6/30/97		NA	44	-44	NA	NA

Table 15.3 Maximum Y-direction horizontal loads (lb.) measured at Boston Museum Towers in June 1997. (NA = not available)

Date	Comments	1st story	2nd story	3rd story	4th story	5th story
7/1/97	13th Story Pouring	2790	4090	2650	NA	NA
7/1/97		NA	4705	5163	2949	NA
7/2/97		NA	5398	5604	2937	NA
7/3/97		NA	5044	5545	3232	NA
7/4/97		NA	4617	5651	3102	NA
7/5/97		NA	4386	5344	2945	NA
7/6/97		NA	4407	5478	3048	NA
7/7/97		NA	4145	5009	2685	NA
7/9/97	14th Story Pouring	NA	NA	NA	NA	NA
7/10/97		3180	NA	5060	3850	NA
7/11/97		3460	NA	5020	3170	NA
7/12/97		3360	NA	4780	3110	NA
7/13/97		3510	NA	4980	5260	NA
7/14/97		3130	NA	4500	4700	NA
7/15/97	15th Story Pouring	NA	NA	NA	NA	NA
7/17/97		3734	6276	NA	5624	6565
7/18/97		3932	5474	NA	5244	6108
7/19/97		2702	3630	NA	2907	3537
7/20/97		2866	3873	NA	3816	3993
7/21/97		2714	3615	NA	3518	NA
7/22/97	16th Story Pouring	2539	3237	NA	2388	NA
7/22/97		NA	4332	4577	NA	3467
7/23/97		NA	4275	4251	NA	3015
7/24/97		NA	3940	3964	NA	3431
7/25/97		NA	3449	3619	NA	3683
7/26/97		NA	3803	4342	NA	5398
7/27/97		NA	3589	4081	NA	4972
7/28/97		NA	3578	4270	NA	5105
7/29/97	17th Story Pouring	NA	3190	3604	NA	4253
7/29/97		NA	NA	3829	4130	NA
7/30/97		NA	NA	4164	4251	NA
7/31/97		NA	NA	3818	4232	NA

Table 15.4 Maximum Z-direction vertical loads measured (lb.) at Boston Museum Towers in July 1997. (NA = not available)

Date	Comments	1st story	2nd story	3rd story	4th story	5th story
7/1/97	13th Story Pouring	NA	-62	148	NA	-28
7/1/97		NA	NA	-73	150	NA
7/2/97		NA	NA	-82	152	NA
7/3/97		NA	NA	-81	155	NA
7/4/97		NA	NA	-83	155	NA
7/5/97		NA	NA	-78	151	NA
7/6/97		NA	NA	-81	152	NA
7/7/97		NA	NA	-72	148	NA
7/9/97	14th Story Pouring	NA	NA	NA	NA	NA
7/10/97		-78	NA	NA	-68	NA
7/11/97		-77	NA	NA	-66	NA
7/12/97		-79	NA	NA	-64	NA
7/13/97		-79	NA	NA	-81	NA
7/14/97		-79	NA	NA	-73	NA
7/15/97	15th Story Pouring	NA	NA	NA	NA	NA
7/17/97		-59	-71	NA	NA	-99
7/18/97		61	-87	NA	NA	-93
7/19/97		15	-88	NA	NA	-66
7/20/97		17	-87	NA	NA	-68
7/21/97		14	-85	NA	NA	NA
7/22/97	16th Story Pouring	14	-84	NA	NA	NA
7/22/97		NA	20	-79	NA	NA
7/23/97		NA	18	-87	NA	NA
7/24/97		NA	12	-87	NA	NA
7/25/97		NA	17	-87	NA	NA
7/26/97		NA	17	-85	NA	NA
7/27/97		NA	13	-87	NA	NA
7/28/97		NA	12	-88	NA	NA
7/29/97	17th Story Pouring	NA	17	-87	NA	NA
7/29/97		NA	NA	18	-89	NA
7/30/97		NA	NA	18	-90	NA
7/31/97		NA	NA	18	-90	NA

Table 15.5 Maximum X-direction horizontal loads measured (lb.) at Boston Museum Towers in July 1997. (NA = not available)

Date	Comments	1st story	2nd story	3rd story	4th story	5th story
7/1/97	13th Story Pouring	NA	37	-47	NA	NA
7/1/97		NA	NA	41	-45	NA
7/2/97		NA	NA	41	-51	NA
7/3/97		NA	NA	42	-47	NA
7/4/97		NA	NA	42	-46	NA
7/5/97		NA	NA	42	-53	NA
7/6/97		NA	NA	43	-47	NA
7/7/97		NA	NA	38	-48	NA
7/9/97	14th Story Pouring	NA	NA	NA	NA	NA
7/10/97		-57	NA	NA	42	NA
7/11/97		-60	NA	NA	41	NA
7/12/97		-60	NA	NA	42	NA
7/13/97		-66	NA	NA	53	NA
7/14/97		-57	NA	NA	47	NA
7/15/97	15th Story Pouring	NA	NA	NA	NA	NA
7/17/97		101	-115	NA	NA	53
7/18/97		100	-109	NA	NA	52
7/19/97		10	-87	NA	NA	40
7/20/97		10	-92	NA	NA	42
7/21/97		12	-84	NA	NA	NA
7/22/97	16th Story Pouring	11	-72	NA	NA	NA
7/22/97		NA	15	-104	NA	NA
7/23/97		NA	10	-99	NA	NA
7/24/97		NA	-5	-93	NA	NA
7/25/97		NA	5	-83	NA	NA
7/26/97		NA	3	-105	NA	NA
7/27/97		NA	-6	-102	NA	NA
7/28/97		NA	-7	-106	NA	NA
7/29/97	17th Story Pouring	NA	-3	-88	NA	NA
7/29/97		NA	NA	7	-102	NA
7/30/97		NA	NA	-8	-106	NA
7/31/97		NA	NA	16	-108	NA

Table 15.6 Maximum Y-direction horizontal loads (lb.) measured at Boston Museum Towers in July 1997. (NA = not available)

Date	Comments	1st story	2nd story	3rd story	4th story	5th story
8/1/97		NA	NA	2428	26	NA
8/2/97		NA	NA	2291	26	NA
8/3/97		NA	NA	2246	30	NA
8/4/97		NA	NA	2261	30	NA
8/4/97	18th Story Pouring	NA	NA	NA	NA	NA
8/8/97	19th Story Pouring					
8/14/97	20th Story Pouring		NA	NA	NA	NA
8/15/97		5065	NA	NA	NA	NA
8/16/97		4952	NA	NA	NA	NA
8/17/97		4948	NA	NA	NA	NA
8/18/97		4221	NA	NA	NA	NA
8/19/97		3888	NA	NA	NA	NA
8/20/97	21st Story Pouring	3646	NA	NA	NA	NA
8/20/97		4023	5970	NA	NA	
8/21/97		4107		NA	NA	
8/22/97		4099		NA	NA	
8/25/97		3966	5584	NA	NA	
8/26/97	22nd Story Pouring	3551	4528	NA	NA	
8/26/97		2730	6300	5900	NA	
8/27/97		3640	6510	6230	NA	
8/28/97		4530	6350	5970	NA	
8/29/97		4340	5410	5370	NA	

Table 15.7 Maximum Z-direction vertical loads (lb.) measured at Boston Museum Towers in August 1997. (NA = not available)

Date	Comments	1st story	2nd story	3rd story	4th story	5th story
8/1/97		NA	NA	19	25	NA
8/2/97		NA	NA	20	25	NA
8/3/97		NA	NA	24	24	NA
8/4/97		NA	NA	24	NA	NA
8/4/97	18th Story Pouring	NA	NA	NA	NA	NA
8/8/97	19th Story Pouring					
8/14/97	20th Story Pouring	NA	NA	NA	NA	NA
8/18/97		-82	NA	NA	NA	NA
8/19/97		-58	NA	NA	NA	NA
8/20/97	21st Story Pouring	-57	NA	NA	NA	NA
8/20/97		83	-77	NA	NA	
8/21/97		93	-79	NA	NA	
8/22/97		91	-77	NA	NA	
8/25/97		60	-32	NA	NA	
8/26/97	22nd Story Pouring	62	-30	NA	NA	
8/26/97		-66	41	-51	NA	
8/27/97		112	44	-58	NA	
8/28/97		105	44	-53	NA	
8/29/97		100	44	-46	NA	

Table 15.8 Maximum X-direction horizontal loads (lb.) measured at Boston Museum Towers in July 1997. (NA = not available)

Date	Comments	1st story	2nd story	3rd story	4th story	5th story
8/1/97		NA	NA	17	-9	NA
8/2/97		NA	NA	19	-9	NA
8/3/97		NA	NA	24	-8	NA
8/4/97		NA	NA	26		NA
8/4/97	18th Story Pouring	NA	NA	NA	NA	NA
8/8/97	19th Story Pouring					
8/14/97	20th Story Pouring		NA	NA	NA	NA
8/17/97		-165	NA	NA	NA	NA
8/18/97		-164	NA	NA	NA	NA
8/19/97		-151	NA	NA	NA	NA
8/20/97	21st Story Pouring	-151	NA	NA	NA	NA
8/20/97		-53	-207	NA	NA	
8/21/97		-56	-272	NA	NA	
8/22/97		-52	-203	NA	NA	
8/25/97		-60	-203	NA	NA	
8/26/97	22nd Story Pouring	-60	-174	NA	NA	
8/26/97		108	-74	-215	NA	
8/27/97		319	-80	-229	NA	
8/28/97		311	-83	-215	NA	
8/29/97		149	-77	-197	NA	

Table 15.9 Maximum Y-direction horizontal loads (lb.) measured at Boston Museum Towers in August 1997. (NA = not available)

16. Comparison of Measured Loads with Those Specified by Codes

16.1 Introduction

At this point the analysis of the shore loads measured at construction sites have only been completed for the loads that were measured at the Beckley WV federal prison. The details of this analysis have been published by Rosowsky et al. (1997). The loads measured at East Ave., Pomeroy Hall, and the Boston Museum Towers are currently undergoing detailed analysis. The results of the analysis of these structures should be completed in the early summer of 1998. The remainder of this section is a detailed analysis of the Beckley data and a comparison of the measured loads with the pertinent shoring codes.

16.2 Applied Loads vs. Load Effects

In order to provide design load values for construction that can be used in the design of formwork and other temporary support systems, information about the load effect rather than simply the applied load is required. This distinction is particularly important for buildings during construction. For these structures, all of the redundancies of the final structure are not yet in place, formwork systems are often much less stiff than the completed structure, and construction loads are often highly localized on the structure. The work by Ayoub and Karshenas (1994) used survey and inventory methods to collect data on the actual loads applied to formwork both before and after concrete placement. Fattal (1983) collected similar information on applied loads keeping extensive written and photographic records. However, adequate characterization of the applied loads, including spatial correlation (Karshenas and Ayoub, 1994), may not be sufficient to describe the actual load effect experienced by the shores. Karshenas and Ayoub (1994) employed the concept of an "influence surface" to develop equivalent uniformly distributed loads (EULDs) that produced the critical load effect in the shores. However, owing to simplifications in the structural model, this approach is unable to account for discontinuities in the formwork, variable installation procedures, and other actual site conditions. Studies by Yen et al. (1995), Peng et al. (1995), and Rosowsky et al. (1995a) have all shown that these can have significant effects on the actual shore loads, and that the spatial variability associated with load effect can be much greater than that associated with the applied loading.

As an alternative to developing more complex structural analysis models, actual shoring load measurements can be taken to provide much needed information on magnitude and variations in load effect. In addition, this information can be used to develop a relationship between the applied loading (i.e., actual loads on the slab) and the shore load effect, thereby providing information on load-structure interaction. A summary of recent and on-going projects in which actual shore load data is being collected is presented in (Rosowsky et al., 1994b).

16.3 Description of Beckley, WV Site

The first site at which extensive data were collected was a low-rise concrete prison facility under construction in Beckley, WV (Huston et al., 1995). The observations described in this paper are based on the data collected from this site. Two specific locations were instrumented and loads were monitored prior to placement of the concrete slab, during concrete placement, and after the slab were completed. Only shoring data were collected since reshores were not used. Two small pour areas were instrumented at the Beckley site. These areas, shown in Figure 12.5, were identical 0.2-m (8-in.) thick slabs with pour areas of approximately 8.10 m 2 (87 ft2). Since these areas were small, only four steel shores were used for vertical support during the pours. All four shores were instrumented for each of the small pour areas. Two steel I-beams were used to support the forms in each of the small pour areas. These I-beams spanned from shores 1/5 to shores 3/8 and from shores 2/7 to shores 4/6 (see Figure 12.5). The steel 1-beams supported wooden stringers that in rum supported the plywood forms.

The large pour area was approximately 51.28 m^2 (552 ft^2) and sixteen steel shores provided vertical support. The slab thickness was 0.2 m (8 in.) and 0.4 m (16 in.), as shown in Figure 12.6. Steel I-beams were used as the primary support for the 0.4-m (16-in.) slab thickness section. Four I-beams were used to span between shores 1-2, 3-4, 5-6, and 7-8 (see Figure 12.6). The I-beams supported aluminum I-beams which spanned the 7.32 m (24 ft.) length of the large pour area. Aluminum I-beams were also used to span from these members to two exterior steel 1-beams also spanning the 7.3'2 m (24 ft.) length, thereby providing support for the 0.2 m (8 in.) thick slab sections. Only those shores indicated in Figure 12.6 were instrumented during the large pour.

16.3 Data Collection, Reduction and Analysis

The data collected at the Beckley site included vertical and lateral shore load effects (one vertical and two lateral load channels per instrumented shore) during both the pouring and curing phases for each pour area. The sampling frequency for the pouring data was 100 Hz. This permitted the collection of sufficient data for later dynamic load analysis. Since the pour durations were several minutes, the data files were typically too large to be manipulated efficiently. For the purposes of data analyses, the data sets were reduced to more manageable sizes by stripping nine out of each ten points from the raw pour data. The effects of this data reduction were not noticeable during graphical comparisons (i.e., no load spikes were lost), however this information might need to be re-included for any dynamic analysis. Although the curing data were sampled at a lower frequency, similar reductions were performed to maximize efficiency during data analyses.

The load effect data were zeroed from the beginning of the individual pours. This procedure provided the load effects due to the pour only, thereby neglecting any residual prepour loads applied to the shores. The lateral load effects were compared to the vertical load effects for each shore and graphical representations of the two were examined to determine the existence of any correlation between them. Additional work included statistical analyses to determine time-dependent average load effects and load multipliers (which, when multiplied by the average shore load at a given time step, give the actual shore load). Design loads for the shoring members were also determined using published values and procedures (i.e., ACI) and compared with the measured load effects.

16.4 Discussion

Lateral load effects in the shores were examined first. Consideration was given to (1) the relative magnitude of the horizontal loads, and (2) the correlation of horizontal loads with vertical loads. Provisions for horizontal design loads for construction are particularly limited. It is, however, widely believed that lateral instability is the primary cause of most formwork collapses. Figure 16.1 shows the lateral load effects (in one direction) for the small pour area as a percentage of the vertical load acting at the same time. The pouring activities occurred approximately between minutes 15 and 30. As Figure 16.1 suggests, when the majority of the vertical load is already applied, the lateral load is about ±10% of the corresponding vertical load. While percentages are somewhat higher earlier during the pour activity, this corresponds to points at which the actual vertical load is low; thus, the lateral load effect would not be large. Nearly identical trends were observed in the other lateral direction as well as for both lateral directions for the large pour area. This value of ±10% provides a simple Guideline for approximating lateral loads on formwork.

Vertical loads were examined next. Figure 16.2 shows the vertical load in the four shores used in one of the small pour areas. Values are shown for the entire construction activity process, including activities on the slab just prior to the concrete being, poured, the actual concrete pouring operations, and a small amount of post-pour activity. By considering the load traces as they reach their maximum values (i.e., toward the end of the pouring activity), along with the average values, some indication of the relative variability in shore loads (i.e., variations shore-to-shore) can be obtained. Recall that these four shores are part of the same single scaffolding unit and are therefore quite close together. In order to examine more clearly this variability, the ratio of individual shore load to average shore load was calculated and is shown in Figure 16.3. Only the actual pouring process is shown (i.e., significant applied loads) starting at minute 18. Figure 16.3 clearly indicates both the relative variability shore-to-shore and the variations of shore loads from the time-dependent average shore load. A shore load multiplier (vertical axis) of 1.0 at the end of the pour would imply that a simple tributary area analysis would be adequate for assigning portions of the total applied load to the individual shore. Figure 16.3 indicates that shore load multipliers in excess of 2.0 were seen in this case.

Figure 16.4 shows a detailed load trace (for the actual pour activity that occurs in the first 24 minutes) of the maximum of the four vertical shore loads in the small pour area along with the average shore load trace. Also shown on this figure are two possible design load values, the ACI design load and the tributary area load. The ACI design load (see ACI 318, 1989 and ACI Committee 347, 1988) is the minimum load suggested by ACI, including concrete and equipment, for the actual slab area. ACT specifies a minimum design dead load of 41.3 N/m^2 (100 psf) for supported slab areas when designing vertical shoring members and shoring placement. This load corresponds to the dead load that would be produced by 0.2 in (8-in.) slab thickness. If the slab thickness exceeds 0.2 in (8 in.), the design dead load should be increased appropriately. In addition, ACI specifies an increase of 20.66 N/m 2 (50 psf) to account for live loads, material storage, impact effects, etc. The tributary area load shown on Figure 16.4 is simply the estimated weight of the completed concrete slab divided by the controlling tributary area for the shores. The tributary area load for each pour was calculated based on the shore that had the largest area of slab to support. For example, the large pour area had many different shore tributary areas, but shores 1 and 2 supported the largest areas. Each of these shores supported a total slab tributary area of 4.44 m^2 (47.8 ft^2), corresponding to a dead load of 27.4 kN (6150 lb.). The design load is therefore simply the tributary area dead load for the shores with an additional loading of 20.66 N/m 2 (50 psf) to account for live loads, material storage, impact loads, etc. The additional loading produces a design load, in the cases of shores 1 and 2, of 38.0 kN (8540 lb.). Note in Figure 16.4 that the ACI design load is very close to the maximum shore load, and the tributary area load is very close to the average shore load. Figure 16.5 shows the period following the pouring activity (i.e.. early curing activity) for the two adjacent small pour areas. Note that this graph covers a time period of nearly three days. During this time, relatively little load was applied to the slab. However, the individual load traces exhibit slight variations on an essentially daily cycle. This graph also illustrates the relative variability among the shore loads and their magnitude relative to the ACI design load.

Figures 16.6 and 16.7 present data obtained from the larger pour area. Figure 16.6 shows a detailed load trace (for the actual pour activity that occurs in the first 48 minutes) of the maximum of the eight vertical shore loads in the large pour area along with the average shore load trace. Also shown on this figure are the two possible design load values described previously. In this case, the tributary area design load (concrete only) appears to be adequate for the maximum shore load, while the higher ACI design load (concrete and equipment) overestimates the actual maximum shore load by about 35%. Since the slab thickness, formwork, and placement procedures are all comparable, this is evidence of a possible area effect. That is, as the effective area increases, currently suggested design loads become more conservative. This may suggest the use of a construction load reduction factor for large pour areas, similar to the live load reduction factor in ASCE 7 (ASCE, 1993). Figure 16.7 shows the period following the pouring activity (i.e., the early cure period) for the large pour area. This graph also illustrates the relative variability among the shore loads and their magnitude relative to the ACI design load. During this time, relatively little load was applied to the slab. However, the individual load traces exhibit definite variations on an essentially daily cycle. These daily fluctuations are much more pronounced than they were for the smaller area. Since no significant loads were being applied or removed during this period, the fluctuations in shore loads must be a result of changes in the ambient environmental conditions at the site. Being early Fall in West Virginia, daily temperature variations can be substantial. During the actual instrumentation period, differences in temperatures from day to night varied by about 17°C (30°F). Steel shores will expand and contract significantly under a 17°'C temperature gradient. Assuming a steel shore (typical) with a diameter of 4.32 cm (1.70 in.), wall thickness of 0.28 cm (0.11 in.), and a shore length of 183 cm (72 in.), the calculated difference in shore length due to thermal expansion would be 0.036 cm (0.014 in.). The change in load carried by a shore would be related to its length (or change in length) by the relationship $\Delta L=(\Delta P)L_O/AE$, where ΔL is the change in length of the shore, L_O is the original length of the shore, A is the cross-sectional area of the shore, E is the elastic modulus of the steel, and ΔP is the calculated change in shore load due to the temperature gradient. For this case, the value of ΔP was found to be 13,800 N (3,110 lb.). As seen in Figure 16.7, changes in shore load of up to 6 kN (1,350 lbs.) were recorded; the difference between the predicted and the observed values may be the result of load sharing.

In addition to these daily fluctuations in load, many of the shore loads in Figure 16.7 exhibit a general decreasing trend with time. Since relatively little load was applied to the fresh slab during this early cure period, and certainly no significant load was removed, this decrease in shore load is likely a function either of creep effects in the concrete or gain in strength and stiffness of the slab. The actual mechanism leading to this apparent decrease in shore load remains to be investigated. However, it is likely that the explanation for this phenomenon will also provide some insight into the evolution of the fresh slab, with essentially no load-carrying capabilities, into a structural element that is carrying part of its self-weight in addition to applied loads. This information may be useful in determining safe shore removal times.

16.5 Additional Investigation

In order to further investigate the possibility of a load reduction, the data collected by Fattal (1983) from a multistory flat-plate type concrete building were considered. The effective slab area (pour area) was similar to that of the large pour area from the Beckley, WN site; however, the design loads (which are functions of the pour area and the slab thickness) were roughly halfway between the values for the small and large Becklev pour areas. While the sampling frequency used by Fattal was far lower than that used in the Beckley investigation, and the data were available only in analog rather than digital form, sufficient information existed to develop figures such as those described above. Figure 16.8 presents the actual shore load data for one pour area along with the average shore load trace. One shore in particular exhibited much higher loads than the others. This began very early in the concrete placement process. This is likely due to some deficiencies in the shore installation. Even before half of the total slab load is placed on the formwork, the load in that shore is far in excess of the ACI design load. The tributary area load is slightly conservative relative to the average shore load. Disregarding the shore with the very high loads, the ACI design load closely predicts the maximum shore load.

Comparing the results from the Beckley site (Figures 16.4 and 16.6) with those from Fattal's study (Figure 16.8) suggests that a load reduction effect may indeed exist but may not simply be a function of the pour area. Rather, a load reduction may be appropriate for certain cases as a function of pour area, slab thickness, formwork arrangement, and perhaps method of placement. Collection of data from additional sites and analytical investigations (structural modeling) are required in order to examine this issue further. Both of these are planned as part of this project and the results are expected to be reported in the next year.

16.6 Shore Removal

Shore removal procedures can induce significant loads, often of an impact nature, on both the supporting formwork elements and the freshly cast slab. The magnitude of these loads is a function of amount for compression in the shore at the time of removal and the procedure used for the removal of that shore. In some cases, this may involve knocking out the shore or the shims with a hammer. while in others it may be accomplished by first slowly relieving the compression in the shore. As part of the data collection activity at the Beckley, VN site, shore loads were recorded during the removal of the eight shores in the large pour area. Figure 16.9 shows the shore loads and clearly indicates when the individual shores were removed. Also shown on this figure are the tributary area load (concrete only) and the ACI design load (including provisions for equipment). The locations of the numbered shores are shown in Figure 12.6.

As can be seen from Figure 16.9, the loads resulting from shore removal take two forms: (1) additional compression in the shore as part of the actual removal procedure, and (2) load redistribution to remaining shores following shore removal. When the first shore was removed (shore 4), only shore 6 saw a significant increase in load. As seen in Figure 12.6, these two shores were very close to each other. Note also that with this redistributed load from shore 4, the load in shore 6 increased above the tributary area load. When shore 2 was removed, the majority of its load appears to have been picked up by shore 5. Note (Figure 12.6) that these two locations are not very close to one another. When shore I was removed, shore 6 was the only shore to see a significant increase in load. Even though two other shores were still 'n-place (7 and 8), they were on the other side of the slab; hence their was limited load sharing (redistribution). At this point, the load in shore 6 was very close to the ACI design load. Finally, when shore 6 was removed, its load was picked up entirely by the slab (i.e., shores 7 and 8 did not see significant increases). In effect, a 40 kN (8990 lbs.) load was applied nearly instantaneously to the fresh slab at shore location 6, near the center of the slab. The potential for increase in load as part of the shore removal operation is illustrated by the removal of shores 2 and 8. When shore 2 was removed, the load increased by about 25%. The removal of shore 8, which appears from Figure 16.9 to have been a two-step process, resulted in an increase in shore load of more than 250%. Clearly, the procedure used to remove shores can significantly affect the shoring (and slab) loads and hence the safety of the structure during construction.

16.7 Conclusions and Implications for Design Loads

A preliminary analysis of shore load data collected during actual concrete construction has been performed and a number of significant observations have been made. These observations shed new light on the load sharing behavior of formwork systems, identify potentially hazardous procedures and conditions during concrete operations, and can be used to assess the adequacy of current construction design loads (i.e., those suggested by ACI). Specific findings reported herein include:

1. The observed lateral shore loads were typically on the order of ±10% of the corresponding (i.e., simultaneous) vertical load.

2. A magnification factor on the order of 2.0 may be appropriate to account for the (spatial) variability among a group of shores in a common pour area. The degree of variability shore-to-shore appears to be a function of the amount of precompression imparted during installation.

3. The suggested ACI design load, including equipment, appears to be adequate for the slab areas considered in this study. The simpler "tributary analysis" design load well approximates the average shore load, while the more conservative ACI load (including equipment) well approximates the maximum shore load. However, an error in the installation of a shore can result in that shore being seriously overloaded.

4. An area-effect may exist which serves to reduce the maximum shore load for a given pour area (i.e., the ACI design load becomes more conservative as the effective slab area increases). A reduction in design load for construction may be a function of pour area, slab thickness, formwork arrangement, and concrete placement procedures.

5. Significant load variations in steel shores may result from large daily (or other) temperature variations. These variations were particularly evident during curing periods, even when there were no additional externally applied loads.

6. A small decrease in shore load was observed during the curing period. This decrease in shore load is likely a function either of creep effects in the concrete or gain in strength and stiffness of the slab. The decrease in load appears to become greater with increasing effective slab area.

7. Shore removal can induce significant loads on the slab and shores, often of an impact nature. The magnitude of these loads is a function of the amount of compression in the shore at the time of its removal and the removal procedure used. Shore removal loads take two forms: (1) additional compression due to the removal procedure, and (2) load redistribution following the removal of a nearby shore. The amount of load redistribution is largely a function of the supporting formwork arrangement. Very large effective impact loads may be imparted to the (early-age) slab during formwork removal.

The work described herein is part of an on-going effort to collect load data during concrete construction and the observations are based only on a limited amount of shore load data. However, it is apparent that a great deal can be learned even from a qualitative analysis of this valuable information. As additional sites are monitored and data are collected and analyzed, much needed information will become available on which to base construction design loads. This, in turn, will lead to improved safety of buildings and temporary formwork systems during construction.

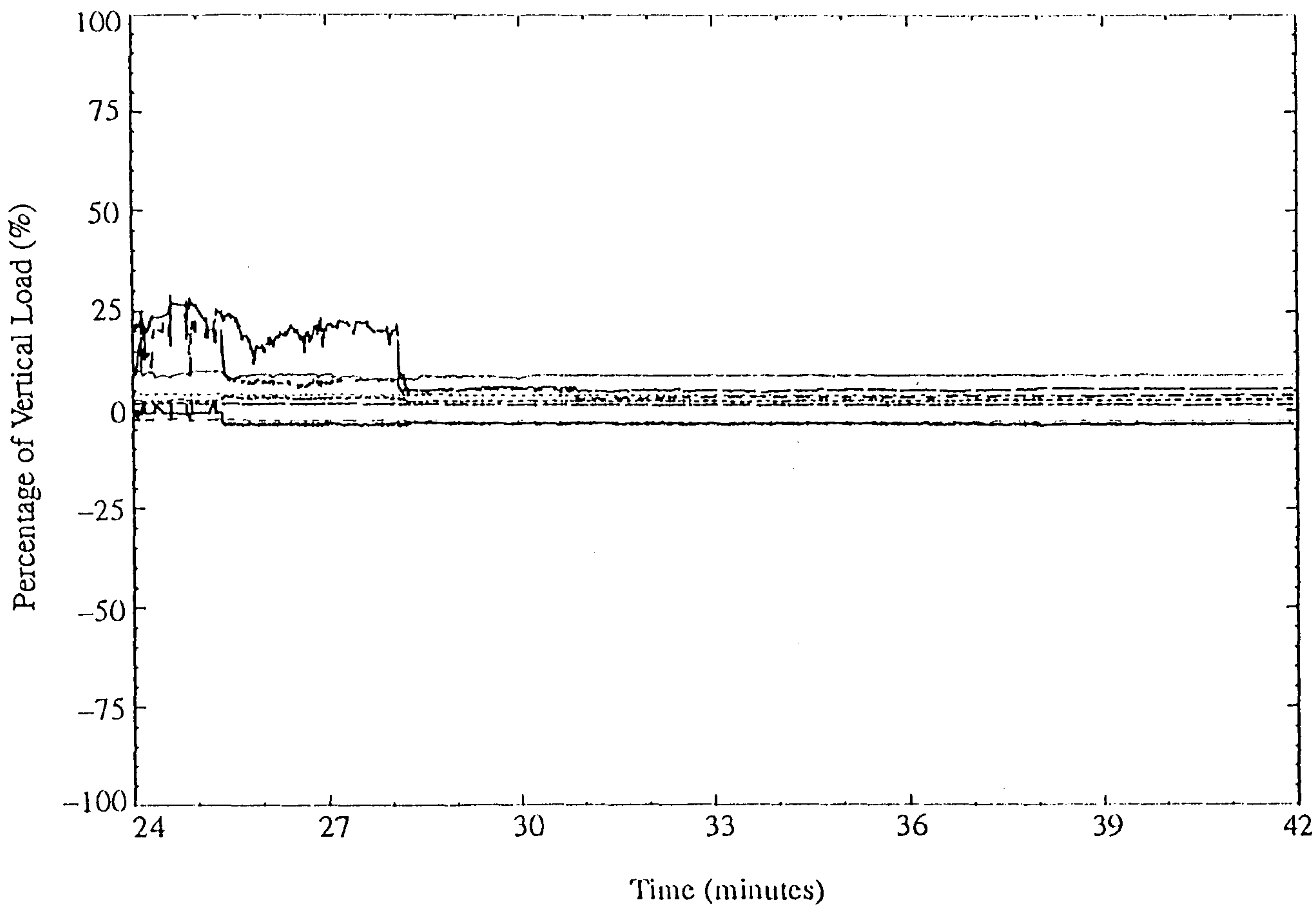

Figure 16.1 Small pour lateral shore loads (Y-direction) as percentage of vertical shore loads at Beckley WV.

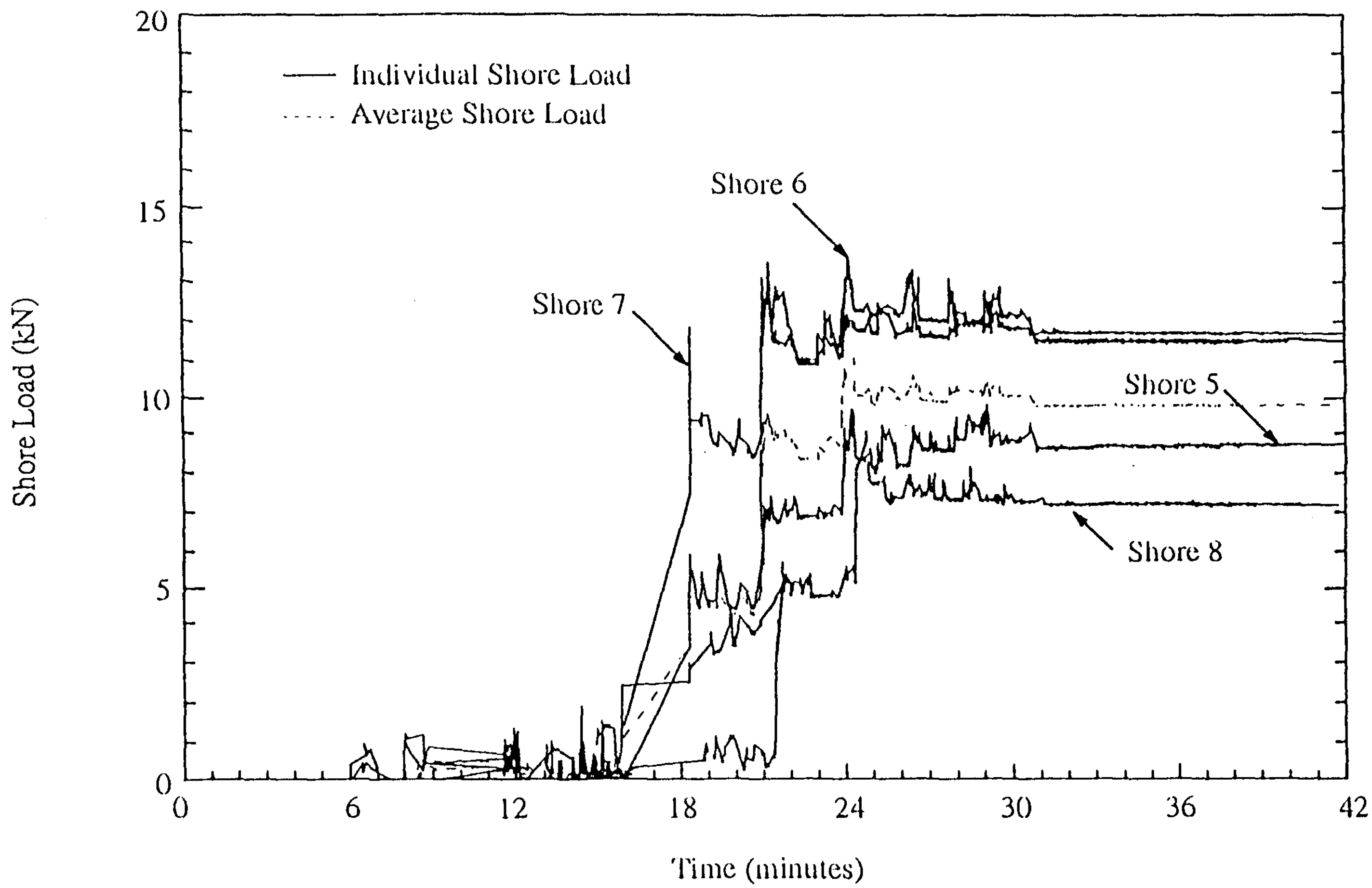

Figure 16.2 Small pour individual vertical shore loads at Beckley WV.

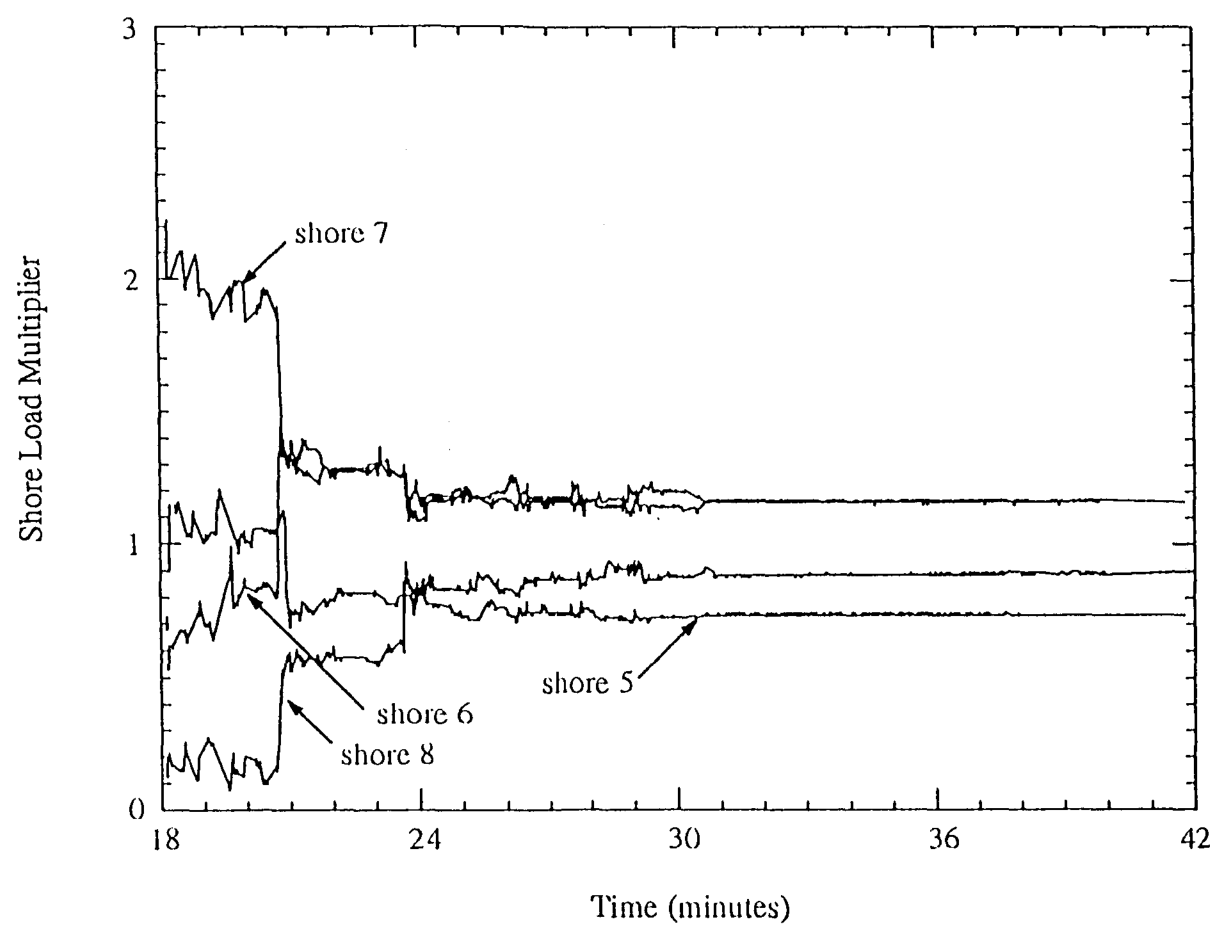

Figure 16.3 Small pour vertical shore load multipliers at Beckley WV.

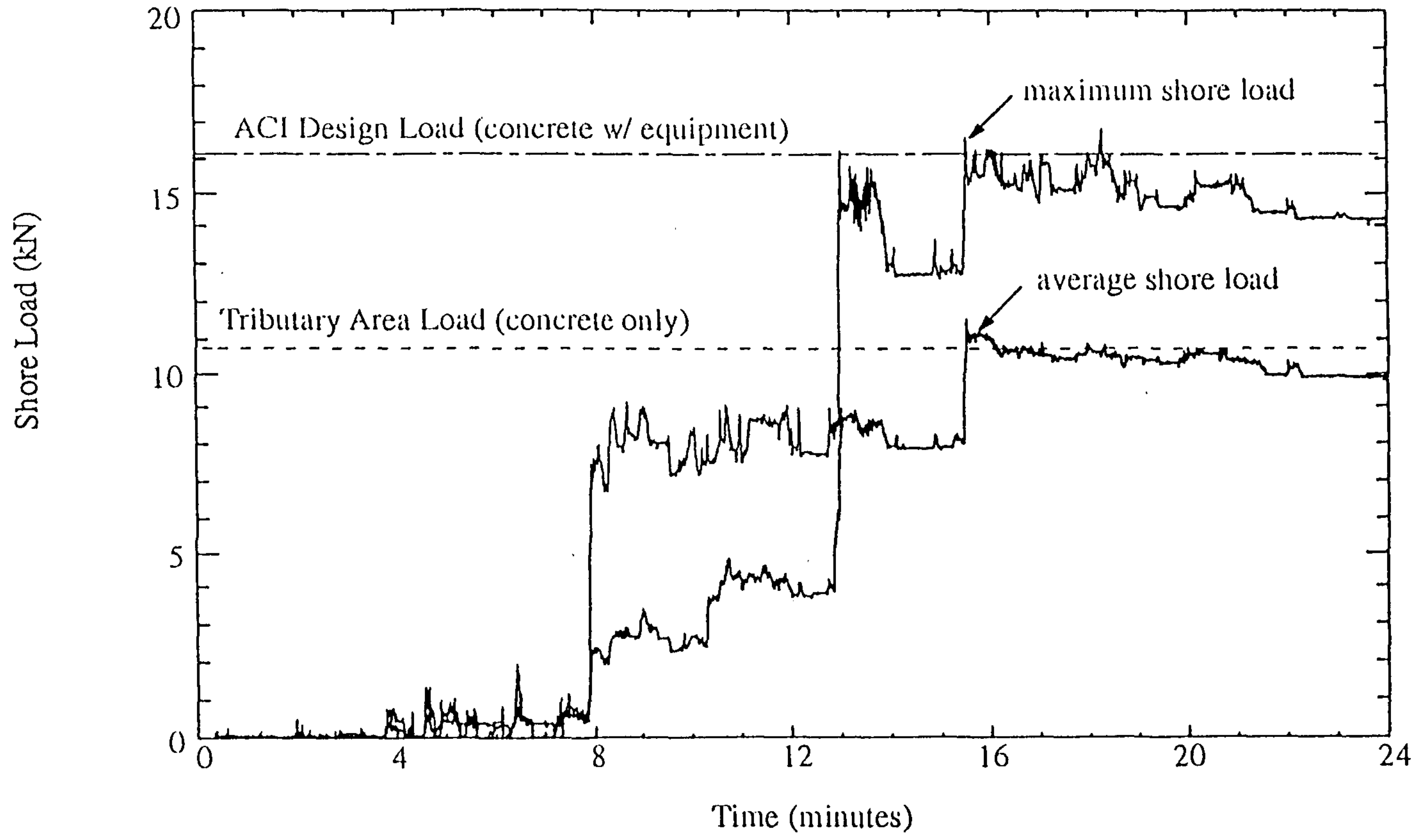

Figure 16.4 Small pour vertical shore loads during pouring at Beckley WV.

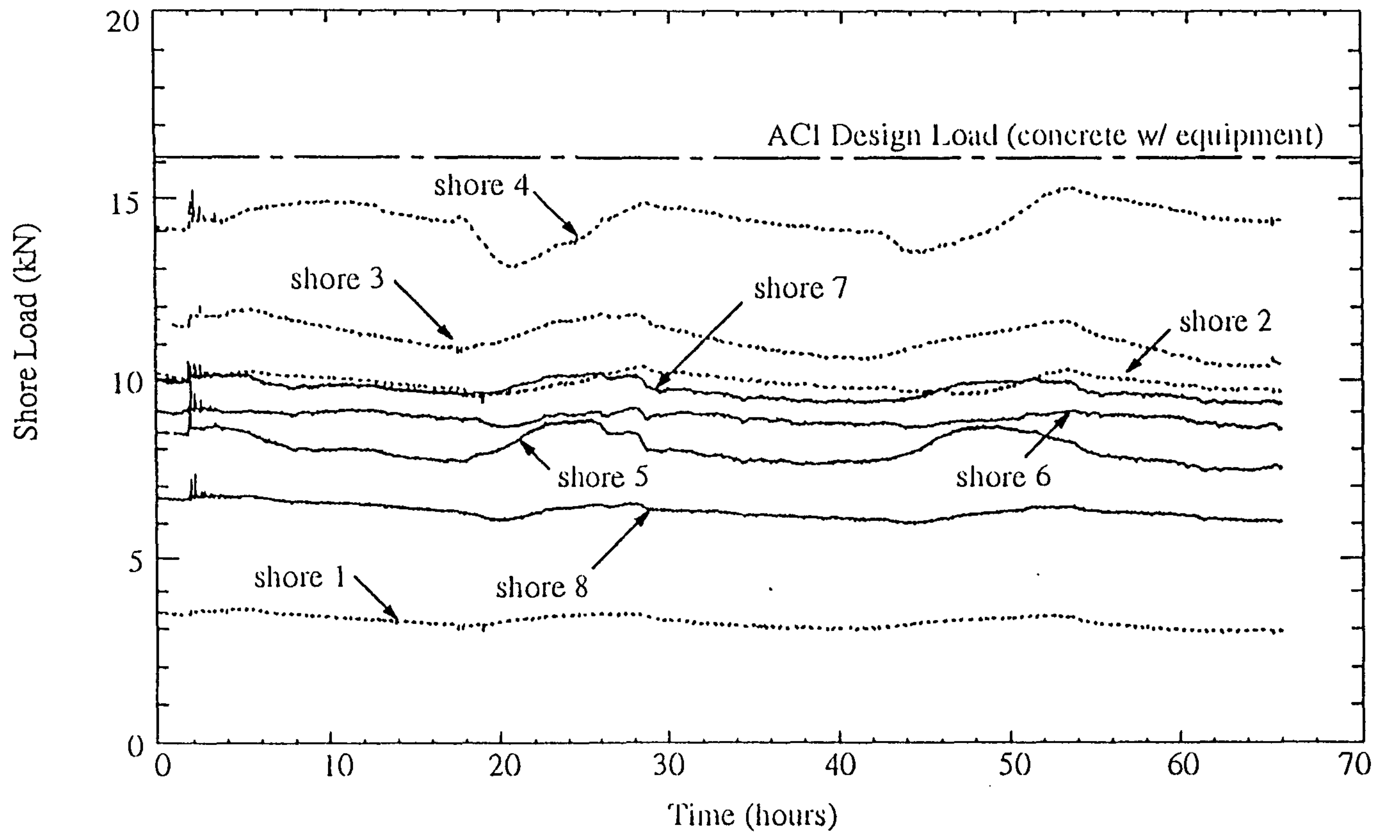

Figure 16.5 Small pour individual vertical shore loads during curing at Beckley WV.

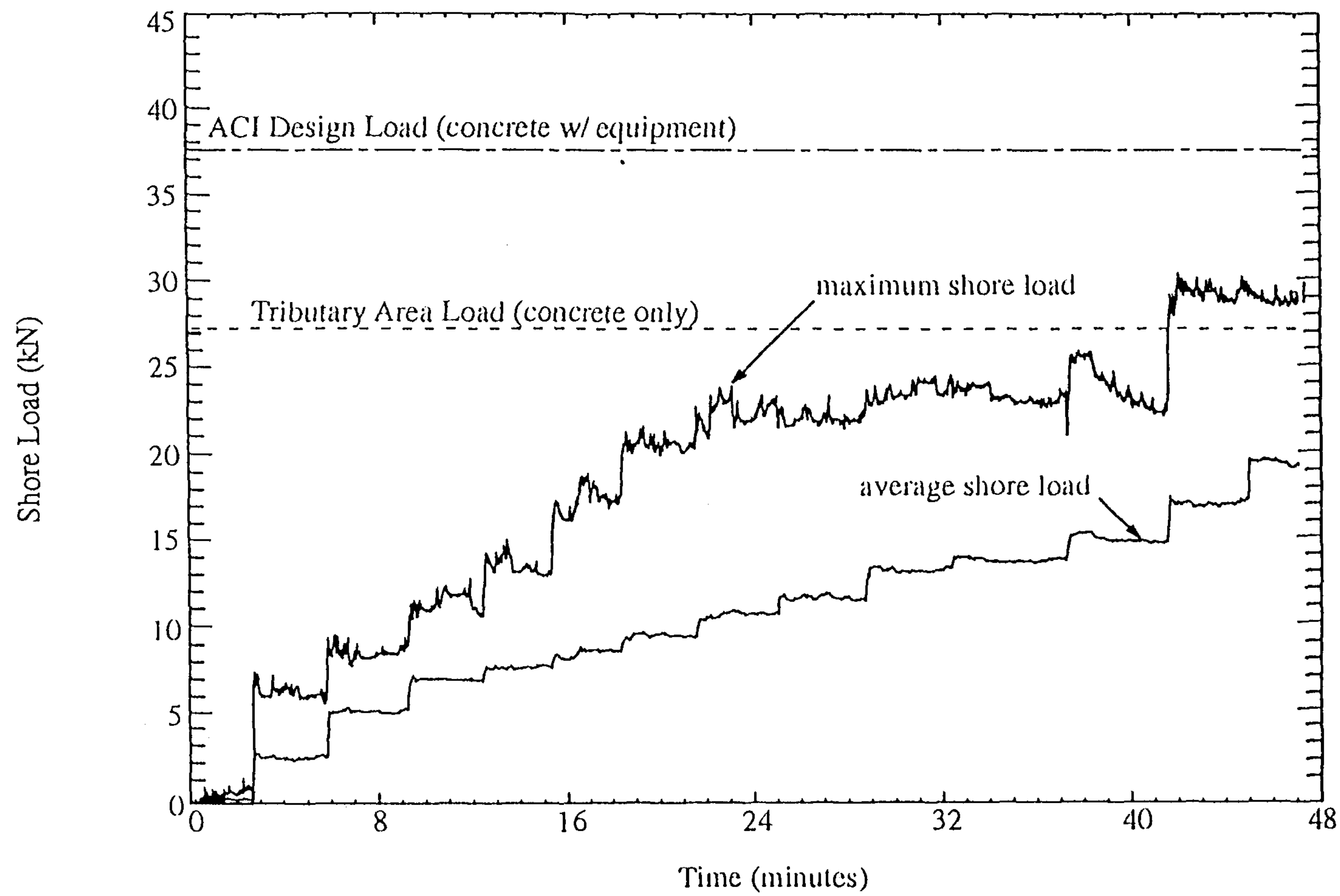

Figure 16.6 Large pour vertical shore loads during pouring at Beckley WV.

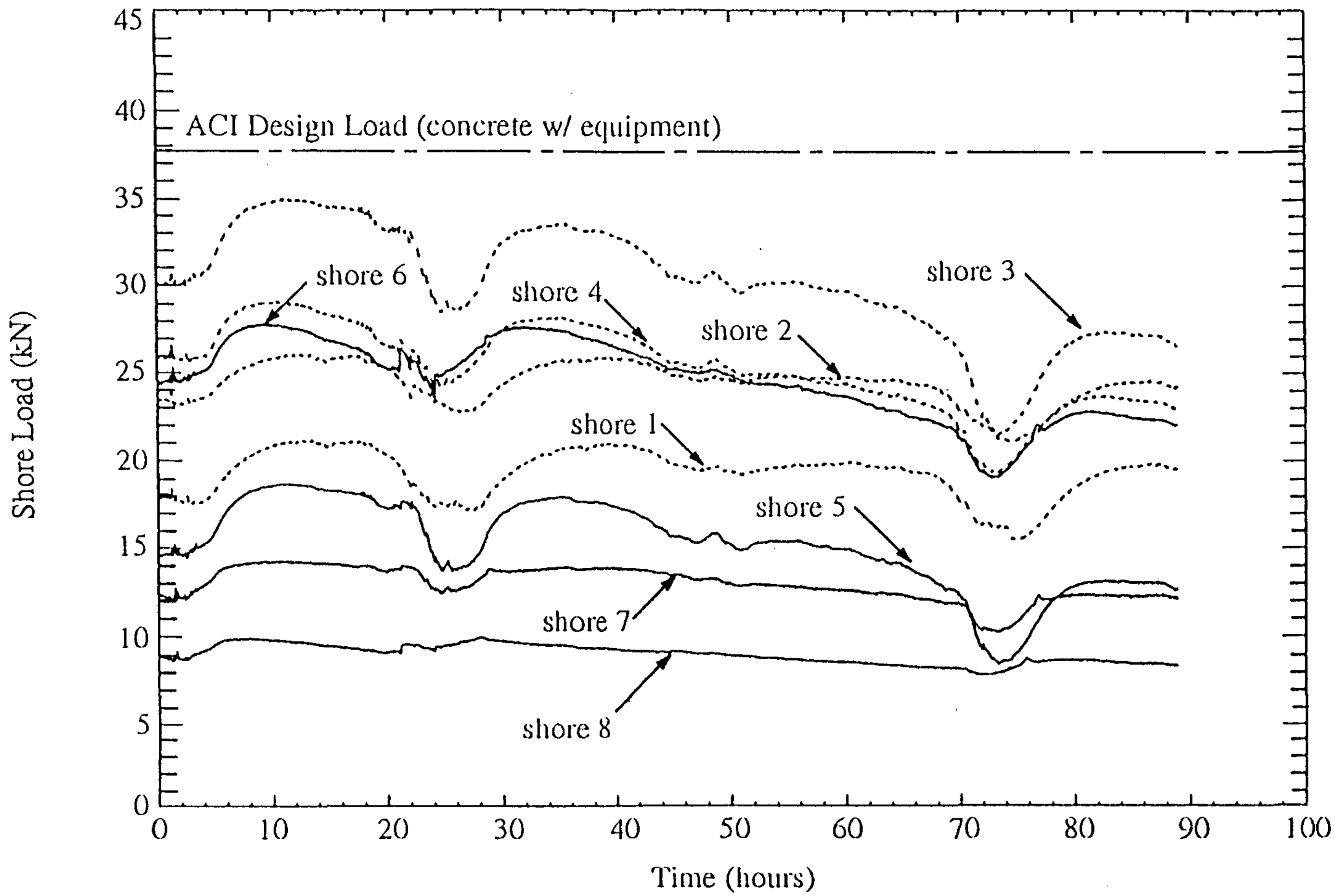

Figure 16.7 Large pour individual vertical shore loads during curing at Beckley WV.

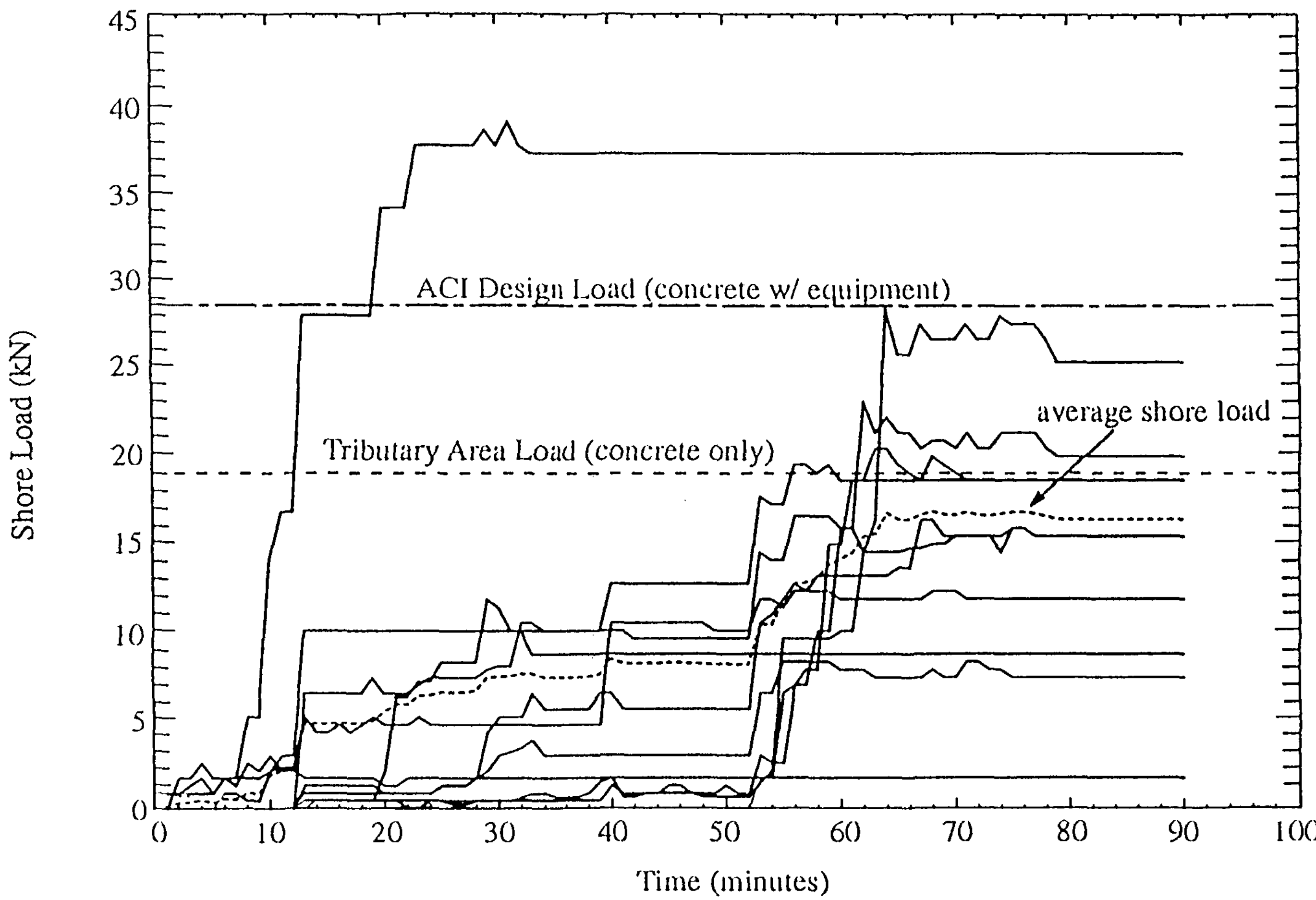

Figure 16.8 Vertical shore loads during pouring (data from Fattal, 1983).

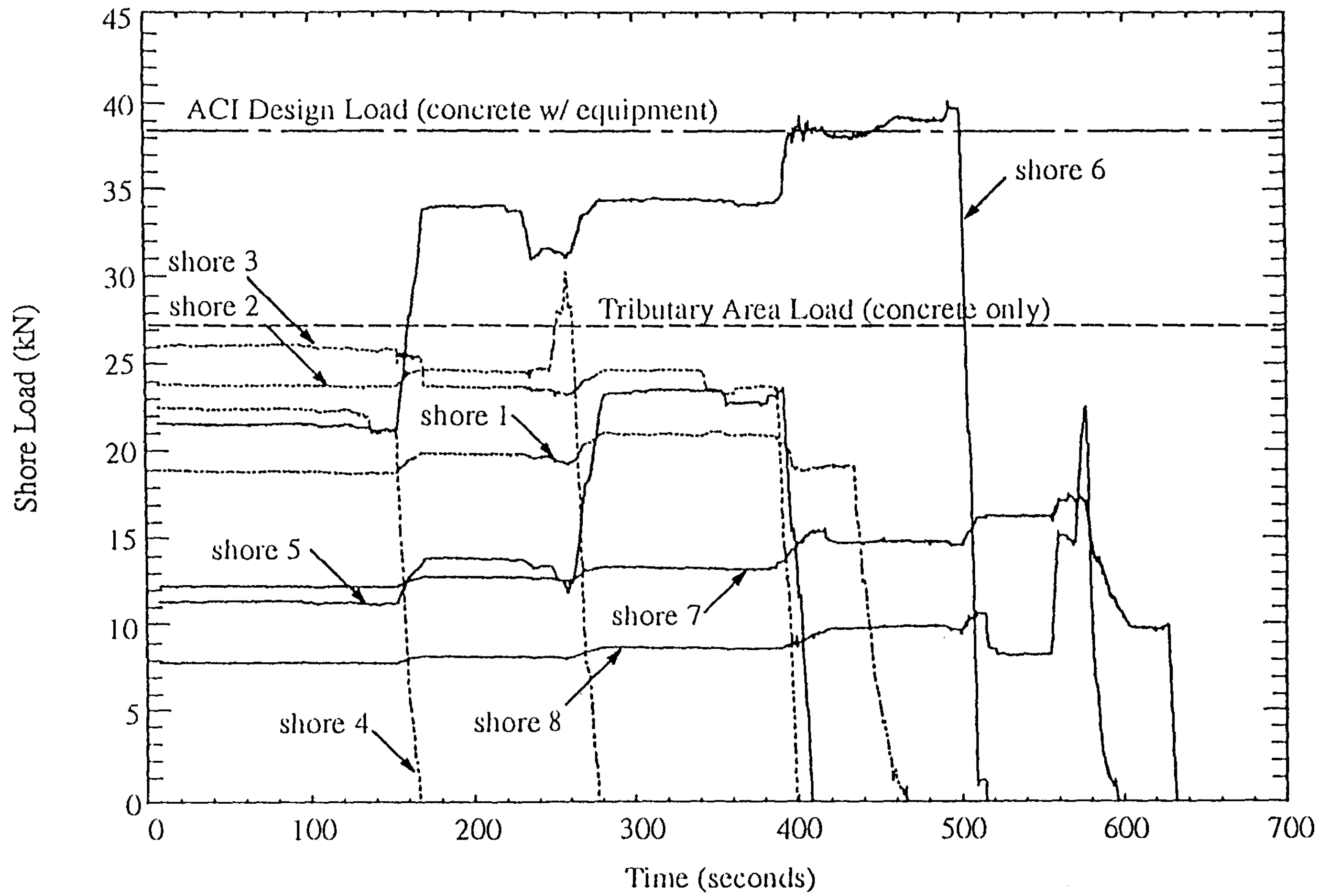

Figure 16.9 Large pour individual vertical shore loads during shore removal at Beckley WV

17. Acknowledgements

This project was supported by grant 5 R01OH03157 from the National Institute for Occupational Safety and Health. The contents of this report are the responsibility of the authors and do not necessarily reflect the official views of the National Institute for Occupational Safety and Health.

The authors would like to thank the construction firms and workers who have aided in the collection of the site data. Without their assistance, this report could not have been written. At the Boston Museum Towers site we were assisted by Dr. James Becker and Walter Turgeon of Beacon/Skanska Construction, and by Dr. Minhaj Kirmani, Suresh Babu, and Juan Pedro of Weidlinger Associates of Cambridge, MA. At the Beckley WV Federal Prison site we were assisted by Alan Haggerty of Pizzagalli Construction. The University of Vermont Architect's office provided assistance in access to the East Ave. and Pomeroy Hall sites.

The authors would also like to thank the students and technicians who contributed their efforts to conducting this research. Students from the University of Vermont include: Timothy Ambrose, Rob Church, Jing Hu, Julie Martin, Madhiv Naik, Matt Nelson, Hongchu Qiu, and Wolfgang Sauter. Students from Clemson University include: AK Kothekar, and T Philbrick, Jr. and B Sockalingam. Mingzhu Duan of from Purdue University also contributed to this research project.

18. List of Present and Future Publications

18.1 Archival Journal Articles Published

Kothekar AV, Rosowsky DV, and Huston DR: Investigating the Adequacy of Vertical Design Loads for Shoring, Journal of Performance of Constructed Facilities, ASCE, 12(1):41-47, 1998

Rosowsky D, Philbrick T, and Huston D. Observations from Shore Load Measurements During Concrete Construction, Journal of Performance of Constructed Facilities, ASCE, 11(1):18-23, 1997

Rosowsky D: Estimation of Design Loads for Reduced Reference Periods. Structural Safety, Vol. 17, 17-32, 1995

18.2 Archival Journal Articles Submitted and Under Review

none

18.3 Archival Journal Articles Planned for Submission

Huston D, Fuhr P, and Kirmani M: Shore Load Measurements at Boston Museum Towers, to ASCE Jnl of Struc Eng

Huston D, Rosowsky D, Chen WF and Fuhr P: Comparison of Shore Load Measurements at Boston Museum Towers with Codes and Models, to ASCE Jnl. of Struc Eng

18.4 Non-Archival Journal Articles Published

Duan M, Chen WF: Design Guidelines for Safe Concrete Construction, Concrete International, Oct. 1996

Rosowsky D, Huston D, Fuhr P, and Chen W-F: Measuring Formwork Loads During Construction, Concrete International, pp. 21-25, November 1994

18.5 Non-Archival Journal Articles Planned for Submission

Huston D, Rosowsky D, Chen WF and Fuhr P: Safe Concrete Building Construction Practices, Concrete International.

18.6 Conference Proceedings Published

Epaarachchi D, Stewart MG, and Rosowsky DV: Reliability of Multi-Story Reinforced Concrete Buildings during Construction, Proceedings 15th Australasian Conference on the Mechanics of Structures and Materials, Melbourne, Australia, pp. 527-532, 1997

Huston DR, Rosowsky, DR, Fuhr PL, and Chen WF: Construction Shoring Load Measurements, Proc. ASCE Structures '95 Conference, Boston MA, pp. 1373-7, April 1995

Huston DR, Fuhr PL, Rosowsky DV, and Chen WF: Load Monitoring and Hazard Warning Systems for Buildings Under Construction, SPIE Smart Structures Conference 2719-10, San Diego, Feb. 1996

Philbrick TW and Rosowsky DV. (1996) "Analysis of Shoring Load Effects Using Field Data," *Proceedings:* ASCE Structures Congress '96, Chicago, IL

Rosowsky DV and Kothekar AV: Partial Safety Factors for Design of Shores Used during R/C Construction, Proceedings 76th International Conference on Structural Safety, and Reliability (ICOSSAR '97), Kyoto, Japan, November 1997

18.7 Conference Proceedings Planned for Submission

Huston DR, Fuhr PL, Rosowsky DV, and Kirmani M: Shoring Measurements at Museum Towers, submitted for presentation at ASCE Structures Congress, New Orleans, April 1999

Khor E, Rosowsky D, and Stewart M: Effect of Early-Age Loading on Serviceability Reliability of Reinforced Concrete Flexural Elements, to appear in *Proceedings:* Structural Engineers World Congress (SEWC) '98, San Francisco, CA, July 1998

18.8 Reports

Duan M, Chen WF. "Chapter 2 - Design considerations for Safe Construction of Concrete Buildings," Project Report, Purdue University, West Lafayette, IN 47907, Dec. 1995

Duan M, Chen WF: Chapter 3 - Improved Simplified Method for Slab and Shore Load Analysis during Construction, Project Report, Purdue University, West Lafayette, IN 47907, Dec. 1995

Duan M, Chen WF: Chapter 4 Effects of Creep and Shrinkage on Slab-Shore Loads and Deflections during Construction, Project Report, Purdue University, West Lafayette, IN 47907, Dec. 1995

Duan M, Chen WF: Decision Making Models for Reliability of Slab and Formwork Systems during Construction, Report No. CE-STR-96-12, School of Civil Engineering, Purdue University, West Lafayette, IN, 1996

Duan M, Chen WF: Effects of Creep and Shrinkage on Slab-shore Loads and Deflections during Construction, Purdue University, School of Civil Engineering, CE-STR-95-24, 1995

Duan M, Chen WF: Effects of Nonuniform and Impact Loading on Slab-Shores in Concrete Placing and Shore Removal during Construction, Purdue University, School of Civil Engineering, Report no CE-STR-95-20, 1995

Duan M, Chen WF: General Design Guidelines for Safe Construction of Concrete Buildings, Purdue University, School of Civil Engineering, Report No. CE-STR-95-22, 1995

Duan M, Chen WF: Improved Simplified Method for Slab and Shore Load Analysis During Construction, Purdue University, School of Civil Engineering, Report No. CE-STR-95-21, 1995

Duan M, Chen WF: Proposed Design Guidelines for Construction Code Requirements of Concrete Buildings, Report No. CE-STR-96-16, Civil Engineering, Purdue Univ., 1996

Kothekar A: Investigation of Adequacy of Vertical Design Loads for Shoring, Project Report, Dept. of Civil Engineering, Clemson University, Clemson, SC 29634-0911

Kothekar A: Reliability Analysis of Shores, Project Report, Dept. of Civil Engineering, Clemson University, Clemson SC 29634-0911

Philbrick, Jr., T: Construction Load Data and Modeling: Literature Review, Project Report, Dept. of Civil Engineering, Clemson University, Clemson SC, Nov. 1994

Philbrick TW, Rosowsky D: Concrete Load Monitoring and Analysis Using Instrumented Shoring: Data Analysis: Beckley, WV Site. Project Report, Clemson University, 28, 1995

Philbrick, Jr. T, and Rosowsky DV: Construction Load Monitoring and Analysis using Instrumented Shoring: Finite Element Model of the Beckley Large Pour Area, Project Report, Dept. of Civil Engineering, Clemson University, Clemson SC, Sept. 1995

Sockalingam B and Rosowsky D: Construction Load Monitoring and Analysis sing Instrumented Shoring: Numerical Modeling of Shore Installation Effects, Project Report, Clemson University, Department of Civil Engineering, Clemson SC Dec. 1995

18.9 Dissertations

Duan M: Design Guidelines for Safe Construction of Concrete Buildings, Ph.D. Dissertation, Purdue University, Civil Engineering, 1996.

Qiu H: Stability and Load Effects of Concrete Construction, PhD Dissertation, University of Vermont, Mechanical Engineering, anticipated completion date – 1999.

19. References

1. ASCE Committee, Structural Standard Division: Proposed Guide/Standard for Design Loads on Structures during Construction. ASCE, 24, 1995

2. ACI Committee 318: Building Code Requirements for Concrete. American Concrete Institute, Detroit, MI, 351, 1995.

3. ACI Committee 347: Guide to Formwork for Concrete. ACI Structural Journal, Vol. 85, No. 5, Sept.-Oct.,22643-22646, 1988

4. ANSI: A10.9 Construction and Demolition Operations - Concrete and Masonry Work, American National Standards Institute, Philadelphia PA, 1983.

5. Agarwal RK, Gardner NJ: Form and Shore Requirements for Multistory Flat Slab Type Buildings. ACI Journal, Vol. 71, No. 11,559-569, 1974

6. Ambrose TP, Huston DR, Fuhr PL, Devino EA, and Werner MP: Shoring Systems for Construction Load Monitoring, Smart Mater. Struc. 3, 26-34 1994

7. Anon.: Avoiding Failures in Concrete Construction, Seminar Course Manual/SCM-19(89), American Concrete Institute, Detroit, 1989.

8. Ayoub H and Karshenas S: Survey Results for Concrete Construction Live Loads on Newly Poured Slabs, ASCE Journal of Structural Engineering, 120(5):1543 -15 62, 1994.

9. Ayyub BM, and Eldukair ZA, Impact of Errors on Safety During Construction, Proc. of Sessions Related to Design, Analysis and Testing, ASCE Structures Congress '89, San Francisco, CA, May 1-5, pp. 835-843, 1989

10. Chalk P and Corotis, R: A Probability Model for Design Live Loads, ASCE Journal of Structural Engineering, 106(10):2017-2033, 1980.

11. Chen WF, Mosallam KH: Concrete Buildings: Analysis for Safe Construction. CRC Press, 221, 1991

12. Corotis RB: Probability-Based Design Codes. Concrete International: Design and Construction, ACI, Vol. 7, No. 8, 42-49, 1985

13. Duan MZ: Design Guidelines for Safe Construction of Concrete Buildings. PhD Dissertation: School of Civil Engineering, West Lafayette, IN, Purdue University, 1995.

14. Duan MZ, Chen WF: Improved Simplified Method for Slab and Shore Load Analysis during Construction. Research Report: CE-STR-95-21, School of Civil Engineering, West Lafayette, IN, Purdue University, 1995a

15. Duan MZ, Chen WF: Effects of Creep and Shrinkage on Slab-Shore Loads and Deflection during Construction. Research Report: CE-STR-95-24, School of Civil Engineering, West Lafayette, IN, Purdue University, 1995b

16. Duan MZ, Chen WF: Effects of non-uniform and Impact Loading on Slab-Shores in Concrete Placing and Shore Removing during Construction. Research Report: CE-STR-95-20, School of Civil Engineering, West Lafayette, IN, Purdue University, 1995c

17. El-Shahhat AM, Rosowsky DV, Chen WF: Partial Factor Design for R/C Buildings during Construction. Research Report: CE-STR-93-11, School of Civil Engineering, Purdue University, West Lafayette, IN, 1993a

18. El-Shahhat AM, Rosowsky DV, Chen WF: Construction Safety of Multistory Concrete Buildings. ACI Structural Journal, Vol. 90, No. 4, 353-341, 1993b

19. El-Sheikh M, Chen WF: Effect of Fast Construction Rate on Deflection of R.C. Buildings. Journal of Structural Engineering, ASCE, Vol. 114, No. 10, 2225-2238, 1988

20. El-Sheikh M. and Chen WF, Behavior and Strength of Telescopic Steel Shores, Proceedings of Materials Congress, ASCE, Denver, CO, July 1990

21. Fattal SG: Evaluation of Construction Loads in Multistory Concrete Buildings, NBS BSS 146, National Bureau of Standards, Washington, DC, 1983.

22. Grundy P, Kabaila A: Construction Loads on Slabs with Shored Formwork in Multistory Buildings. ACI Journal, Vol. 60, No. 12, 1729-1738, 1963

23. Hadipriono FC, Wang HK: Analysis of Causes of Formwork Failures in Concrete Structures. Journal of Construction Engineering and Management, ASCE, Vol. 112, No. 1,112-121, 1986

24. Huang YL: Load and Resistance Factor Design Guidelines for High-Clearance Scaffold Systems, Ph.D. Thesis, Purdue University, 1995

25. Hurd MK: Formwork for Concrete. American Concrete Institute, Detroit MI, Fifth Edition, 1989

26. Huston DR: Construction Load Monitoring at Beckley site" Personal Correspondence, 1995

27. Huston, DR, Smart Civil Structures - An Overview, SPIE Paper No. 1588-21, Proc. SPIE Fibers '91 Symposium, Boston, MA, Sept. 1991

28. Huston D, Beliveau J-G, and Durham D, Wind-Induced Failure of Bar-Cable on the Cornish-Windsor Cable-Stayed Bridge, Proc. 6th U.S.-Japan Bridge Engineering Workshop, pp. 27-34, A.M. Abdel-Ghafar, ed., Lake Tahoe, NV, May 7-8, 1990

29. Huston DR, Rosowsky, DR, Fuhr PL, and Chen WF: Construction Shoring Load Measurements, Proc. ASCE Structures '95 Conference, Boston MA, pp. 1373-7, April 1995

30. Huston DR, Fuhr PL, Rosowsky DV, and Chen WF: Load Monitoring and Hazard Warning Systems for Buildings Under Construction, SPIE Smart Structures Conference 2719-10, San Diego, Feb. 1996

31. Lee HM, Liu XL, Chen WF: Creep Analysis of Concrete Buildings during Construction. Journal of Structural Engineering, ASCE, Vol. 117, No. 10, 3135-3148, 1991

32. Karshenas S, Analysis of Construction Loads in Multistory Buildings, ASCE Structures Congress, Baltimore, MD, May 1990

33. Karshenas S and Ayoub H: Analysis of Concrete Construction Live Loads on Newly Poured Slabs, ASCE Journal of Structural Engineering, 120(5):1525-1542, 1994.

34. Kothekar AV, Rosowsky DV, and Huston DR: Investigating the Adequacy of Vertical Design Loads for Shoring, ASCE Jnl. of Performance of Constructed Facilities, 12(1):41-47, 1998

35. Kubo Y, Watanabe A, Kuga N, Tokuyama S, Katao K, and Morimoto M, Full Scale Observation of Aerodynamic Responses of a PC Cable-Stayed Bridge During its Erection, Proc. ASCE Struc. Cong., pp. 628-637, San Francisco, May 1989

36. Liu XL, and Chen WF, Probability Distribution of Maximum Wooden Shore Loads in Multistory R.C. Buildings, Jnl. of Structural Safety, pp. 197-215, 1987

37. Liu XL, Chen WF, Bowman MD: Construction Load Analysis for Concrete Structures. Journal of Structural Engineering, ASCE, Vol. 3, No. 5, 1019-1036, 1985

38. Liu XL, Chen WF: Effect of Creep on Load Distribution in Multistory Reinforced Concrete Buildings during Construction. ACI Structural Journal, Vol. 84, No. 3, 190-200, 1987

39. Liu XL, Lee HM, Chen WF: Analysis of Construction Loads on Slabs and Shores by Personal Computer Concrete International, pp. 21-30, June 1988.

40. Masahiro Y, Sakurai J, Ohsaka K, Makuta H., and Habu S., Precision Control System under Construction of Yokohama Bay Bridge, Proc. 6th U.S.-Japan Bridge Engineering Workshop, Lake Tahoe, NV, May 1990

41. Nielsen KEC, Load on Reinforced Concrete Slabs and Their Deformation During Construction, Bulletin No. 15, Final Report, Swedish Cement and Concrete Research Institute of Technology, Stokholm, 1952

42. OSHA: Occupational Safety and Health Standards for the Construction Industry (29 CFR Part 1926) Commerce Clearing House, Inc., Chicago IL, Amended Nov. 1, 1993

43. Peng, JL, Rosowsky DV, Pan AD, Chen WF and Yen T, Analysis of Concrete Placement Load Effects Using Influence Surfaces, ACI Structural Journal, 1995

44. Philbrick TW, Rosowsky D: Concrete Load Monitoring and Analysis Using Instrumented Shoring: Data Analysis: Beckley, WV Site. Project Report, Clemson University, 28, 1995

45. Rosowsky D: Estimation of Design Loads for Reduced Reference Periods. Structural Safety, Vol. 17, 17-32, 1995

46. Rosowsky DV, Huang YL, Chen WF and Yen T: Modeling Concrete Placement Loads during Construction, Structural Engineering Review, 6(2):71-84, 1994.

47. Rosowsky D, Huston D, Fuhr P, and Chen W-F: Measuring Formwork Loads During Construction, Concrete International, pp. 21-25, November 1994

48. Rosowsky DV, Philbrick TJ, and Huston DR: Observations from Shore Load Measurements During Concrete Construction, ASCE Jnl. of Per. of Const. Fac., 11(1):18-23, 1997

49. Sbarounis JA: Multistory Flat Plate Buildings: Construction Load and Deflection. Concrete International: Design and Construction, ACI, Vol. 6, No. 2, 70-77, 1984a

50. Sbarounis JA: Multistory Flat Plate Buildings: Effect of Construction on Long-Term Deflections. Concrete International: Design and Construction, ACI, Vol. 6, No. 4,62-67, 1984b

51. Sbarounis JA: Multistory Flat Plate Buildings: Measured and Computed One-Year Deflections. Concrete International: Design and Construction, ACI, Vol. 6, No. 8, 31-34, 1984c

52. Tanaka H, Kamai M, and Kaneyoshi M, Cable Tension Adjustment by Structural System Identification, Proc. Intl. Conf. on Cable-Stayed Bridges, Cable-Stayed Bridges: Experiences and Practice, W. Kanok-Nukuchi, Bangkok, 1987

53. Taylor PF, Effect of Formwork Stripping Time on Deflection of Flat Slabs and Plates, Australian Civil Engineering and Construction, (Melbourne) , No. 2, pp. 31-35, February 1967

54. Yen T. Huang YL, Chen WF and Lin YC, Design of Scaffold Systems for Concrete Buildings During Construction, Structural Engineering Report, CE-STR-95-4, Purdue University, W. Lafayette, IN, 1995

55. .